The impact of recent advances in laboratory astrophysics on our understanding of the cosmos

D W Savin[1], N S Brickhouse[2], J J Cowan[3], R P Drake[4], S R Federman[5], G J Ferland[6], A Frank[7], M S Gudipati[8], W C Haxton[9], E Herbst[10], S Profumo[11], F Salama[12], L M Ziurys[13] and E G Zweibel[14]

[1] Columbia Astrophysics Laboratory, Columbia University, New York, NY 10027, USA

[2] Harvard-Smithsonian Center for Astrophysics, 60 Garden Street, Cambridge, MA 02138, USA

[3] Homer L Dodge Department of Physics and Astronomy, University of Oklahoma, Norman, OK 73019, USA

[4] Department of Atmospheric, Oceanic and Space Sciences, University of Michigan, Ann Arbor, MI 48109, USA

[5] Department of Physics and Astronomy, University of Toledo, Toledo, OH 43606, USA

[6] Department of Physics, University of Kentucky, Lexington, KY 40506, USA

[7] Department of Physics and Astronomy, University of Rochester, Rochester, NY 14627, USA

[8] Science Division, Jet Propulsion Laboratory, California Institute of Technology, Pasadena, CA 91109, USA

[9] Department of Physics, University of California, Berkeley, and Lawrence Berkeley National Laboratory, Berkeley, CA 97420, USA

[10] Departments of Chemistry, Astronomy and Physics, University of Virginia, Charlottesville, VA 22904, USA

[11] Department of Physics, ISB 325, University of California, 1156 High Street, Santa Cruz, CA 95064, USA

[12] Space Science Division, NASA Ames Research Center, Moffett Field, CA 94035, USA

[13] Departments of Chemistry and Astronomy, Arizona Radio Observatory and Steward Observatory, University of Arizona, Tucson, AZ 85721, USA

[14] Departments of Astronomy and Physics, University of Wisconsin, 6281 Chamberlain Hall, 475 North Charter Street, Madison, WI 53706, USA

Abstract

An emerging theme in modern astrophysics is the connection between astronomical observations and the underlying physical phenomena that drive our cosmos. Both the mechanisms responsible for the observed astrophysical phenomena and the tools used to probe such phenomena—the radiation and particle spectra we observe—have their roots in atomic, molecular, condensed matter, plasma, nuclear and particle physics. Chemistry is implicitly included in both molecular and condensed matter physics. This connection is the theme of the present report, which provides a broad, though non-exhaustive, overview of progress in our understanding of the cosmos resulting from recent theoretical and experimental advances in what is commonly called laboratory astrophysics. This work, carried out by a diverse community of laboratory astrophysicists, is increasingly important as astrophysics transitions into an era of precise measurement and high fidelity modeling.

(Some figures may appear in colour only in the online journal)

This article was invited by S Ritz.

Contents

1. Introduction

Laboratory astrophysics and complementary theoretical calculations are the foundations of astronomy and astrophysics and will remain so into the foreseeable future. The impact of laboratory astrophysics ranges from the scientific conception for ground-based, airborne and space-based observatories, all the way through to the scientific return of these projects and missions. It is our understanding of the underlying physical processes and the measurement or calculation of critical physical parameters that allows us to address fundamental questions in astronomy and astrophysics.

The field of laboratory astrophysics comprises both theoretical and experimental studies of the underlying physics that produce the observed astrophysical processes. We have identified six areas of physics as relevant to astronomy and astrophysics[15]. Astronomy is an observational science focused primarily on detecting photons generated by atomic, molecular and condensed matter physics. Chemistry is implicitly included here as part of molecular and condensed matter physics. Our understanding of the universe also relies on knowledge of the evolution of matter (nuclear and particle physics) and of the dynamical processes shaping it (plasma physics). Planetary science, involving *in situ* measurements of solar system bodies, requires knowledge from atomic, molecular, condensed matter and plasma physics. Hence, our quest to understand the cosmos rests firmly on scientific knowledge in six areas: atomic, molecular, condensed matter, plasma, nuclear and particle physics.

Here we review recent advances in our astrophysical understanding of the cosmos arising from work in laboratory astrophysics. We focus primarily on the past decade. Our work complements that of previous reviews on laboratory astrophysics in atomic physics (Beiersdorfer 2003, Kallman and Palmeri 2007, International Astronomical Union (IAU) Commission 14 2011), molecular physics (Salama 1999, Tielens 2005, Herbst and van Dishoeck 2009, IAU Commission 14 2011), condensed matter physics (Draine 2003, Whittet 2003), plasma physics (Drake 1999, Remington *et al* 2006, Zweibel and Yamada 2009, Yamada *et al* 2010), nuclear physics (Käppeler *et al* 2011, Wiescher *et al* 2010,

Adelberger *et al* 2011) and particle physics (Grupen 2005, Aprile and Profumo 2009).

Because laboratory astrophysics, as implied by its name, is astrophysically motivated, we have structured our report into five broad categories which blanket the field of astronomy and astrophysics. This helps us to bring out the synergy between the various subareas of laboratory astrophysics. The specific categories are as follows: planetary systems and star formation (section 2), stars and stellar evolution (section 3), the galactic neighborhood (section 4), galaxies across time (section 5) and cosmology and fundamental physics (section 6). This structure parallels the scientific divisions used by the recent US National Research Council Astro 2010 Survey on Astronomy and Astrophysics (Blandford *et al* 2010a). These five sections are further subdivided into relevant subareas of laboratory astrophysics. Space limitations prevent these subsections from being exhaustive. Rather they are aimed at giving the reader an overview of recent successes in the field and appropriate citations to provide entry into the relevant research. We conclude with a brief discussion and outlook for the future in section 7.

2. Planetary systems and star formation

Planetary systems and star formation encompass 'solar system bodies (other than the Sun) and extrasolar planets, debris disks, exobiology, the formation of individual stars, protostellar and protoplanetary disks, molecular clouds and the cold ISM[16] (interstellar medium), dust, and astrochemistry' (Blandford *et al* 2010a).

2.1. Atomic physics

2.1.1. Young late-type stars. In accreting stellar objects with strong magnetic fields (such as young late-type stars, x-ray binaries with neutron stars and magnetic cataclysmic variables (CVs)), the stellar magnetic field truncates the accretion disk and channels the accreting material toward a 'hot spot' near the pole of the star (Konigl 1991). This material accelerates in the gravitational field of the star, reaching supersonic velocities and producing a shock which emits in x-rays. For low-mass young stars, the free-fall velocity (the maximum velocity obtained by material accelerated from infinity) is

---

[15] The authors comprise past and current members of the American Astronomical Society Working Group on Laboratory Astrophysics.

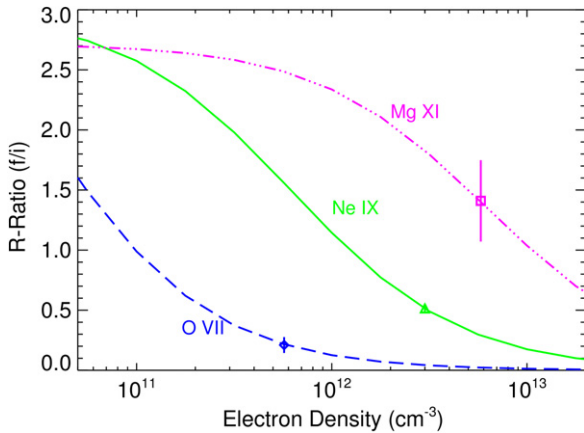[16] A list of acronyms used throughout the text is given in the appendix.

Figure 1. Theoretical He-like ion forbidden to intercombination line *R*-ratios (f/i) as a function of density (curves) overplotted with the observed line ratios from the *Chandra* spectrum of the young star TW Hya (points with 1σ error bars). As discussed in the text, the electron temperature and density are determined using accurate atomic data. Accretion shock models are in good agreement with the Ne XI and Mg XI densities and temperatures at the shock front. However, the models fail to match the observed O VII density, from Brickhouse *et al* (2010).

$\sim$500 km s^{-1} and the expected shock temperatures are around a few MK (Calvet and Gullbring 1998, Kastner *et al* 2002). High electron densities of $\sim 10^{13}$ cm^{-3} are also expected at the shock, assuming the ram pressure of the gas balances the stellar atmospheric pressure. Electron temperature and density diagnostics are available using He-like lines observed in x-ray spectra from O VII, Ne IX and Mg XI. However, atomic theoretical models of these diagnostic lines have only recently become accurate enough to test shock models (Chen *et al* 2006, Smith *et al* 2009). Applying the new atomic data to a long observation (500 ks) of TW Hya with the *Chandra X-ray Observatory* High Energy Transmission Grating, Brickhouse *et al* (2010) showed that the shock models work well at the shock front. But, again using accurate diagnostics, the standard model fails to describe the spectra of the post-shock cooling gas. In the standard model, the electron density increases as the shocked gas cools and recombines, but instead the opposite is observed: the observed density of the cooler O VII is lower than that of the hotter Ne IX by a factor of 4 (figure 1) and lower than the model prediction by a factor of 7. In contradiction to the post-shock models of cooling and 'settling' gas, the shock heats a significant mass of stellar atmosphere to soft x-ray emitting temperatures. This discovery has implications for coronal heating and wind driving in the presence of accretion.

2.1.2. Cometary x-ray emission. The discovery of x-ray and extreme ultraviolet emission from comet C/Hyakutake (Lisse *et al* 1996) was a great surprise. The subsequent identification of the emission mechanism as charge exchange with the highly charged ions of the solar wind (Cravens 1997, Krasnopolsky *et al* 1997) has led to tremendous progress in understanding the solar system (see Bhardwaj *et al* (2007)). High spectral resolution observations revealed the classic signature of charge exchange, namely dominant features from high angular momentum states and thus high principal quantum levels

(Kharchenko and Dalgarno 2000, Krasnopolsky and Mumma 2001, Lisse *et al* 2001). Calculations and experiments of charge exchange are now incorporated into x-ray studies of the interaction between the solar wind and planets, comets and the heliosphere. Cravens *et al* (2001) predicted that charge exchange of solar wind ions in the heliosphere and geocorona could produce half the soft x-ray background. The long-standing mystery of the soft x-ray background (and one of the key goals of *Chandra*) is now being solved: perhaps all or most of this background comes from charge exchange of the solar wind within the heliosphere (Koutroumpa *et al* 2006), with important implications for the interstellar environment surrounding the solar system. Experimental measurements continue to be important for quantitative analysis of charge exchange spectra (see, e.g., Beiersdorfer *et al* (2000), Greenwood *et al* (2000), Beiersdorfer *et al* (2003) and Otranto and Olson (2011)). Dennerl (2010) provides a good review of this field.

2.1.3. Exoplanetary discovery. Nearly 500 planets around other stars have been discovered to date using a variety of techniques, with many more expected from the *Kepler* mission (Borucki *et al* 2010). The ~100 exoplanets that transit their host stars are scientifically invaluable since both the mass and radius of the planet can be determined (see, e.g., Maxted *et al* (2010)). Transit searches involve two main stages: repeated photometric detection of transits of acceptable depth and duration, followed by spectroscopic confirmation. The first exoplanet discovered by the transit method exploited a detailed stellar atmosphere model of the star, cross-correlated with the observed spectra, in order to determine radial velocities (Konacki *et al* 2003, 2004, Sasselov 2003). This approach has now become a standard tool in the field, with many refinements added (Torres *et al* 2011). These atmosphere models incorporate an enormous database of atomic and molecular line transitions (Kurucz and Bell 1995, Castelli *et al* 1997). The precision in radial velocity that can be achieved depends strongly on the fraction of spectral lines in the model that match the observation; hence, ongoing efforts to improve the line lists go hand in hand with continuing discoveries in this field.

2.2. Molecular physics

2.2.1. Molecular clouds: diffuse interstellar bands. The diffuse interstellar absorption bands (DIBs) are ubiquitous absorption features observed in the line of sight to stars that are obscured by diffuse or translucent interstellar clouds. Close to 500 bands have been reported to date in local and extragalactic environments spanning from the near ultraviolet (UV) to the near infrared (IR) (Snow and McCall 2006). Various candidates have been proposed as carriers for the bands, ranging from impurity-doped dust grains, to molecules, to atoms. Today the DIBs are widely thought to be associated with carbon molecules and ions (polycyclic aromatic hydrocarbons (PAHs), carbon chains, fullerenes) that are part of an extended size distribution of interstellar dust (Sarre 2006, Snow and McCall 2006). Astronomers
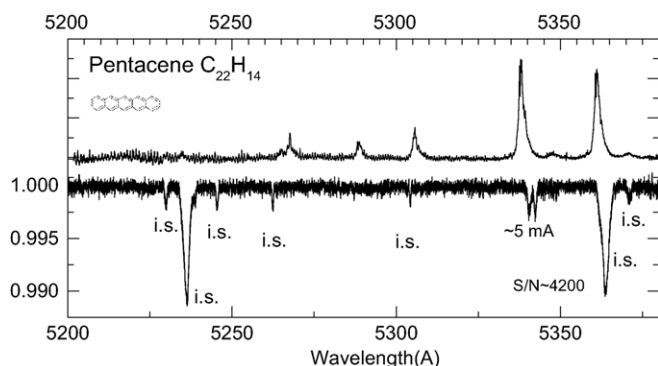
Figure 2. The top trace shows the (inverted) laboratory absorption spectrum (in arbitrary units) of the neutral PAH molecule pentacene ($C_{22}H_{14}$) prepared in a cold supersonic free jet expansion. The lower trace shows the average absorption spectrum of interstellar translucent clouds (in normalized flux units) providing, for the first time, accurate upper limits for the abundances of interstellar PAHs in the optical. S/N refers to signal-to-noise, i.s. to interstellar and 5 mÅ is the resolution (from Salama *et al* (2011)).

are very interested in the molecules that carry the DIBs, because these molecules may make up the largest cache of organic material in the universe. Recent advances in laboratory techniques have made it possible to measure the spectra of cold molecules and ions under conditions that are relevant to astrophysics (Salama 2008). As a result, accurate upper limits for the abundances of PAH molecules along the lines of sight of translucent clouds have been reported for the first time (Salama *et al* (2011), figure 2), while coincidences with naphthalene ($C_{10}H_8^+$) and anthracene ($C_{14}H_{10}^+$) cation bands have been tentatively reported for DIBs in the line-of-sight of Cernis 52 (BD +31 640), an early type reddened star behind the Perseus supernova remnant (SNR) that shows anomalous microwave emission (Iglesias-Groth *et al* 2008, 2010). A near coincidence between a DIB and a weak absorption feature of the diacetylene cation ($C_4H_2^+$) was also detected in the average spectrum of 11 reddened stars (Krełowski *et al* 2010), while a coincidence was tentatively reported between a weak DIB observed in the lines of sight of two objects and a band associated with propadienylidene (H_2C_3) by Maier *et al* (2011). All coincidences reported to date are tentative and point to hydrocarbon molecules.

2.2.2. Molecular clouds: molecular anions. Molecular anions were predicted many years ago to be abundant in the interstellar medium (ISM) (Sarre 1980, Herbst 1981). Subsequent chemical considerations by Terzieva and Herbst (2000) indicated that efficient electron attachment occurs once a carbon chain reaches six atoms. Molecular anions, however, have only recently been detected in space through a combination of spectroscopic laboratory measurements and observations of the molecular envelope of the star IRC+10216 and of the dense Taurus molecular cloud TMC-1 (McCarthy *et al* 2006). McCarthy *et al* (2006) showed that the unidentified harmonic sequence found by Kawaguchi *et al* (1995) in IRC+10216 was C_6H^-. The number of detected molecular anions has increased dramatically as a result of laboratory studies since then. These include C_4H^- in IRC+10216 by

Cernicharo *et al* (2007), C_8H^- in TMC-1 by Brünken *et al* (2007) and in IRC+10216 by Remijan *et al* (2007), CN^- in IRC+10216 (Agúndez *et al* 2010), and C_3N^- in the same object (Thaddeus *et al* 2008). Sakai *et al* (2010) detected C_4H^-, C_6H^- and C_8H^- in a starless core of a molecular cloud (Lupus-1A). This wealth of observational data has renewed interest in the effects of molecular anions on interstellar chemistry (see, e.g., Walsh *et al* (2009)).

2.2.3. Molecular clouds: polyaromatic hydrocarbons. These emission features, known as the unidentified infrared (UIR) bands, were first discovered by Gillet *et al* (1973) and attributed to ~10 Å size grains by Sellgren (1984). These UIR bands are now generally attributed to PAHs (see Salama (2008) and references therein). The features of this universal spectrum provide information on the physical conditions in the emitting regions and the nature of the molecular carriers. Puget and Léger (1989) and Allamandola *et al* (1989) have proposed a model dealing with the UIR interstellar emission features where PAHs are present as a mixture of radicals, ions and neutral species. The ionization states reflect the ionization balance of the medium while the size, composition and structure reflect the energetic and chemical history of the medium. The proposed excitation mechanism of the IR bands is a one-photon mechanism that leads to the transient heating of the PAHs by stellar photons. The IR emission bands are associated with the molecular vibrations of molecular PAH species (discrete bands) and larger carbonaceous grains (continuum-like structures). In this model, PAHs constitute the building blocks of interstellar carbonaceous dust grains and play an important role in mediating energetic and chemical processes in the ISM. However, exploitation of these features as astrophysical probes has been slow in developing because the IR properties of PAHs under interstellar conditions were largely unknown for at least 20 years after the bands were discovered. During the past two decades, advanced experimental and computational laboratory astrophysics programs have been developed to collect data to test and refine the PAH hypothesis. The information for hundreds of PAH molecular species is now compiled in databases that allow astronomers to quantitatively interpret their observations for a variety of environments in our local galaxy and in extragalactic environments (Malloci *et al* 2007, Bauschlicher *et al* 2010).

2.2.4. Dark interstellar clouds. The chemistry that occurs in dark interstellar clouds, and especially in the denser regions of such clouds known as cold cores, is an unusual one. Although organic molecules appear to grow in these regions, they are very unsaturated and consist mainly of bare carbon clusters, radicals of the C_nH and species with two hydrogen atoms, such as c-C_3H_2. This unusual pattern of growth exists despite the fact that molecular hydrogen is the dominant species in the gas and might be expected to hydrogenate the molecular species into more saturated forms. Although the basic mechanism for the growth of unsaturated species in these cold regions was worked out in the early 1970s (Watson 1973, Herbst and Klemperer 1973), the last ten years have

witnessed some very important laboratory work in rounding out the picture. Before then, it was thought that all organic neutrals are produced via syntheses based entirely on ion–molecule reactions, which synthesize precursor organic ions that do not react with H_2, but instead come apart following dissociative recombination reactions with electrons. This picture was incomplete because (a) there was little evidence concerning the actual products of dissociative recombination and (b) the growth of neutral species via reactions involving radicals and regular neutral species was not considered because it was assumed not to occur at low temperatures. Thanks to laboratory astrophysics, the picture has changed. The products of dissociative recombination have now been studied in the laboratory mainly by the use of storage rings in Denmark, Sweden and Germany (Geppert and Larsson 2008, Petrignani *et al* 2009) in which molecular ions can be cooled down before reaction with electrons. Rapid radical neutral reactions have been studied with Laval nozzles to temperatures down to near 10 K in laboratories in Rennes, France, and Birmingham, UK (Chastaing *et al* 2001, Sims 2006). Between these two sets of experiments, our knowledge of the chemical mechanism of molecular growth in cold clouds has become much more complete down to near 10 K.

2.2.5. Pre-stellar cores. Pre-stellar cores have begun the evolutionary journey to form low- and medium-mass stars. They have temperatures of around 10 K and a gas density of approximately $10^4 \, cm^{-3}$. At this stage, the collapse is isothermal because any heat developed is radiated away by atoms and molecules. The gaseous cores are dominated by hydrogen, helium and deuterium, as many, if not most, of the heavier molecules are depleted onto dust particles. For example, the abundance of CO drops precipitously toward the center of pre-stellar cores (Bacmann *et al* 2002, 2003). The evidence is not as clear cut for other heavy species but their low abundance is determined indirectly by detailed simulations of the deuterium fractionation chemistry, which show a huge fractionation effect in which deuterated isotopologues (e.g. H_2D^+) can be very abundant (Roberts *et al* 2004). Such a large effect can only occur in the near absence of heavy reactive species (Vastel *et al* 2006). The chemical simulations are based heavily on experimental measurements of rate coefficients involving deuterated species, such as those obtained in an ion trap (Schlemmer *et al* 2006). The extent of depletion of species such as CO is confirmed by measurements on the rate of desorption of this species from dust particles, which is not rapid enough to keep a large amount of material in the gas (Öberg *et al* 2009a).

2.2.6. Hot cores and corinos. Hot cores and corinos are warm objects (100–300 K) associated with low-mass protostars or young stellar objects of high mass. In these objects, the inventory of gas-phase organic molecules is quite different from what it is in cold interstellar clouds, where the molecules are mainly unsaturated (hydrogen-poor). Instead, in hot cores and corinos the organic molecules are much more terrestrial-like and consist of simple alcohols, esters, ethers and nitriles. For many years, it was thought that gas-phase reactions might

produce these molecules, but laboratory experiments (Horn *et al* 2004) show that some of the reactions suggested do not occur or are inefficient. A new school of thought has arisen that the molecules can be produced on the surfaces of dust particles and then desorbed or evaporated into the gas. Several suggestions were made including the production of organic molecules on cold grains, mainly via atomic addition reactions, and the production of these molecules via radical–radical association reactions during the actual heating up of a cold cloud into a hot core because of star formation (Herbst and van Dishoeck 2009). The production of radicals in this latter view comes from photon bombardment of simple surface species such as methanol, produced during the cold era (Garrod and Herbst 2006). Although laboratory experiments have not completely ruled out the idea that more complex species can be produced on cold surfaces, new experiments seem to confirm the radical–radical hypothesis (Öberg *et al* 2009b).

2.2.7. Protoplanetary disks. Protoplanetary disks are dense objects of gas and dust that rotate around newly formed low-mass stars and may be the precursors of solar-type systems. Astronomers have obtained both rotational and vibrational spectra of molecules in these disks and the molecular inventory is a strong function of how far the molecules lie from the central star and how high they lie off the midplane of the disk. The chemical models used to simulate the chemistry of these complex objects owe much to laboratory astrophysics. One recent success has been an understanding of how some CO can be in gaseous form at temperatures well below its sublimation point despite the high density of dust particles, which should guarantee that all CO should be in the form of ice mantles. Recent experiments on the photodesorption of CO indicate that the efficiency per photon of photodesorption for UV radiation is approximately 10^{-3}, which under the conditions of protoplanetary disks can explain why CO can be detected in the gas phase (Öberg *et al* 2009a, Hersant *et al* 2009). The recent detection of acetylene (C_2H_2) and HCN in hotter regions near the central star can be explained by chemical models that make use of numerous laboratory studies of reactions at temperatures much higher than 300 K (Agúndez *et al* 2008a, Harada *et al* 2010).

2.2.8. Metal hydride spectra of L and T type stars. Refractory hydrides such as FeH, CrH, CaH and MgH have recently been found to be abundant in the atmospheres of M, S and L sub-dwarf-type stars (Kirkpatrick 2005), as deduced from optical spectroscopy of these objects. In fact, the shift from prominent spectra of metal oxides to metal hydrides is dramatic in the transition from M type to L and T type sub-dwarfs (Burrows *et al* 2002). These brown sub-dwarfs, especially the L types, are extremely important for the understanding of planet formation, as they trace the intermediate stage between stars that undergo nucleosynthesis and those that do not, i.e. planets. Hydride spectra such as that of CrH are also excellent tracers of very cool stellar atmospheres (Burrows *et al* 2002) and may be an important key in identifying planets. None of this work would have occurred without laboratory spectroscopic measurements, conducted across a broad spectral range (see,

e.g., Harrison *et al* (2006)). Laboratory studies of CrH, for example, have been carried out using a variety of spectral techniques, including laser-induced florescence (Chowdhury *et al* 2005), Fourier transform infrared (FTIR) spectroscopy (Bauschlicher *et al* 2001) and millimeter/sub-mm direct absorption methods (Halfen and Ziurys 2004). Such hydrides are not stable under terrestrial conditions and must be created by unusual synthetic techniques involving laser ablation, hollow cathode sources and Broida-type ovens. Such work has provided not only wavelengths for spectral identification, but other important physical properties such as electronic state terms, energy levels and Einstein A coefficients, which are essential for astrophysical interpretation of stellar/planetary atmospheres (see, e.g., Burrows *et al* (2005)). Not all hydrides have been as well characterized as CrH, however, and much lab work needs to be done for species such as FeH and TiH.

2.2.9. Comets. Comets offer a unique opportunity to study organic astrochemistry, knowledge of which till recently has largely been obtained from remote astronomical observations and from laboratory simulations of the formation and evolution of organic molecules in various cosmically relevant environments. Comets are considered as the most primitive objects in the solar system. The composition and the structure of cometary nuclei contain a record of the primordial solar nebula at the time of their formation. Cometary nuclei are made of refractory solids and frozen volatiles. The composition of the volatile component is similar to that observed in dense molecular clouds reflecting the close relationship between cometary materials and interstellar icy grain mantles. Hence, in comets the composition of the volatile ices is largely dominated by H_2O ice (about 70–90%) while other major components include CO, CH_3OH, CO_2 and H_2CO (Salama 1998, Bockelée-Morvan *et al* 2004, Fink 2009).

Comets are also thought to have been a major source for the volatile ices on planetary bodies. Thus, cometary ices constitute a link between interstellar and solar system materials. The captured materials from sample return missions provide new insight into the formation of our solar system. The *Stardust* mission flew through the near-nucleus coma of comet 81P/Wild 2 on 2 January 2004, swept up material using aerogel collectors and returned these samples to the Earth on 15 January 2006. *Stardust* is the first space mission to bring back solid material from a known body other than the Moon. One of the key questions that the *Stardust* samples addressed is the origin of primitive organic matter in the solar system. After the recovery of the Sample Return Capsule, the returned material from *Stardust* was examined in the laboratory with the goal to determine the nature and amount of the returned samples (Brownlee *et al* 2006, Hörz *et al* 2006, Sandford *et al* 2006, McKeegan *et al* 2006, Keller *et al* 2006, Flynn *et al* 2006, Zolensky *et al* 2006).

Laboratory astrophysics played a crucial role in the optimization of the knowledge gained from the return of these extraterrestrial samples. An impressive battery of advanced laboratory astrophysics techniques was called upon to help decipher the information contained in the returned samples. The techniques involved transmission electron microscopy (TEM), Raman and FTIR spectroscopy, time of flight secondary ion mass spectrometry (TOF-SIMS) and scanning electron microscopy using energy-dispersive x-ray (SEM-EDX) analyses, among others. These laboratory studies show the highly heterogeneous nature of the collected cometary grains and reveal an interesting distribution of organic material, including the detection of amide, carboxy and alcohol/ether groups (see, e.g., Cody *et al* (2008) and Clemett *et al* (2010)) and the amino acid glycine (Elsila *et al* 2009). While concerns remain as to the organic purity of the aerogel collection medium and the thermal effects associated with hypervelocity capture, the majority of the observed organic species appear indigenous to the impacting particles and are hence of cometary origin. Additionally, though the aromatic fraction of the total organic matter present is believed to be small, it is notable in that it appears to be N rich. Spectral analyses in combination with instrumental detection sensitivities suggest that N is incorporated predominantly in the form of aromatic nitriles (R–CN) (Clemett *et al* 2010).

2.2.10. Exoplanetary atmospheres. In addition to mass and radius, other properties of an exoplanet (e.g. temperature and composition) can be determined using spectral changes during eclipses. Since the first thermal emission from an exoplanet was discovered (Charbonneau *et al* 2005, Deming *et al* 2005), a number of other firsts have been reported. One was the discovery of strong evidence for water vapor in the atmosphere of an exoplanet (Tinetti *et al* 2007). Signatures of water and carbon dioxide are now observed both in absorption and emission in a number of exoplanet atmospheres (Knutson *et al* 2008, Charbonneau *et al* 2008, Grillmair *et al* 2008). The measurement of temperature differences between the night-side and day-side of a tidally locked close-in hot Jupiter has emphasized the role of stellar radiation on the planetary atmosphere (Knutson *et al* 2007). While the composition of exoplanets at or above Jupiter in mass is not in doubt (they must be gas giants composed of hydrogen and helium), spectroscopy is needed to determine the composition of the smallest planets discovered to date (the so-called 'super-Earths'), since they may also be rocky (like the Earth) or icy. Near IR spectroscopy of one such super-Earth has ruled out hydrogen gas, unless there are thick clouds (Bean *et al* 2010). These observations are also consistent with the presence of hot water vapor (steam), in which case the planet might have an icy rather than rocky core. All these discoveries rely heavily on spectroscopic modeling of the stellar atmosphere (Hauschildt *et al* 2009), as well as the exoplanet atmosphere (Seager *et al* 2005, Miller-Ricci *et al* 2009, Kaltenegger and Sasselov 2010) and thus on the supporting laboratory astrophysics and atomic and molecular line data (Castelli and Kurucz 2004, Rothman *et al* 2005).

2.3. Condensed matter physics

2.3.1. Outer solar system ice. The connection between the ISM and solar systems profoundly influences our understanding of the birth and death cycles of stars in our Galaxy. Present models of star formation suppose that interstellar amorphous ice grains accreted to form the outer

rim of the solar system from Oort cloud to Kuiper belt objects (KBOs) (Jewitt 1999). Based on these models, outer solar system icy bodies with surface temperatures $<100\,$K form amorphous ices. At these temperatures amorphous ices remain stable over the lifetime of our star ($4.5 \times 10^9\,$yr). Galilean icy satellites like Europa at 5 AU with surface temperatures $\sim$120 K are crystalline. Beyond Jupiter, the rest of the outer solar system icy bodies have equilibrium surface temperatures $<100\,$K and hence are expected to contain amorphous ices. These are Saturnian icy moons and rings at 10 AU ($\sim$100 K), Uranian satellites around 20 AU, trans Uranian objects and KBOs ($\sim$50 K) at 40 AU from the Sun and the Oort cloud ($\sim$30 K) spanning up to several thousands of AU towards the local ISM.

Near IR spectroscopic studies carried out in the laboratory (Grundy and Schmitt 1998) revealed that amorphous ices show significantly different absorption features in this region compared with the crystalline ices, as shown in the lower part of figure 3. Recent spectrally resolved observations showed that the surface ices of trans Uranian icy bodies (Grundy *et al* 2006), trans Neptunian objects (TNOs) (Trujillo *et al* 2007, DeMeo *et al* 2010) and KBOs (Jewitt and Luu 2004) are significantly crystalline, based on comparison of these spectra with the laboratory data. Some recent models attribute the surface crystallinity to micrometeorite impacts (Porter *et al* 2010). This counter-intuitive observation, supported by laboratory data, has opened up a new chapter in our understanding of the evolution of icy bodies in the solar system and in the ISM.

Recently it has also been shown in the laboratory (Zheng *et al* 2009) that the crystallinity of ice at $>$50 K is not destroyed or altered to amorphous-like form by electron irradiation under conditions similar to those that exist on KBOs and comets originating from them. However, it is still unclear how the amorphous ice grains in the ISM are converted into the crystalline surface layer of KBOs and whether the subsurface of KBOs is amorphous or crystalline and hence the comets originating from them. More laboratory studies are needed in order to resolve this amorphous–crystalline puzzle that connects the ISM with the outer solar system.

2.3.2. Cometary ice, chemistry and the origins of life? One of the working postulates of the origins of life is that cometary impacts brought organic chemicals and water to the Earth (Whittet 1997, McClendon 1999, Matthews and Minard 2006). Comets are expected to retain the interstellar amorphous ice structure. Organic rich comets have been found to be highly porous (Richardson *et al* 2007, A'Hearn 2008). One of the outstanding questions is whether the delicate building blocks of life survived the comet impacts on Earth. With a very similar ice grain composition between comets (Crovisier *et al* 2004) and interstellar ice grains (Gibb *et al* 2004), these ices are dominated by H_2O, followed by CO_2, CO, methanol (CH_3OH), hydrocarbons, nitrogen-containing molecules (NH_3 and derivatives) and sulfur-containing molecules such as OCS, as well as minerals such as silicates. All these ingredients (H, C, N, O, S and minerals containing these elements) are essential for all forms of life on Earth as is also phosphorus (P), which is yet to be positively detected in comets. Laboratory

studies using the primitive molecules mentioned above and simulating the composition of comet and interstellar ice grains have shown that radiation processing of these ices indeed produced building blocks of life upon subsequent heating to evaporate ice (Dworkin *et al* 2001, Bernstein *et al* 2002, Deamer *et al* 2002, Muñoz Caro *et al* 2002, Elsila *et al* 2007, Nuevo *et al* 2009). These laboratory studies are critical, corroborating one of the possible origins of life on Earth.

Recent laboratory studies have also enhanced our understanding of the mechanisms involved in the radiation processing of organic molecules in ices that result in the formation of complex building blocks of life (Gudipati 2004, Gudipati and Allamandola 2004, 2006, Bouwman *et al* 2010). Using PAHs as probes embedded in ices, these laboratory studies have shown that radiation induced ionization of PAHs is an important first step, forming electron and PAH radical cation pairs in ice, which subsequently lead to the formation of oxidized PAHs. These laboratory studies have opened up a new understanding of chemistry in ices, involving charged species, bringing us one step closer to understanding how ices evolve under irradiation. Charged ice grains behave differently compared with their neutral counterparts due to strong long-range Coulomb forces. The implications of these studies to astrophysics and planetary sciences are slowly unfolding (Kalvans and Shmeld 2010).

2.4. Plasma physics

2.4.1. Accretion disks and magnetorotational instability. Accretion disks form in various astrophysical systems including young stars, protostars and some CVs. The accretion disk forms because the accreting matter brings substantial angular momentum, which must be transported away in order for the matter to move inward. Physical viscosity is far too small and it is generally believed that magnetohydrodynamic (MHD) turbulence is responsible for the angular momentum transport. At present, the leading candidate to drive such turbulence is magnetorotational instability (MRI) (Balbus and Hawley 1991, 1998), with the turbulence itself produced by secondary instabilities that convert the structures generated by the MRI into multiscale turbulent fluctuations (Pessah 2010, Pessah and Goodman 2009). A major challenge in coming to understand the MRI comes from the limitations of various approaches. Analytic and semi-analytic theories have made great progress (Julien and Knobloch 2010) but always struggle to define turbulent states. The astrophysical systems have very large *Re* and *Rm*, where *Re* is the usual viscous Reynolds number and *Rm* is the analogous magnetic Reynolds number, characterizing how slowly the magnetic structures are dissipated by resistive heating of the plasma. Numerical simulations cannot reach the astrophysical regime, being very limited in *Re* and having values of *Rm* that can be larger but remain limited. The past decade has seen laboratory experiments that reported observation of the MRI (Stefani *et al* 2006) and a helical variant (Sisan *et al* 2004). These experiments complement the simulations, having larger values of *Re* than the simulations can produce but smaller values of *Rm*. Experiments to date have been performed with a liquid

metal conducting fluid, a system well described by MHD theory. The combination of experiments, simulations and observations now provides a more complete set of information for theoretical work that seeks to identify the important scaling parameters and to provide a unified understanding of MRI across all regimes.

2.4.2. Young stellar objects: jet structure. Many open questions remain in the study of jets emanating from young stellar objects (YSOs) (Reipurth and Bally 2001). These non-relativistic beams of hypersonic plasma are likely magnetized and are known to cool effectively via radiation losses. Of particular interest for astrophysics are issues related to the internal jet structure. Are the hypersonic beams of plasma (hyperfast mode in the case of MHD jets) structurally smooth or inherently inhomogeneous?

Depending on the stability conditions of the jets this question speaks directly to the launch mechanisms of the jets as structurally smooth jets, implying time independent conditions at the central engine launching the jet. Recent observations using *Hubble Space Telescope* and other high-resolution platforms indicate that jets may contain significant sub-radial structure ($\delta x < r_{jet}$), which implies that jets may be inherently heterogeneous or 'clumpy' phenomena (Hartigan and Morse 2007, Hartigan *et al* 2011).

Recent experimental studies have attempted to explore this issue by developing platforms that can create steady jet beams as a starting point for further work. Of particular note have been the pulsed power studies of Lebedev *et al* (2002) who were able to develop stable hypersonic radiative jets. These jets have high Mach numbers ($M \sim 20$) and have been shown to propagate without disruption over long distances, achieving aspect ratios of 10 or more. Shorter duration jets have also been produced in a number of studies (Foster *et al* 2005). In some cases these experimental platforms have allowed researchers to explore the interaction of jets with large-scale obstacles (Hartigan *et al* 2009). This is an astrophysically relevant issue as jets from young stars are observed, in some cases, to be deflected by clumps or clouds in their path. Deflection of jets by winds induced by the motion of the jet source through a background has also been observed and this process has been studied in the laboratory as well (Lebedev *et al* 2004).

Thus experimental studies to date have shown that stable hypersonic jets can propagate over long distances and that even when interacting with side winds the jets are not fully disrupted. Future studies should focus on the generation and propagation of 'clumps' within the beams.

2.4.3. Young stellar objects: magnetized jets. Astrophysical jets are believed to form via a combination of accretion, rotation and magnetic fields (Pudritz *et al* 2007). The central engine may be a star, a compact object like a black hole or surrounding accretion disk. YSO jets are also believed to form via magnetized accretion disks and many open issues remain concerning both the magneto-centrifugal launch processes and the propagation of the magnetized jet at large distances from the central engine. In general theorists expect the fields to be

strong to moderate as characterized by the plasma beta which is the ratio of gas (g) to magnetic (B) pressures $\beta = P_g/P_B \leqslant 1$.

Using a planar magnetized coaxial plasma gun, Bellan (2005) and Bellan *et al* (2005) have developed a platform to study MHD jet launching. The premise behind the experiments is that the basic magnetic dynamics near a star-disk system, namely the winding up of poloidal field lines generated by the central disk+star rotation, can be simulated in the laboratory by applying a voltage across coaxial electrodes in the presence of a background colloidal field. The magnetic helicity injection with these boundary conditions leads naturally to collimated unstable plasmas whose dynamics may be indicative of disk-driven jets and plasmoids.

A second approach to the study of magnetized YSO jets comes from experiments using radial plasma sources, which consist of a pair of concentric electrodes connected radially by thin metallic wires or a thin foil (Lebedev *et al* 2005, Ciardi *et al* 2009). Resistive heating of the wires or foil produces a plasma. If wires are used, when they break, toroidal flux from below drives a magnetic bubble ($\beta < 1$) and a collimated jet forms on the axis. The jet goes unstable due to kink modes and evolves into a series of hypersonic clumps. When a foil disk is used, the process becomes episodic with a series of magnetic bubbles and jets forming one after the other.

Laboratory studies of magnetized jets relevant to YSOs have offered a new window into the three-dimensional (3D) dynamics of magnetized plasma systems. Helicity injection and kink mode instabilities have been followed in ways that already demonstrate new pathways of jet evolution not previously considered in analytic or computational studies.

2.4.4. Young stellar objects: radiative jets. Along with magnetic fields, radiative cooling is another important process occurring in YSO jets. In this context radiative cooling means that optically thin emission from shock excited atoms and ions will carry away a significant amount of energy from the system. Systems are radiatively cooling when the timescale for energy loss ($t_{cool} = e/\dot{e}$) is less than the characteristic hydrodynamic timescale ($t_h = L/c$) where e, $\dot{e}$, L and c are thermal energy, thermal energy loss rate, system scale and speed of sound, respectively. As has been shown in numerous studies, radiative cooling will produce dramatic differences in the evolution of jet systems compared with adiabatic flows (Blondin *et al* 1990). In particular, the collapse of bow shocks onto the jet body will occur when thermal pressure generated at the shock is removed via the radiative cooling. Resolution issues hamper numerical simulations of jet dynamics with radiative cooling. A detailed understanding of instabilities at cooling bow shocks, for example, has not yet been achieved.

Experiments have produced radiative jets by creating radially imploding plasmas having an axial velocity component. In early work lasers were used to irradiate conically shaped targets (Farley *et al* 1999). Work using wire arrays (Lebedev *et al* 2002) created stagnation of plasma flow on the axis of symmetry, forming a standing conical shock effectively collimating the flow in the axial direction. This scenario is essentially similar to that discussed by Canto *et al* (1988) as a purely hydrodynamic mechanism for jet formation

in astrophysical systems. In both types of experiments, the diameter of the jet decreased with increasing atomic number, providing direct evidence of radiative cooling. In a more recent experiment, a ring-shaped laser spot was employed to produce an imploding Cu plasma, generating a jet that penetrated into adjacent gas (Tikhonchuk *et al* 2008). Analysis showed the experimental parameters to be rigorously well scaled to astrophysical cases. Structure was seen in the shocked ambient medium, providing evidence relevant to the instabilities at cooling bow shocks.

Thus experiments have produced radiative hypersonic jets in laboratory settings, allowing existing theories of jet dynamics to be explored and opening up new domains of investigation beyond the reach of existing analytic methods and simulations.

2.4.5. Hydrodynamic stability of protoplanetary accretion disks. It is widely accepted that MRI plays an important role in generating turbulence that transports angular momentum outward in accretion disks (Balbus and Hawley 1998). The electrical conductivity of portions of protoplanetary disks is thought to be so low, however, that the magnetic field is not well coupled and that MRI cannot operate. It was proposed that hydrodynamic Keplerian flow can be unstable to finite amplitude perturbations and that this could lead to angular momentum transport. Recent laboratory experiments of hydrodynamic Keplerian flow between two cylinders have found no evidence of such an instability, up to Reynolds numbers of 2×10^6 (Ji *et al* 2006, Schartman *et al* 2011). This negative result weighs against instability of Keplerian flow as an angular momentum transport mechanism in accretion disks and encourages us to look for other mechanisms.

2.4.6. Equation of state for planetary interiors. Present-day observations of planets can determine only their mass, size and perhaps surface composition. One wants to know much more such as the structure of the planet, the properties of the interior matter and whether gas-giant planets required an ice and rock core to nucleate their formation. One seeks a self-consistent model in which the local density at some radius is determined by the materials present and the local pressure, while the integrated density profile within the observed planetary radius corresponds to the mass of the planet (see the recent review by Fortney and Nettelmann (2010)).

The relations between density, pressure and other thermodynamic quantities are the equations of state (EOS). For the specific case of Jupiter, Saumon and Guillot (2004) have shown that the uncertainties in the EOS are the dominant limitation to understanding the structure of the planet. Laboratory measurements are essential to advance this field; the relevant EOS theory is difficult, both intrinsically and with regard to choosing appropriate assumptions. The first two first-principles models, using very similar methods, implied different amounts and distributions of heavy elements in Jupiter (Fortney *et al* 2009). Laboratory data have been used to adjust other EOS models (Fortney and Nettelmann 2010) and researchers are actively acquiring more data (Eggert *et al* 2008, Hicks *et al* 2009).

Figure 4 shows a comparison of state-of-the-art data and theory for the pressure and density produced by a strong shock wave in cryogenic He after compression to some initial density (adapted from Fortney *et al* (2009)). The theory curves were produced by first-principles calculations using a combination of path-integral-Monte-Carlo and density-functional-theory, molecular-dynamics calculations (Militzer 2009). The data points were inferred from direct measurements of shock velocity in He and in quartz, using standard techniques (Eggert *et al* 2008). There is reasonable agreement between data and theory for high pre-compressions, but not for low pre-compressions. This indicates that more work is needed to fully understand the compression of He.

Further advances are needed in order to obtain a fully validated account of the properties of He at relevant densities and pressures. Progress in these areas will complement improved measurements of the abundance of oxygen and of the detailed gravitational field structure by the *Juno* orbiter (Bolton 2006). Other space missions will identify hundreds of additional Neptune-like to Jupiter-like planets. EOS research during the last decade has provided data that constrain planetary models and demonstrated methods that will produce further data going forward.

3. Stars and stellar evolution

Stars and stellar evolution covers 'the Sun as a star, stellar astrophysics, the structure and evolution of single and multiple stars, compact objects, supernovae, gamma-ray bursts, solar neutrinos and extreme physics on stellar scales' (Blandford *et al* 2010a).

3.1. Atomic physics

3.1.1. Solar and stellar abundances of rare earth elements. Accurate heavy-element abundances have recently been determined for the rare earth elements in the Sun and in old, metal-poor Galactic halo stars. These abundances provide insight into the nature of the earliest stellar generations and element formation in the Galaxy. The updated values are the result of extensive new laboratory data for atomic transition probabilities. Data have been published for numerous spectra including La II (Lawler *et al* 2001a), Ce II (Palmeri *et al* 2000, Lawler *et al* 2009), Pr II (Ivarsson *et al* 2001), Nd II (den Hartog *et al* 2003), Sm II (Xu *et al* 2003, Lawler *et al* 2007), Eu I, II and III (den Hartog *et al* 2002, Lawler *et al* 2001c), Gd II (den Hartog *et al* 2006), Tb II (den Hartog *et al* 2001, Lawler *et al* 2001b), Dy I and II (Curry *et al* 1997, Wickliffe *et al* 2000), Ho I and II (den Hartog *et al* 1999, Lawler *et al* 2004), Er II (Lawler *et al* 2008a,2008b), Tm I and II (Anderson *et al* 1996, Wickliffe and Lawler 1997), Lu I, II, and III (den Hartog *et al* 1998, Quinet *et al* 1999, Fedchak *et al* 2000), Hf II (Lawler *et al* 2007), Os I and Ir I (Ivarsson *et al* 2003), Pt I (den Hartog *et al* 2005), Th II and III (Biémont *et al* 2002, Nilsson *et al* 2002b) and U II (Lundberg *et al* 2001, Nilsson *et al* 2002a).

These new transition probabilities have culminated in more precise solar and stellar abundances of Pr, Dy, Tm, Yb and Lu (Sneden *et al* 2009). As a result, it is now
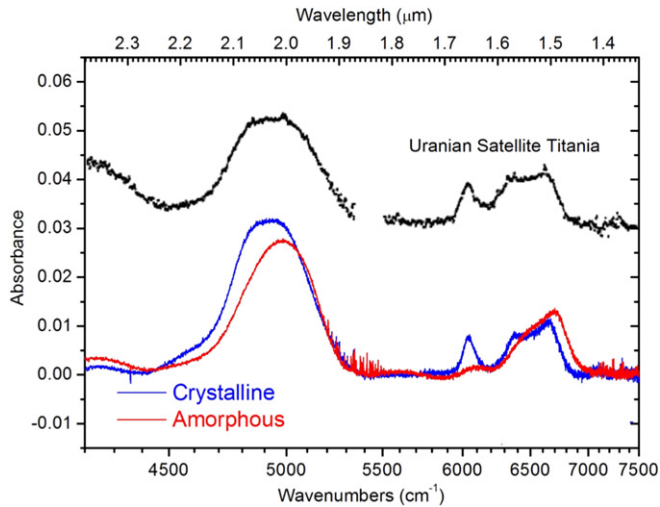
Figure 3. Observed near IR (black) of the Uranian satellite Titania (Grundy *et al* 2006), compared with the laboratory spectra of amorphous (red) and crystalline (blue) water ice at 10 K (courtesy of M Gudipati, private communication, and in excellent agreement with the published results of Grundy and Schmitt (1998) and Mastrapa and Brown (2006)). The absorption around 6000 cm^{-1} (1.65 μm) is the most prominent feature of the crystalline ice that is not present in amorphous ices. Other subtle spectral differences can also be seen in the laboratory spectra.

conclusively demonstrated that the abundance pattern for the heaviest elements in the oldest metal-poor halo stars is consistent with the relative solar system abundances for rapid neutron capture (r-process) only elements. This indicates that the r-process that operated in the early Galaxy, soon after the first stars formed, must share some common features with—and perhaps is identical to—the r-process that operates now. Thus, the star-to-star relative abundances of these elements should be the same and also consistent with the solar system values. This can be seen in figure 5 where the abundances of three metal-poor halo stars (CS 22892-052, BD +17 3248 and HD 115444) are compared with meteoritic and solar system r-process abundances (den Hartog *et al* 2006, Sneden *et al* 2008). Additional elements have been measured since the publication of that figure and the abundance analyses have now been extended to more stars (see, e.g., Sneden *et al* (2009)).

3.1.2. The solar abundance problem. Three-dimensional, time-dependent, hydrodynamical solar atmosphere models are a remarkable computational achievement of the past decade. These models require significantly lower abundances of C, N, O and Ne to match photospheric spectra (Asplund *et al* 2004), compared with previous results based on one-dimensional, static non-local-thermodynamic-equilibrium (non-LTE) models (see, e.g., Vernazza *et al* (1976)). However, the new abundances do not agree with helioseismology observations (Bahcall *et al* 2005a). Christensen-Dalsgaard *et al* (2009) and others have suggested that increased opacity could bring the helioseismology models back into agreement with observations, but that would require about a 30% increase in atomic abundances at the base of the convection zone and a few percent in the solar core.
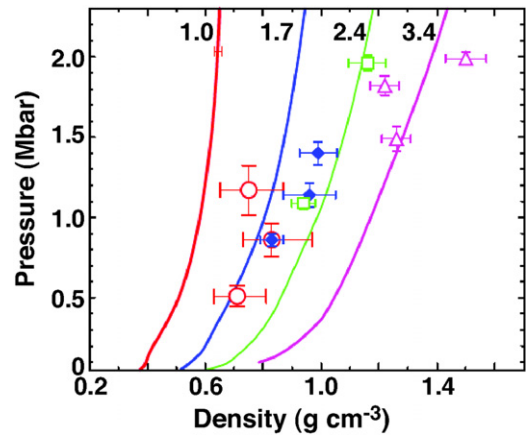

Figure 4. Equation of state data and theory for He. The He is first precompressed, in a diamond-anvil cell, by the factor that labels each curve and then is shocked to high pressure, which allows one to access densities and pressures relevant to gas-giant planets. The density of the He before precompression is the zero-pressure density of cryogenic He (0.123 g cm^{-3}). This figure, adapted from Fortney *et al* (2009), shows experimental data from Eggert *et al* (2008) and first-principles theory from Militzer (2009).
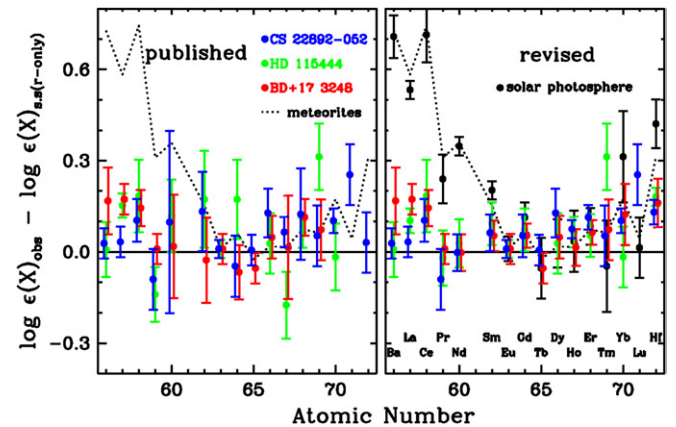

Figure 5. The observed abundances $\epsilon(X)_{\rm obs}$ relative to the solar system r-process only abundances $\epsilon(X)_{\rm s.s.(r-only)}$ as a function of atomic number for element X. The left panel results are based upon older published atomic data. A large scatter is readily apparent from star-to-star and with respect to the dashed horizontal line, representing the solar system r-process only line (normalized to the element Eu). The right panel shows the relative abundances with the newly determined laboratory data (labeled 'revised'). For those elements discussed in section 3.1.1 with new atomic data, the star-to-star scatter has largely disappeared and the new abundances are also consistent with the solar r-process only abundances. Adapted from den Hartog *et al* (2006) and Sneden *et al* (2008).

The convergence of various opacity calculations over the past decade (including large contributions from atomic theory and experiment) is a considerable success and thus an opacity increase as large as 30% may not be reasonable (Christensen-Dalsgaard *et al* 2009). Furthermore, new Z-pinch experimental tests of the iron opacity, under conditions approximating the base of the solar convection zone, show good agreement with the most recent and advanced opacity models (see section 3.4.4; Bailey *et al* (2007) and Mancini *et al* (2009)). Additional experiments are needed to test the opacity models under other relevant physical conditions (see Bailey *et al*

(2009)). For now, opacities alone do not appear to resolve all the problems fitting helioseismology data and the solution may well lie elsewhere, such as in the EOS (Lin *et al* 2007, Basu 2010).

3.1.3. The solar corona. Despite decades of research, we still do not understand how the temperature of the solar atmosphere rises from ∼6000 K at the photosphere to more than 10^6 K in the corona. Fe XVII is an important system for studying the corona, producing some of the strongest lines seen. It is formed near the peak temperatures of active regions and emits a number of useful diagnostic line ratios for temperature, density and opacity. Resonant line scattering in the strongest solar coronal x-ray line (Fe XVII 3d $^1P_1$ to ground $^1S_0$, known as 3C) has long been thought to contribute to its observed weakness relative to the nearby Fe XVII 3d $^3D_1$ to $^1S_0$ line (known as 3D). Even at a relatively low optical depth, resonant line scattering could in principle also account for morphological effects in images of loop structures (Wood and Raymond 2000). If this were the case, efforts to increase spatial resolution of solar coronal imaging instruments to ∼0.1 arcsec might not be worthwhile. Theoretical calculations of the 3C/3D line ratio have until recently been significantly larger than any of the solar observations. Over the past decade a number of experimental measurements (Brown *et al* 1998, Laming *et al* 2000, Brown *et al* 2001, Gillaspy *et al* 2011) and ongoing theoretical work (see, e.g., Doron and Behar (2002), Loch *et al* (2006) and Chen (2008)) have produced convergence on the appropriate line ratio for comparison with observations. With the Fe XVII 3C/3D line ratios on solid ground, Brickhouse and Schmelz (2006) showed that the solar x-ray corona is optically thin in Fe XVII 3C and, by extension, in all the coronal lines. The blurring seen in some images (e.g., Fe XV from the *Transition Region and Coronal Explorer* (*TRACE*) satellite) is thus the result of unresolved spatial structure near the peak temperature. Efforts to observe the solar corona at still higher spatial resolution are thus warranted.

3.1.4. O star winds. Advances in our understanding of the elemental evolution of the cosmos has come about from spectroscopic observations of O stars carried out using *Chandra* and the *X-ray Multi-Mirror Mission-Newton* (*XMM-Newton*) coupled with new laboratory astrophysics data. The powerful radiatively driven winds of O stars are important sources of chemical enrichment in the universe. Recent analyses of UV P Cygni profiles and x-ray emission line profiles have been used to determine mass loss rates (Fullerton *et al* 2006, Cohen *et al* 2010). These studies used the best available wavelengths (accurate to a few mÅ) and a relatively complete database of important x-ray emission lines coupled with data on relative line strengths in coronal plasmas, in order to accurately account for blended complexes of Doppler broadened emission lines. The mass loss rate from O stars was found to be a factor of 3–6 less than previously thought (Cohen *et al* 2010), a result deriving from recent improvements in atomic data from laboratory and theoretical calculations. This changes our understanding of chemical enrichment of galaxies, especially during their early starburst phase.

3.1.5. Type Ia supernovae. Type Ia supernovae (SNe) are used as standard candles to study dark energy and the expansion of the universe. *Chandra* and *XMM-Newton* x-ray observations of young supernova remnants (SNRs) have deepened our understanding of these standard candles. X-ray observations of young SNRs in the Milky Way and the Magellanic Clouds offer a detailed view of Type Ia supernova (SN) ejecta and provide invaluable constraints on the physics of these explosions and the identity of their progenitor systems. Utilizing public domain atomic data, it is now possible to model this x-ray emission and distinguish SNRs resulting from bright and dim Type Ia SNe. This technique has been validated by the detection and spectroscopy of SN light echoes for the Tycho SNR (Badenes *et al* 2006, Krause *et al* 2008) and SNR 0509-67.5 in the Large Magellanic Cloud (LMC) (Badenes *et al* 2008a, Rest *et al* 2008). A key advantage of these x-ray studies of nearby SNRs over optical studies of extragalactic SNe is that the SNRs are close enough to examine the circumstellar medium sculpted by the progenitor systems (e.g., the Kepler SNR, Reynolds *et al* (2007)) and also to study the resolved stellar populations associated with them (Badenes *et al* 2009). Recent x-ray spectroscopic observations have also discovered emission from Mn and Cr in young Type Ia SNRs which can be used to measure the metallicity of the progenitor system (Badenes *et al* 2008b), one of the key variables that might affect the cosmological use of Type Ia SNe and which cannot be determined for extragalactic SNe.

3.2. Molecular physics

3.2.1. Evolved star envelopes: characterizing gas and dust chemistry. Mass loss from evolved stars (asymptotic giant branch (AGB), red giants and supergiants) contributes about 85% of the material to the ISM (Dorschner and Henning 1995). Such mass loss creates large envelopes of dust and gas surrounding the central star, extending to ∼1000 stellar radii. Establishing the chemical content of stellar envelopes is important in evaluating the overall composition of the ISM. These envelopes can either be oxygen-rich (O > C) or carbon-rich (C > O). Such shells also have large temperature and density gradients (see, e.g., Ziurys (2006), Kim *et al* (2010), Maercker *et al* (2008), Patel *et al* (2011), Tenenbaum *et al* (2010a), Polehampton *et al* (2010) and Schoier *et al* (2011)). Close to the stellar photosphere, chemical species, as well as dust condensates, form under thermodynamic equilibrium. As the material flows from the photosphere, abundances become 'frozen-out', but then are altered by photochemistry at the shell edge (see, e.g., Cordiner and Millar (2009)). Circumstellar envelopes are consequently unusual chemical factories. The C-rich shell of the AGB star IRC + 10216, for example, has been found to contain over 70 different chemical compounds (Ziurys 2006, Agúndez *et al* 2008b, Tenenbaum *et al* 2010a, 2010b). Oxygen-rich stars also have complex chemistries, as observations of the envelope of VY Canis Majoris have demonstrated (Tenenbaum *et al* 2010a, 2010b). The chemical richness of circumstellar envelopes is illustrated in figure 6. Here composite spectra of the envelopes of IRC + 01216 and VY Canis Majoris are shown at 1 mm in wavelength.
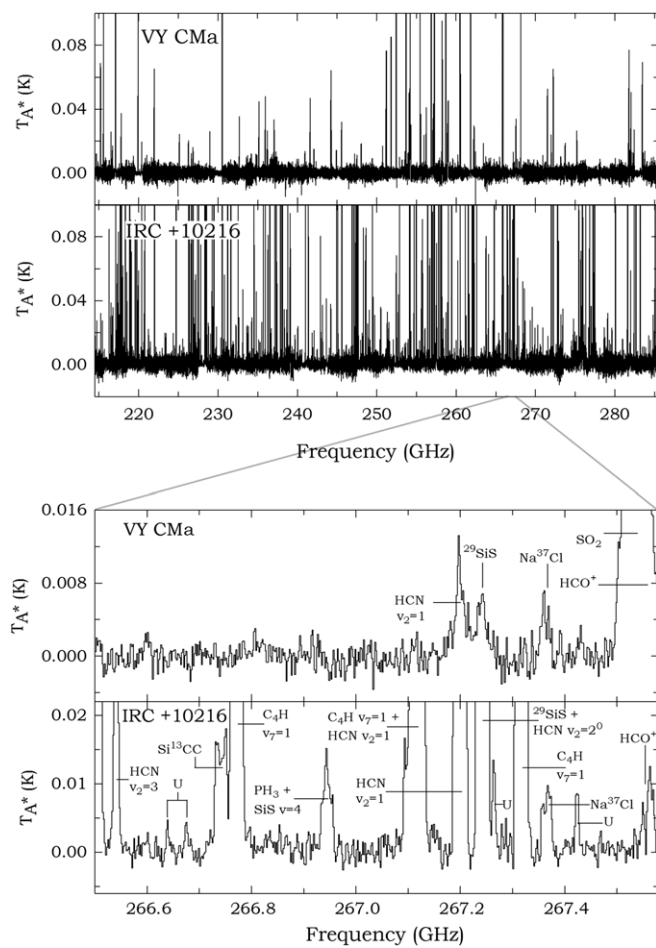
Figure 6. The composite spectra of VY CMa and IRC + 10216 across the entire 214.5–285.5 GHz frequency region, showing the rich chemical complexity of both sources (Tenenbaum *et al* 2010a). The intensity scale is the same for both sources and has been truncated to show the weaker lines. The inset panel displays a select 1 GHz section, centered at 267 GHz. The inset panel highlights some of the molecular identifications such as HCN $v_2 = 1^{1d} (J = 3 \to 2)$, ^{29}SiS $(J = 15 \to 14)$, Na^{37}Cl $(J = 21 \to 20)$ and HCO$^+$ $(J = 3 \to 2)$. The IRC+10216 spectrum at 267 GHz shows a tentative line of PH$_3$ and various other vibrationally excited HCN features. Without laboratory spectroscopic studies, not a single line in these spectra could be securely identified.

Most circumstellar species have been detected on the basis of their pure rotational spectra, which occur at millimeter and sub-mm wavelengths. IR spectra have also been important for species with no dipole moments, such as HCCH. The input of laboratory spectroscopy, which supplies the critical 'rest frequencies' for line identification, has been crucial in this regard. Recent examples include the identification of negative ions, such as C$_4$H$^-$ and C$_3$N$^-$ (Thaddeus *et al* 2008) and KCN (Pulliam *et al* 2010).

3.2.2. Evolved star envelopes: refractory-element-bearing species. Condensation models predict that dust in circumstellar shells take on a variety of forms, depending on whether the environment is oxygen or carbon-rich (Lodders and Fegley 1999). Almost all the refractory elements (Si, P and metals) are predicted to be in some sort of mineral grain.

In C-rich shells, silicon is contained primarily in SiC, but in O-rich objects in oxide condensates. Phosphorus is thought to be in the form of schreibersite, (Fe, Ni)$_3$P. Magnesium is contained in silicon and aluminum oxides in O-rich shells and primarily in MgS in C-rich shells.

Refractory elements in circumstellar environments are not all contained in dust grains, however, as millimeter observations have clearly shown. Nine molecules have been found in circumstellar shells that contain silicon and eleven that contain metals, in the chemist's sense. In C-rich envelopes, the metals are either found in halides (NaCl, KCl, AlF and AlCl) or metal cyanides (MgCN, AlNC, MgNC, KCN and NaCN; Pulliam *et al* 2010); in oxygen-rich shells, oxides and hydroxides such as AlO and AlOH dominate (Tenenbaum and Ziurys 2010). Aluminum is thought to be condensed into Al$_2$O$_3$ in O-rich stars (Lodders 2003). The presence of AlO and AlOH indicates that photospheric shocks are likely disrupting grains.

In addition, phosphorus-containing molecules appear to be prevalent in circumstellar shells, as evidenced by the recent discoveries of CCP, PN, HCP, PO and, tentatively, PH$_3$ (see, e.g., Agúndez *et al* (2007), Tenenbaum *et al* (2007), Milam *et al* (2008) and Tenenbaum and Ziurys (2008)). Phosphorus is an important biogenic element and has consequences for the origin of life. Until very recently, few molecules containing this relatively rare element have been observed in the ISM.

Gas-phase, high-resolution, laboratory spectroscopy has been absolutely crucial in establishing the presence of metal and phosphorus-bearing species in circumstellar gas. Recent discoveries, such as CCP or AlOH, have relied on such work, in particular those employing millimeter direct absorption and Fourier transform microwave methods (see, e.g., Apponi *et al* (1993) and Halfen *et al* (2009)). Many potential species of this type are highly reactive, and require unusual, non-equilibrium synthesis methods.

3.2.3. Evolved star envelopes: contributions to the ISM. The matter lost from evolved stars becomes part of the ISM via planetary nebulae. It has usually been assumed that the molecular content of circumstellar shells is returned to the atomic state as the central star becomes a strong UV emitter, defining the planetary nebula stage. Yet, observations toward the Helix Nebula, which is 10 000 years old, have demonstrated that CO is present in a large clumpy shell surrounding the central star and that HCO$^+$, HCN, HNC and CN exist as well (Bachiller *et al* 1997, Young *et al* 1999). Studies conducted recently by Tenenbaum *et al* (2009) have resulted in the detection of CCH, C$_3$H$_2$ and H$_2$CO in the Helix. Furthermore, mapping of HCO$^+$ and H$_2$CO in the Helix suggests that these species are as widespread as CO (Zack *et al* 2012). All of these molecules have been studied via their mm rotational spectra. Higher energy transitions are likely to be found in these regions; recent laboratory spectroscopy (see, e.g., Lattanzi *et al* (2007)) will make such studies possible.

The discovery of complex molecules in old planetary nebulae is surprising; such species have been subjected to intense UV radiation for thousands of years. Theoretical calculations have shown that instabilities in the stellar wind

can create finger-like clumps with densities as high as 10^5 cm^{-3} (Redman *et al* 2003). *Spitzer Space Telescope* IR images show the presence of finger-like dust structures in the Helix (Hora *et al* 2006). Such clumps, composed of gas-phase molecules mixed with dust, become self-shielding. It could be that these clumps survive on sufficient timescales to bring molecular material to the diffuse ISM. Recent observations by Liszt and collaborators (see, e.g., Liszt *et al* (2006)) have demonstrated that polyatomic molecules such as H_2CO, HCO^+ and C_3H_2 are abundant in diffuse clouds.

The cycling of molecular material in the ISM has yet to be fully evaluated. Without knowledge of the gas-phase rotational spectra, our understanding of the molecular ISM would be negligible (Ziurys 2006). Furthermore, such spectra could not be interpreted without additional laboratory measurements or theoretical calculations. Knowledge of dipole moments, transition strengths, Einstein coefficients and energy levels are essential in the analysis of molecular data. Collisional cross-sections, photodestruction rates and radiative absorption cross-sections are also important. When combined, all these data enable detailed interpretation of gas-phase molecular spectra, producing a clearer picture of the nature of the dense ISM.

3.2.4. Evolved stellar envelopes: fullerenes. Fullerene molecules such as C_{60} and C_{70} have been prime observational targets ever since their discovery in laboratory experiments designed to simulate the chemistry of carbon star outflows (Kroto *et al* 1985). However it is only recently that observations with *Spitzer* have revealed for the first time the spectroscopic signatures of C_{60} and C_{70} in a variety of astronomical environments. The detections would not have been possible without spectroscopic data from laboratory measurements (Krätschmer *et al* 1990, Frum *et al* 1991, Martin *et al* 1993, Nemes *et al* 1994, Fabian 1996, Sogoshi *et al* 2000). The laboratory data provided the wavelengths and line strengths to confirm the astronomical detections.

C_{60} and C_{70} were first detected in a hydrogen-poor planetary nebula (Cami *et al* 2010). The hydrogen-poor conditions were thought to be necessary in light of laboratory measurements on fullerene production (De Vries *et al* 1993, Wang *et al* 1995). Other *Spitzer* observations reveal the presence of C_{60} in the reflection nebulae NGC 7023 and NGC 2023 (Sellgren *et al* 2010) and in planetary nebulae in our Galaxy and the Small Magellanic Cloud (SMC) (García-Hernández *et al* 2010). The latter work shows that the fullerenes are present in a variety of environments, including hydrogen-rich ones. García-Hernández *et al* (2010) suggest that the photochemistry of hydrogenated amorphous carbon plays a key role.

3.3. Condensed matter physics

3.3.1. Carbonaceous dust in outflows of late-type stars. Cosmic dust particles span a continuous size distribution from large molecules to μm-sized particles and play an essential role in the evolution of the ISM (Tielens 2005). Carbonaceous dust particles are primarily formed in the outflow of carbon stars, through a combustion-like process where small carbon

chains form PAHs that nucleate into larger-size PAHs and, ultimately, into nanoparticles (Henning and Salama 1998). According to this model, nucleation occurs for temperatures above 2000 K, followed by the growth of amorphous carbon on the condensation nuclei in the 1500 K temperature range. As the temperature falls to around 1100 K, aromatic molecules begin to form in the gas phase and condense onto the growing particles forming graphitic microstructures that will ultimately aggregate into larger structures such as seen in soot formation (Pascoli and Polleux 2000). Very little was known until recently about the formation of cosmic dust due to the difficulty of forming and isolating these large species and in tracking their evolutionary path under realistic astrophysical laboratory conditions. Much effort has been made in this direction leading to new laboratory tools and breakthrough results (Jager *et al* 2007, Ricketts *et al* 2011). Carbon pyrolysis and plasma-induced combustion experiments on mixtures of small hydrocarbons indicate that the product distribution is dominated by PAHs and partially hydrogenated PAHs. The condensates produced in the experiments consist of soot particles with graphene layers and PAHs. The formation process starts with small molecules recombining to form aromatic benzene rings, followed by the growth of larger PAHs through subsequent C_2 addition to the aromatic rings and the final growth of grains by the condensation of large PAHs on the surfaces of the nuclei. These results demonstrate that low-temperature condensation is a very likely formation process of soot and PAHs in AGB stars, confirming the model predictions.

3.3.2. Silicates in envelopes of late-type stars. Silicates are an important component of cosmic matter. Silicates form in the winds of AGB stars and are processed in the diffuse ISM. They are also an important component of dust in protoplanetary and debris disks where they help regulate thermal exchanges (Henning 2010). The detection at IR and millimeter wavelengths of silicate dust grains containing O, Si, Fe and Mg, as well as some Ca and Al, provides an important constraint on dust chemical composition and on grain size (Bouwman *et al* 2001, van Boekel *et al* 2005, Chiar and Tielens 2006, Sargent *et al* 2009, Juhasz *et al* 2009). Cosmic silicates are mostly found in the amorphous state, characterized by broad and structureless IR bands at 10 and 18 μm that can be attributed to Si–O stretching and O–Si–O bending modes, respectively (Draine 2003). In circumstellar environments, however, evidence for crystalline silicates is found both around (post-)AGB stars and in disks around Herbig Ae/Be stars, T Tauri stars and brown dwarfs (Henning 2010, Molster and Waters 2003). Silicates are also found in cometary environments (Crovisier *et al* 1997, Kelley and Wooden 2009, Hanner and Zolensky 2010), in spectra from asteroids (Emery *et al* 2006) and in interplanetary dust particles (Bradley 2010). These findings have only been possible thanks to vigorous laboratory programs that have helped characterize the basic properties of silicates that are needed to detect their signature in astronomical spectra. A vast amount of data resulting from laboratory studies dealing with both amorphous and crystalline silicates is now available in the literature, making it possible to derive information on topics as diverse as the evolution of

cosmic dust, transport in protoplanetary and debris disks and redshifts in high-*z* objects (for recent reviews see Henning (2010) and references therein).

3.4. Plasma physics

3.4.1. Ion heating in the solar corona and solar wind. UV spectroscopy of the solar corona has revealed that ion temperatures vary among species and that ion distribution functions are non-Maxwellian and anisotropic. These effects are most pronounced in certain minor ions and in particular increase with particle mass (Kohl *et al* 2006, Cranmer *et al* 2008, Landi and Cranmer 2009). These anisotropies may be a signature of heating by high-frequency turbulence, possibly driven by magnetic reconnection. Similar effects have been observed in laboratory plasmas. Brown *et al* (2002) reported an energetic ion population associated with 3D magnetic reconnection in the Swarthmore Spheromak Experiment device. Recently, ion heating associated with magnetic reconnection events in the Madison Symmetric Torus (MST) has been studied, revealing similar anisotropies and mass dependences (Tangri *et al* 2008, Fiksel *et al* 2009). The physical mechanism may be related to the reconnection driven turbulent cascade also recently studied on MST (Ren *et al* 2009). Thus, the experiments have shown that ions can be heated anisotropically, in a mass-dependent way, by MHD turbulence generated in reconnection events. This suggests that turbulent heating is responsible for the species-dependent temperature and anisotropy observed in the solar corona and that the turbulence could be generated by reconnection.

3.4.2. Reconnection in stars. Magnetic reconnection is a key process in stellar astrophysics. It is the leading candidate for the energy release mechanism in flares and may be an important mechanism for coronal heating. It must also occur in stellar interiors, as part of the magnetic dynamo. Laboratory experiments have made essential contributions to reconnection studies. Two recent review articles discuss these contributions in depth (Zweibel and Yamada 2009, Yamada *et al* 2010). Highlights include laboratory studies of flux rope dynamics, including reconnection in line tied plasmas and relaxation to a lower energy state (Bergerson *et al* 2006, Cothran *et al* 2009, Sun *et al* 2010), a criterion for the onset of fast collisionless reconnection mediated by the Hall effect (Yamada 2007) and studies of the electron diffusion layer, which clarify the mechanisms responsible for breaking the fieldlines and the apportionment of energy in the reconnection region (Ren *et al* 2008). These studies thus suggest a possible mechanism for triggering fast reconnection in solar flares and provide detailed information on how energy is apportioned among thermal and non-thermal electron and ion populations in solar reconnection.

3.4.3. Stellar dynamos. Although magnetic cycles are well established on the Sun and other stars, a theoretical explanation of stellar dynamos is still lacking and experimental confirmation is sparse. For many years, dynamo theory has been dominated by kinematic studies in which a mean field is built up from infinitesimal values by small-scale turbulence and large-scale shear. Recently, dynamo action has been reported in a number of liquid sodium experiments (Gailitus *et al* 2000, Monchaux *et al* 2007, Spence *et al* 2007). Liquid sodium, like stellar interior plasmas, is much more resistive than it is viscous. These experiments are being used to understand saturation mechanisms, the surprising role of turbulence in suppressing the growth of large-scale magnetic fields and the electromotive forces produced by large-scale and small-scale turbulent flows. These experiments are influencing the development of a new dynamo paradigm, in which dynamos are essentially non-linear and maintained by large-scale flows rather than small-scale turbulence.

3.4.4. Stellar opacities. Heating by fusion reactions deep within stellar cores produces thermal x-ray radiation and the outward transfer of this radiation is an essential element of stellar dynamics and evolution. The rate of attenuation of such radiation is the opacity. One can calculate opacities from fundamental atomic physics, but in even moderately complex elements such as iron this involves the interaction of many millions of transitions. Because of this complexity, calculations of opacity are uncertain and experimental measurements are essential to determine which calculations are correct. This has led to a quest to produce in the laboratory conditions present in stellar interiors so as to measure relevant opacities (Bailey *et al* 2009). During the 1990s, laboratory research and atomic theory resolved the issue of understanding pulsations in Cepheid variable stars (Rogers and Iglesias (1994), Springer *et al* (1997); see also the review by Remington *et al* (2006)). More recently, research has turned to the challenging issue of understanding solar structure. The Sun has an inner, radiative heat conduction zone that gives way to a convective zone nearer the surface. Solar models typically find a location of the boundary between these zones that differs from the measured one by more than 13 standard deviations (Basu and Antia 2008). One possible cause of this is knowledge of the energy-averaged opacity, which indeed must be accurate to ∼1% in order to fix the boundary to within the uncertainties of the observation (Bahcall *et al* 2004). By producing conditions of the stellar interior and measuring the detailed spectral structure of the opacity, researchers are now able to address this issue (Bailey *et al* 2007, 2009, Mancini *et al* 2009). These measurements showed that while very recent opacity models were nearly accurate enough under the conditions studied, previous opacity models were much less accurate. Challenges going forward are to produce accurate measurements in hotter, denser plasmas, in effect moving deeper into the Sun, while also addressing the other uncertainties discussed in section 3.1.2.

3.4.5. Photoionized gas. CVs are binary star systems composed of a white dwarf and (most often) a normal star. Mass from the normal star falls toward the white dwarf, producing a wide variety of phenomena. Recent laboratory work has focused on shock phenomena (Falize *et al* 2009a, 2009b, 2011) and on photoionization. CVs emit x-ray radiation from the accreting matter. Such emission

is also important in other accreting systems, for example, neutron stars, black holes and star-forming regions. The radiation photoionizes the nearby matter, producing plasma that is 'overionized' (ionized far beyond the level that would be produced by collisional ionization at the local electron temperature). One needs experiments to assess the accuracy of radiative rates across a wide range of transitions. An early effort in this direction (Foord *et al* 2004) used the radiation pulse produced by imploding a cylindrical array of metal wires to vaporize and then photoionize very thin foils of Fe and NaF. They later compared the measured charge state distributions to those calculated by photoionization codes (Foord *et al* 2006), finding broad agreement but some differences. To obtain more uniform photoionized plasma, present-day experiments use radiation from an imploding wire array to create plasma in a gas cell (Bailey *et al* 2001, Mancini *et al* 2009). The radiation from a Z-pinch machine has also been used to photoionize a gas cell (Cohen *et al* 2003). In an alternative approach, a laser source is used to heat a gold cavity whose emission produces a moderately overionized plasma in a gas cell (Wang *et al* 2008). More recently, Fujioka *et al* (2009) used a laser-driven implosion to produce a $\sim$5 MK blackbody radiation source, which in turn photoionized a laser-ablated, Si plasma. The photoionization experiments to date have shown that detailed comparisons of code results with laboratory data can improve our understanding of photoionized systems.

3.4.6. Instabilities in type II supernovae. Core-collapse SNe (ccSNe) involve much uncertain physics. Their complete physics and full range of dynamics are far beyond what can now be simulated. As a result, theories or simulations of these events must employ reduced physics, creating a need to test those simplified models. The potential for discovery is high, as unanticipated interactions of the physical processes may arise. Laboratory work relevant to ccSNe is currently limited to the 'late' phase of explosion, after the initial core collapse and after the shock wave forms that blows apart most of the star. It is now widely accepted that unstable mixing of stellar materials occurring during that phase is essential to explain observations of supernova SN 1987A (Arnett *et al* 1989, Chevalier 1992), but early simulations including these effects failed to do so (Muller *et al* 1991). This, combined with the observed asymmetry of SN ejecta, led to the hypothesis that such explosions were jet-driven (Wang *et al* 2001), although the mechanism that would cause this remains unidentified. Meanwhile, and quite unexpectedly, simulations employing improved traditional explosion models produced relevant levels of asymmetry (Kifonidis *et al* 2000, 2003, 2006, Guzman and Plewa 2009). This seems to be a nice story with an endpoint, yet all its elements remain uncertain without experimental evidence that other unanticipated coupling does not exist. Simulations cannot for example test the hypothesis that small-scale dynamics may feed back on the large-scale hydrodynamic evolution (Leith 1990).

Experiments have been developed to examine unstable hydrodynamics in a regime relevant to late-phase ccSNe dynamics. Work through 2005 is reviewed by Remington *et al* (2006). Such experiments can be well scaled in detail (Ryutov

et al 1999) to local conditions in ccSNe. To date the large-scale behavior they have seen has been consistent with a variety of simulations (Kuranz *et al* 2009), showing that on a large scale our understanding of instabilities in the late phase of ccSNe is correct. However, to explain the observations it requires only that $\sim$1% of the inner material in the star finds a way to reach its outer layers with high velocity, and a number of small details have not been consistent between simulations and experiments (Calder *et al* 2002, Miles *et al* 2004, Kuranz *et al* 2010). Further work is seeking to understand the origin of the differences between observations and simulations, and to develop experiment designs relevant to the global dynamics of the explosion (Grosskopf *et al* 2009).

3.4.7. Radiative shocks in type II supernovae. During the explosion, the radiation pressure in the shocked matter produced by a type II SN exceeds the material pressure, but because the mean free path for thermal radiation is small compared with other scale lengths in the system, the shock wave behaves as a hydrodynamic shock with a polytropic index $\gamma = 4/3$ (Ryutov *et al* 1999). This changes as the shock wave breaks out of the star and radiation can escape ahead of the shock. The shock enters a regime in which the thermal energy produced by the shock is mostly radiated away even though the layer behind the shock is many mean-free-path thick. A dense shell forms, which may be unstable (see sections 4.3.1 and 4.3.2). Current astrophysical instruments are beginning to observe such shock-breakout events (Calzavara and Matzner 2004, Chevalier and Fransson 2008, Soderberg *et al* 2008). Experiments have begun to produce and study shock waves in the same radiation-hydrodynamic regime as the shock-breakout events, with strong radiation emission, escape of the radiation ahead of the shock, and trapping of the radiation behind the shock (Bouquet *et al* 2004, Reighard *et al* 2006, Doss *et al* 2009, 2010). Such experiments are a subset of radiative-shock experiments more broadly (Bozier *et al* 1986, Grun *et al* 1991, Edwards *et al* 2001, Edens *et al* 2005, Hansen *et al* 2006, Koenig *et al* 2006, Busquet *et al* 2007). They typically involve producing a low atomic number Z plasma 'piston' moving at $\gtrsim$100 km s^{-1} and using it to drive a shock wave in Xe or some other high-Z gas. In the experiments the radiation transport is dominated by broadband thermal emission and absorption, while that in the star is more complex. Even so, the experiments are a vehicle to better understand the radiation-hydrodynamic behavior of this type of system and they have the potential to discover unanticipated behavior. To date, the experiments have shown that the Vishniac-like instability to which such dense shells are subjected is not so virulent as to greatly distort the shock. Ongoing work is developing scaling connections to SNe and SNRs (Doss 2011) and simulating the observed behavior (van der Holst *et al* 2011). These experiments constrain astrophysical simulation models, which cannot be expected to correctly model the SN if they cannot model these data.

3.4.8. Compact objects and gamma ray bursts: relativistic collisionless shocks. Most astrophysical shocks are collisionless shocks, in which electromagnetic turbulence

randomizes the motion of the incoming particles, replacing the role of collisions in ordinary shocks. Astrophysical observations often imply that relativistic collisionless shocks must be present, as for example in gamma ray bursts (GRBs) (Piran 1999, Waxman 2006). Yet the observed emission from GRBs, attributed to synchrotron emission by electrons, required magnetic fields orders of magnitude larger than could be produced by mechanisms known to be present in the 1990s. The shocks involved are too complex to be fully described by a first-principles analytic or semi-analytic theory. The past decade has seen an explosion of work on such shocks (only some of which can be cited here), made possible primarily by the application of particle-in-cell (PIC) simulation methods on ever-larger computers. The first 3D PIC simulation of colliding electron–positron plasmas (Silva *et al* 2003), which are thought to occur in GRBs and elsewhere, found that the 3D Weibel instability produces both long-lived magnetic fields whose energy density is near that of the ions and non-thermal particle acceleration. This supported the theory (Medvedev and Loeb 1999) that the Weibel instability was the key process, which previously was only one of many theories. Further simulations studied initially unmagnetized (Spitkovsky 2008) and initially magnetized (Murphy *et al* 2010) electron–ion shocks, both also considered important in GRBs. In both cases one also sees the Weibel instability and the generation of strong magnetic fields, in addition to significant electron heating. The results of Murphy *et al* (2010) in combination with observations of polarization in emission from GRBs provide evidence for a significant primordial magnetic field in such events. Applying a similar model to relativistic electron–positron jets, Nishikawa *et al* (2009) found that the gamma-ray emission should come primarily from the shocked jet material rather than from the shocked ambient medium, confirming this interpretation of the observations of those objects. In this way large PIC simulations have become an important tool to advance understanding of relativistic astrophysical systems.

3.5. Nuclear physics

3.5.1. Nuclear synthesis via neutron capture. Elements beyond the iron peak are produced primarily by neutron (n) capture in the s- (slow) and r- (rapid) processes. The main s-process occurs in low-mass AGB stars while the weak s-process takes place in the He- and C-burning shells of massive stars. There is uncertainty about site or sites of the r-process, with Type II SNe (and their associated neutrino-driven winds) and neutron star mergers being leading candidates (Qian and Wasserburg 2007).

The fractional contributions of the weak and main s-processes have been deduced from studies of solar system (including meteorite) abundances. The r-process must account for 'shielded' or other n-capture isotopes off the s-process path, and for other differences between observed abundances and those attributable to the s-process. Discussions can be found in Raiteri *et al* (1993), Arlandini *et al* (1999), The *et al* (2007) and Heil *et al* (2008). These studies attribute the light n-capture elements (e.g. Sr and Zr) with high-mass stars and heavier s-process elements, such as Ba, with low-mass stars

(Busso *et al* 1999). Recent laboratory data for s-process cross-sections are summarized by Käppeler *et al* (2011), updating Käppeler *et al* (1989).

Although the sites of the r-process are uncertain, data from metal-poor stars show that an r-process operated in the early galaxy at a frequency typical of ccSNe (Cowan and Thielemann 2004, Sneden *et al* 2008) (see also section 3.1.1). While properties of lighter r-process nuclei have been determined in the laboratory (Kratz *et al* 2000, Pfeiffer *et al* 2001, Möller *et al* 2003), much of the r-process path is through short-lived, very neutron-rich nuclei that are difficult to produce. Future facilities (e.g., the Facility for Rare Isotope Beams (FRIB)) will allow more extensive measurements of relevant masses and β-decay rates.

Interstellar abundances, however, do not appear to match solar system values. The abundances of Ga and Ge are 25% of the meteoritic value for low-density, warm gas, where depletion onto interstellar grains is expected to be minimal (Cartledge *et al* 2006, Ritchey *et al* 2011). The inferred Rb abundance is about 35% of the meteoritic value (Federman *et al* 2004, Walker *et al* 2009). The noble gas Kr, which does not deplete onto grains, has an average abundance of 50% of the solar system value (Lodders 2003, Cartledge *et al* 2003). Ga, Ge, Kr and Rb are predicted to form primarily in high-mass stars. In contrast, Cd and Sn, which are mainly synthesized in low-mass stars, are not depleted for low density lines of sight (Sofia *et al* 1999), despite similarities between Ga, Ge, Rb, Cd and Sn condensation temperatures (Lodders 2003). The observed depletion patterns cannot be attributed to imprecise oscillator strengths, which are well known from laboratory and theoretical work (Morton 2000, 2003, Schectman *et al* 2000, Alonso-Medina *et al* 2005, Oliver and Hibbert 2010). Additional interstellar studies of other n-capture elements are needed.

3.5.2. Stellar nuclear fusion: pp chain. The proton–proton or pp chain is the principal mechanism by which low-mass hydrogen-burning stars like the Sun produce energy through $4p \rightarrow {}^4\mathrm{He} + 2e^+ + 2\nu_e$ where e^+ represents a positron and ν_e an electron neutrino. The competition between the three cycles of the pp chain (ppI, ppII and ppIII) depends sensitively on the stellar core temperature, as the reactions require Coulomb barrier penetration, and on the specific rates of the reactions, which are conventionally given in terms of the astrophysical S-factor, from which the highly energy-dependent S-wave Coulomb behavior of the cross-section has been removed (Adelberger *et al* 2011). Laboratory measurements of S-factors are important to both solar neutrino physics and helioseismology. The uncertainties in laboratory S-factor measurements limit the precision of the standard solar model (SSM) neutrino flux and sound speed predictions (Bahcall *et al* 2005b). Associated astrophysics challenges include demonstrating through neutrino spectrum distortions that matter effects influence neutrino oscillations, detecting day–night effects and resolving discrepancies discussed in section 3.1.2 between the SSM and helioseismology measurements related to solar metallicity (Haxton and Serenelli 2008, Aharmin *et al* 2010, Abe *et al* 2011).
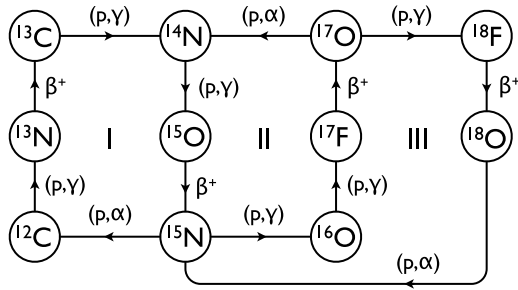
Figure 7. The three pathways that dominate the CNO cycles at lower temperatures. Recent experiments on the branch-point reactions involving ^{15}N and ^{17}O are discussed in the text. Adapted from Wiescher *et al* (2010).

Recent key advances in laboratory astrophysics include a series of precise measurements of the reactions ^{3}He(^{3}He, 2p)^{4}He (Bonetti *et al* 1999) and ^{3}He(^{4}He, γ)^{7}Be (Singh *et al* 2004, Bemmerer *et al* 2006a, Brown *et al* 2007, Confortola *et al* 2007, Gyurky *et al* 2007, di Leva *et al* 2009) which control the ratio of ppI solar neutrino flux to that of the ppII and ppIII. There have also been several new and precise measurements of ^{7}Be(p, γ)^{8}B (Hammache *et al* 1998, 2001, Strieder *et al* 2001, Junghans *et al* 2002, 2003, 2010, Baby *et al* 2003a, 2003b), until recently the limiting nuclear physics uncertainty in predicting the flux of ppIII solar neutrinos. These measurements will have an important impact on the analysis of the currently running Borexino experiment (Arpsella *et al* 2008) which, in conjunction with the Sudbury Neutrino Observatory (SNO) (Aharmin *et al* 2010) and Super-Kamiokande (Abe *et al* 2011), will provide a direct test of matter effects on neutrino oscillations. They also impact the comparison between the total SSM ^{8}B flux and that measured in SNO, which is sensitive to SSM parameters such as core metallicity. Recent progress in *S*-factor determinations came from technological advances like the Laboratory for Underground Nuclear Astrophysics (LUNA) (Costantini *et al* 2009, Broggini *et al* 2010), a specialized low-energy accelerator operating at great depth, allowing nearly background-free measurements of important cross-sections.

3.5.3. Stellar nuclear fusion: CNO cycle. Heavier hydrogen-burning stars produce their energy primarily through the carbon–nitrogen–oxygen (CNO) cycles, where nuclear reactions are characterized by higher Coulomb barriers. Hence energy production rises steeply with temperature, $\epsilon_{\mathrm{CNO}} \sim T^{18}$, compared with $\epsilon_{\mathrm{pp}} \sim T^4$ at solar temperatures. Unlike the pp chain, the CNO cycle requires pre-existing metals (in the astronomer's sense meaning all elements heavier than He). These serve as catalysts for hydrogen burning, with the energy production at a fixed temperature proportional to metallicity. The CNO cycle is responsible for about 1% of solar energy generation, but dominates hydrogen burning in stars with central temperatures $\gtrsim 2 \times 10^7$ K.

The rate-controlling step in the carbon–nitrogen (CN) cycle, denoted by I in figure 7, is ^{14}N(p, γ)^{15}O. The nuclear physics of this reaction is complex, with contributions from several ^{15}O resonances both above and below threshold. Work

on this reaction over the past decade has been intense. New measurements have been made with both direct methods (Formicola *et al* 2004, Imbriani *et al* 2005, Runkle *et al* 2005, Bemmerer *et al* 2006b, Lemut *et al* 2006, Marta *et al* 2008) and indirect methods, covering the energy range between 70 and 480 keV (see Wiescher *et al* (2010) and Adelberger *et al* (2011) for summaries). After summing all transitions $S_{1\ 14}^{\mathrm{tot}}(0) = 1.66 \pm 0.12$ keV barn was obtained (Adelberger *et al* 2011), a value nearly a factor of two below previously recommended values. This has had significant consequences for astrophysics, such as increasing the age estimate for the oldest globular cluster stars by nearly a billion years (Runkle *et al* 2005). The increased precision of the *S*-factor will be critical to the analyses of data from the neutrino detector SNO+ (http://snoplus.phy.queensu.ca/Home.html) now under construction. By measuring the CNO neutrino flux, SNO+ may directly determine the carbon and nitrogen content of the solar core.

While ^{14}N(p, γ) controls the cycling rate of the CN cycle, other reactions determine the flow rate out of this cycle toward oxygen and heavier metals. The turn-on of these branches influences the opacity evolution and temperature profile of hydrogen-burning stars. Competition between ^{15}N(p, α)^{12}C and ^{15}N(p, γ)^{16}O governs the division of the flow between the left two cycles illustrated in figure 7. Here α represents an ^{4}He nucleus. Recent work on the second reaction (Bemmerer *et al* 2009) has led to corrections in earlier results (Adelberger *et al* 2011). The new measurements were done at novae energies and reduce the final nucleosynthesis yield of ^{16}O by up to 22%, depending on the nova temperature (Bemmerer *et al* 2009). There is a similar competition between ^{17}O(p, α)^{14}N, which closes CNO cycle II of figure 7, and ^{17}O(p, γ)^{18}F, which leads either to the more complicated reaction network of the hot CNO cycles or to CNO I and II via ^{18}F($\beta^+\nu$)^{18}O(p, α)^{15}N. Recent work has led to significant cross-section changes affecting the flow toward the hot CNO cycle in novae (Fox *et al* 2005, Chafa *et al* 2007).

3.5.4. Stellar nuclear fusion: hot CNO burning. At temperatures greater than approximately a few times 10^8 K a more complicated set of reactions allows mass flow to heavier nuclei (Wiescher *et al* 2010). In addition, the equilibrium abundances characterizing previously described cycles change: the rates of key radiative capture reactions increase to the point that they match or exceed those of the β decays of ^{13}N and ^{15}O, for example, so that weak rates now govern the cycling time and rate of energy production, while rapid (p, γ) reactions competing with β decay open up new pathways. The hot CNO network involves reactions on unstable nuclei that require laboratory tools that only recently have become available, with the development of radioactive ion beam facilities. The resulting advances include the following.

- The cycle ^{12}C(p, γ)^{13}N(p, γ)^{14}O($\beta^+\nu$)^{14}N(p, γ)^{15}O ($\beta^+\nu$)^{15}N(p, α)^{12}C opens up when the radiative capture rate on ^{13}N exceeds the β decay rate. The key resonance governing the capture was measured in inverse kinematics, using an intense ^{13}N radioactive beam of 3×10^8 s^{-1} (Decrock *et al* 1991, Delbar *et al* 1993). The direct capture

contribution was recently determined from the asymptotic attenuation coefficient (Li *et al* 2006, Guo and Li 2007). These measurements together have led to a substantial increase in the recommended low-energy cross-section (Wiescher *et al* 2010), lowering the ignition temperature for the hot CNO cycle. This cross-section impacts models of novae, including the $^{13}C/^{12}C$ ratio in nova ejecta, as well as the predicted abundance of ^{13}C, an important s-process neutron source (Arnould *et al* 1992).

- A critical branching in the hot CNO cycle depends on the competition between $^{18}F(p, \alpha)^{15}O$ and $^{18}F(p, \gamma)^{19}Ne$. These destruction channels for radioactive ^{18}F are also the largest nuclear physics uncertainty affecting γ-ray emission from novae (Hernanz *et al* 1999). The development of high-intensity ^{18}F beams of $\sim10^5$ particles s^{-1} have allowed experimenters to determine the dominant ^{18}F reaction rates for temperatures characterizing ONeMg novae (Bardayan *et al* 2000, 2002, Chipps *et al* 2009, Murphy *et al* 2009).

3.5.5. Core-collapse supernovae. Nuclear physics governs three important aspects of ccSNe, the core bounce (and ultimately the structure of the neutron star), energy transport and nucleosynthesis.

The core bounce depends on the nuclear EOS at densities that could range up to six times that of ordinary nuclear matter, at temperatures of tens of MeV and at extremes of isospin. The conditions at maximum compression are beyond the direct reach of experiment, but are constrained by astrophysical observations, including the stability of the 1.396 ms pulsar Terzan 5 (Hessels *et al* 2006) and the recent determination of a two-solar-mass neutron star measured by Shapiro delay (Demorest *et al* 2010) as well as by laboratory measurements of nuclear compressibilities. Laboratory measurements of giant monopole resonance energies in nuclei with and without neutron excesses constrain the compressibility for isospin symmetric matter and the symmetry energy K_τ critical to neutron-dominated matter (Piekarewicz 2010). New measurements, carried out in Sn isotopes, has led to $K_\tau = -395 \pm 40$ MeV (Garg *et al* 2007), increasing the error bar on compressibility estimates (Piekarewicz 2010).

In a core-collapse supernova explosion the energy released through gravitational collapse must be preferentially transferred to the mantle of the star, to enable ejection. This is thought to be accomplished through the combined effects of the shock wave and neutrino heating. The neutrino heating and associated physics—neutrino opacity, neutrino cooling, β decay rates important to lepton number emission and nucleosynthesis—are governed in part by nuclear Gamow–Teller and first-forbidden responses (Langanke and Martinez-Pinedo 2003). The Gamow–Teller responses have been mapped in the laboratory using forward-angle (p, n) and (n, p) scattering (Rapaport and Sugarbaker 1994) and then incorporated into nuclear models used in SN simulations. The resulting modern electron capture and β decay rates have been found to increase the electron mass fraction Y_e throughout the iron core. As the size of the homologous core and thus the shock radius is proportional to Y_e^2, this has significantly

increased calculated shock wave strengths (Heger *et al* 2001, Bronson-Messer *et al* 2003). These improvements have also led to changes in neutrino (ν) process nucleosynthesis yields for key isotopes such as ^{11}B and ^{19}F (Heger *et al* 2005).

Recent studies of metal-poor halo stars (Cowan and Sneden 2006) have associated early Galaxy r-process events with ccSNe, which provide in their ν-driven winds and mantles conditions under which an r-process might occur. The rate of nucleosynthesis is controlled by weak interactions, as new neutrons can be captured only after neutron holes are opened by β decay. Thus the rate of β decay is critical to determining which SN zones might be able to sustain the necessary nucleosynthetic conditions for the requisite time. Recent laboratory β decay measurements for very-neutron-rich isotopes near mass number $A = 100$ have demonstrated that half-lives are a factor of two or more shorter than previously believed, which significantly relaxes constraints on the r-process time scale (Nishimura *et al* 2011).

4. The galactic neighborhood

The galactic neighborhood includes 'the structure and properties of the Milky Way and nearby galaxies and their stellar populations and evolution, as well as interstellar media and star clusters' (Blandford *et al* 2010a).

4.1. Atomic physics

4.1.1. Galactic chemical evolution. The early chemical evolution of the Galaxy can be studied from abundances of the iron-peak elements. These elements are synthesized in SN explosions and the stellar abundance trends with metallicities (i.e. [Fe/H]) provide important constraints on the explosion mechanisms of type II and Ia events. Early work by McWilliam (1997) demonstrated that as [Fe/H] decreased below -2.4, Cr/Fe decreased while Co/Fe increased, leading to a rising trend of Cr/Co with decreasing Fe/H. This behavior provides clues to synthesis from SNe in the Galaxy as a function of metallicity. For example, models with α-rich conditions tend to produce more elements heavier than Fe, such as Co, in contrast to lighter elements such as Cr. It is also possible to reproduce these abundance trends by varying such effects as the explosion energies, neutron excess, mass cut position and progenitor masses in explosive SN nucleosynthesis. Additional studies have recently been completed, focusing on the iron-peak elements Ti, V, Cr, Mn, Fe, Co and Ni as a function of [Fe/H] (Henry *et al* 2010). The derived abundance trends have been based upon utilizing neutral (and less abundant) species for the Fe-peak element species and assuming LTE conditions.

Recent laboratory determinations of atomic data (e.g. oscillator strengths) have been obtained for Cr I (Sobeck *et al* 2007), Cr II (Nilsson *et al* 2006), Mn I and II (den Hartog *et al* 2011), Co I (Nitz *et al* 1999) and Co II (Crespo Lopez-Urrutia *et al* 1994). These new experimental data have led to increasingly more accurate abundance values for the iron-peak elements in old halo stars. As a result of these new precise values, we are getting a clearer picture of the

nature, and sources, of the earliest element formation in the Galaxy. In addition these new abundance values are providing increasingly stringent constraints on models (e.g. mass cut, energies, progenitor masses, elemental content of the ejecta, etc) of SN explosions and nucleosynthesis. Finally, an examination of the abundance trends of the iron-peak elements over different stellar metallicities is providing direct insight into the chemical evolution of the Galaxy.

4.2. Molecular physics

4.2.1. Interstellar medium chemical complexity. Recent developments in detector technology for ground-based measurements and the launch of the *Herschel Space Observatory* provide new opportunities to improve our understanding of interstellar chemistry. This has been particularly true for molecular ions and radicals which are important intermediate species in chemical networks describing the molecular evolution of interstellar clouds. Intermediates which have been detected spectroscopically include SH^+ (see section 5.2.1), H_2Cl^+, OH^+, H_2O^+ and CH^+. Accurate transition frequencies are required for observational searches of these species, many of which have transitions at sub-millimeter and far-IR wavelengths. For SH^+ a combination of laser (Hovde and Saykally 1987), microwave (Savage *et al* 2004) and IR (Brown and Müller 2009) measurements provided the needed accuracy. The measurements in the THz range for H_2Cl^+ by Araki *et al* (2001) yielded the required transition frequencies. The frequencies for OH^+ come from the study of Bekooy *et al* (1985). The H_2O^+ frequencies are given by Mürtz *et al* (1998). CH^+ data come from the spectroscopic work of Amano (2010). Lastly, there are numerous spectroscopic studies of NH and NH_2, which have been compiled into the Cologne Database for Molecular Spectroscopy (Müller *et al* 2005).

Herschel has detected many of the above species. Lis *et al* (2010) discovered H_2Cl^+ in absorption toward the star-forming region NGC 6334I in both ^{37}Cl and ^{35}Cl isotopologues. They found that the HCl/H_2Cl^+ ratios are consistent with chemical models, but the H_2Cl^+ column densities greatly exceeded model predictions. The OH^+ and H_2O^+ ions, which lead to H_2O in ion–molecule chemical schemes, were seen in several star-forming clouds and the intervening diffuse clouds (see, e.g., Gupta *et al* (2010), Neufeld *et al* (2010) and Schilke *et al* (2010)). For example, Neufeld *et al* (2010) detected these ions in absorption toward the cloud W49N. The OH^+/H_2O^+ abundance ratio indicated that the ions formed in clouds with small fractions of H_2. Since these ions are produced by cosmic ray ionization of atomic and molecular hydrogen, an ionization rate could be inferred. The values are consistent with other recent determinations. Falgarone *et al* (2010) observed absorption from $^{12}CH^+$ and $^{13}CH^+$. As the absorption from $^{12}CH^+$ is optically thick, they were only able to set a lower limit of 35 on the isotope ratio. This value is consistent with other determinations of the $^{12}C/^{13}C$ ratio in ambient gas. Lastly, we note that Persson *et al* (2010) detected NH and NH_2 in absorption in diffuse gas. Neither gas-phase nor grain-surface chemical models adequately explain the data; clearly further investigations into nitrogen chemistry are required.

4.2.2. Cosmic ray measurements. Energy input from Galactic cosmic rays, mainly relativistic protons and helium ions, drives important processes in the ISM. Ionization of H and H_2 heats the gas and initiates chemical reactions. Cosmic rays interacting with the gas break apart ambient C, N and O nuclei in a process called spallation, producing significant quantities of stable Li, Be and B isotopes. The interactions with H and H_2 also lead to γ-ray production through the decay of neutral pions. Many of these processes are dominated by low-energy cosmic rays (tens of MeV), which are shielded from the Earth by the magnetic field of the Sun.

One way to obtain the cosmic ray ionization rate involves measurements of H_3^+ in diffuse molecular clouds (Snow and McCall 2006). The analysis is dependent on an accurate determination of the dissociative recombination rate coefficient, which until recently was poorly known. Measurements using storage rings (McCall *et al* 2003, Kreckel *et al* 2005, 2010, Tom *et al* 2009) and afterglows (Glosík *et al* 2008, 2009, Kotrík *et al* 2010), as well as theoretical calculations (Dos Santos *et al* 2007), are now converging on the most appropriate value for the rate coefficient. The cosmic ray ionization rate in diffuse molecular clouds inferred from H_3^+ observations is now more secure (e.g. Indriolo *et al* (2007)). One implication of this work is that the shape of the cosmic ray spectrum may differ from what has commonly been assumed (Indriolo *et al* 2009).

4.3. Plasma physics

4.3.1. Supernova remnants: radiative shock thermal instabilities. During the SN phase, a contact surface forms at the change in density gradient where the stellar envelope gives way to the stellar wind, between the driven forward shock and an eventual reverse shock. This contact surface is unstable and is subject to instabilities such as those discussed in sections 3.4.6 and 3.4.7. Other issues that arise in SNRs involve the predicted role of radiation. Here and in section 4.3.2 we discuss two of these issues.

As the shocks produced by SNe or other circumstances propagate across the ISM, the newly shocked material cools by the emission of radiation. The rate of cooling varies with temperature and there are regimes in which linear theory and simulations find that this produces an instability, causing oscillations in the shock velocity (Chevalier and Imamura 1982, Innes *et al* 1987, Kimoto and Chernoff 1997). Observational evidence of cooling that might be part of such an instability has been reported (Raymond *et al* 1991). The instability also would be expected to occur in accreting systems such as TW Hydrae and other T Tauri stars (Koldoba *et al* 2008), but recent observations find no evidence of it (Drake *et al* 2009, Gunther *et al* 2010). This creates a focused need for the observation of such instabilities in a laboratory environment, to show if they can in fact exist. This was accomplished (Hohenberger *et al* 2010) by the production of cylindrical shock waves by focusing a 1.4 ps laser pulse into a medium composed of Xe gas clusters (Moore *et al* 2008, Symes *et al* 2010). Measurements of the shock trajectory clearly showed velocity oscillations attributed to this

instability. Future experiments can proceed toward systems that are more closely scaled to specific astrophysical cases.

4.3.2. Supernova remnants: Vishniac instabilities. SNRs at times produce very thin dense shells of material by radiative cooling, driven outward by the pressure within the SNR and decelerating as they accumulate more mass. Vishniac (1983) showed such shells to be unstable. Ryu and Vishniac (1991) showed that blast waves producing a density increase above about 10 to 1 are likewise unstable. This instability also may operate in other contexts where one finds a thin, dense shell, such as shocks emerging from SNe (see sections 3.4.6 and 3.4.7). Clumping in simulations of SNRs is often attributed to this process (van Veelen *et al* 2009). In observations, it is most often difficult to say whether the observed clumping is due to this instability as opposed to inhomogeneity in the medium being shocked (Grosdidier *et al* 1998) or to other instabilities such as Rayleigh–Taylor. However, the underlying theory is highly simplified, involving several assumptions including that the shell is infinitesimally thin and an unusual definition of the sound speed in the shell. This created the need for experimental tests. Experiments have produced the instability by driving a blast wave through Xe gas, generating the required large density increase by radiative cooling. Grun *et al* (1991) reported the first observation attributed to this process, but it was only recently that Edens *et al* (2005) reported a test of the predicted growth rate. Laming (2004) has discussed the common physics underlying these instabilities in astrophysical and laboratory systems and the connection of the Vishniac process with the thermal instability discussed above.

4.3.3. Shock–clump interaction. High-resolution images of astrophysical environments reveal that, in general, circumstellar and interstellar plasma distributions are essentially heterogeneous. Strong density perturbations over the ambient density, $\delta\rho/\rho_{amb} \geqslant 1$, exist on a range of scales. The origin of such heterogeneity may lie in turbulent motions which exist in many astrophysical environments or through thermal or dynamical instabilities. Any supersonic flows through these environments will necessarily involve so-called *shock–clump interactions*. The importance of such clumpy flows cannot be understated as critical issues such as mixing, transport and global evolution will all differ in clumpy as opposed to smooth flows. The observational literature shows many clump studies addressing these issues in environments ranging from SN to active galactic nuclei (AGNs) (Smith and Morse 2004, Chugai and Chevalier 2006, Byun *et al* 2006, Westmoquette *et al* 2007, Fesen *et al* 2011).

Theoretical studies of shock–clump interactions have relied heavily on numerical simulations as the problem is essentially multi-dimensional and non-linear interactions dominate. Many studies of adiabatic shocks interacting with a single clump have been performed (see, e.g., Klein *et al* (1994)). Studies of magnetized and radiatively cooled single shocked clumps also exist but are fewer in number. Only a handful of multiple clump studies have been published (Fragile *et al* 2004, Yirak *et al* 2008). Because 3D simulation studies are often resolution limited (Yirak *et al* 2012) laboratory studies

can offer relatively clean platforms for deeper exploration of shock–clump interactions. A robust literature reporting a host of shock–clump high energy density laboratory astrophysics (HEDLA) studies has emerged over the last decade.

The first HEDLA studies of shock–clump interactions focused on single clumps interacting with a passing shock (Kang *et al* 2000, Robey *et al* 2002, Klein *et al* 2003). These works, along with simulations and analytical work, were able to explore key features of shocked clump evolution including the breakup of downstream vortices by the Widnall instability. Characteristic density distributions of the clump as it is flattened by the passage of the shock along with break up of the vortex ring were well characterized in both experiments and simulations. The data shown in Klein *et al* (2003) were used to interpret the evolutionary stage of an observed structure in Puppis A by direct comparison with experimental data (Hwang *et al* (2005), see also figure 8). Recent studies have begun focusing on shock interactions with multiple clumps (Rosen *et al* 2009). Issues such as the interaction of bow shocks from nearby clumps as well as the effect of upstream clumps enhancing the breakup of downstream clumps in their dynamic shadow are currently being explored (Poludnenko *et al* 2004).

5. Galaxies across time

Galaxies across cosmic time covers 'the formation, evolution, and global properties of galaxies and galaxy clusters, as well as active galactic nuclei and [quasi-stellar objects (QSOs)], mergers, star formation rate, gas accretion, and supermassive black holes' (Blandford *et al* 2010a).

5.1. Atomic physics

5.1.1. Active galactic nuclei warm absorbers. Early *Chandra* and *XMM-Newton* observations of the AGN IRAS 13349+2438 detected a new absorption feature in the 15–17 Å range (Sako *et al* 2003). This spectral feature is believed to originate in the warm absorber material surrounding the central supermassive black hole in AGNs and has since been observed in a number of other AGNs (see, e.g., Pounds *et al* (2001), Blustein *et al* (2002), Kaspi *et al* (2002, 2004), Behar *et al* (2003), Sako *et al* (2003), Steenbrugge *et al* (2003, 2005), Gallo *et al* (2004), Matsumoto *et al* (2004), Pounds *et al* (2004), Krongold *et al* (2005) and McKernan *et al* (2007)). These unresolved transition arrays (UTAs) were quickly identified as 2p–3d innershell photoabsorption in iron M-shell ions (Sako *et al* 2003). New atomic calculations were soon carried out which demonstrated that the shapes, central wavelengths and equivalent widths of these features can be used to diagnose the properties of AGN warm absorbers such as wind and outflow velocities, ionization and elemental structure and mass loss rates and relative abundances (Behar *et al* 2001, Gu *et al* 2006). However, the ability to diagnose these properties was initially hindered by a lack of reliable ionization balance calculations, proper line identification and wavelengths and accurate absorption strengths.

Initial AGN models which matched absorption features from second- and third-row elements failed to correctly
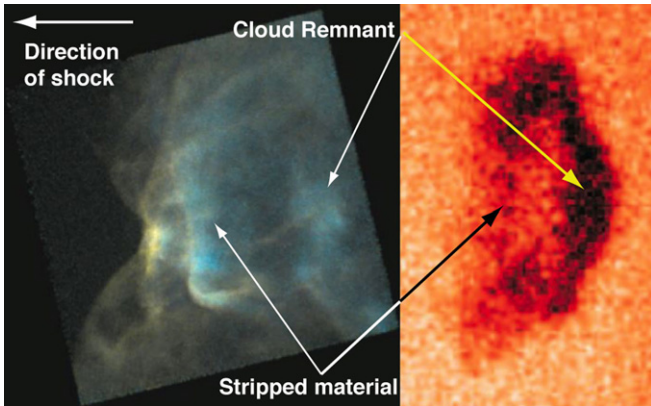
Figure 8. Astrophysical data from *Chandra* (left) and from the laboratory Nova laser (right) showing one phase of shock–clump interaction. Hwang *et al* (2005) used the laboratory data of Klein *et al* (2003) to interpret the astrophysical image. Adapted from Rosner and Hammer (2010).

reproduce the observed absorption from the fourth-row element iron (see, e.g., Netzer *et al* (2003)). The models predicted too high an iron ionization level. This was attributed to an underestimate in the models of the low temperature dielectronic recombination rate coefficients for the Fe M-shell ions (Netzer 2004, Kraemer *et al* 2004). This motivated a series of theoretical calculations (Gu 2004, Badnell 2006a, 2006b, Altun *et al* 2006, 2007) and experimental studies (Schmidt *et al* 2006, 2008, Lukić *et al* 2007, Lestinsky *et al* 2009) which found dielectronic recombination rate coefficients up to orders of magnitude larger than the data previously available. These data improved agreement of the models with observations, though a number of issues still remain (Kallman 2010).

Comprehensive spectral models of the deep *Chandra* observation of the warm absorber in NGC 3783 suggested two ionization components in pressure equilibrium (Krongold *et al* 2003), with similar kinematic velocities. Netzer *et al* (2003) found three ionization components each with two sets of velocities and all three in pressure equilibrium. Subsequent theoretical calculations by Gu *et al* (2006) indicated only a single component in the wind, supporting the idea of pressure equilibrium (see section 5.1.2). Until recently, benchmark measurements capable of testing such bound–bound photoabsorption calculations did not exist. This has now become possible with the use of a portable electron beam ion trap which can be coupled to third or fourth generation light sources (Epp *et al* 2007, Simon *et al* 2010). The results of Simon *et al* (2010) largely verified the calculation of Gu *et al* (2006) for Fe xv. As a result of the photoabsorption work described here and the dielectronic recombination work mentioned above, more reliable models of AGN warm absorbers are now being developed. An example of this is discussed in section 5.1.2.

5.1.2. Thermal stability of active galactic nuclei emission line regions. Many models of the origin of the emission lines of AGNs have been proposed (see chapter 14 of Osterbrock and Ferland (2006), hereafter AGN3). Possibilities include winds from stars or the accretion disk, an ionized layer above the surface of the disk, or distinct clouds confined by a surrounding
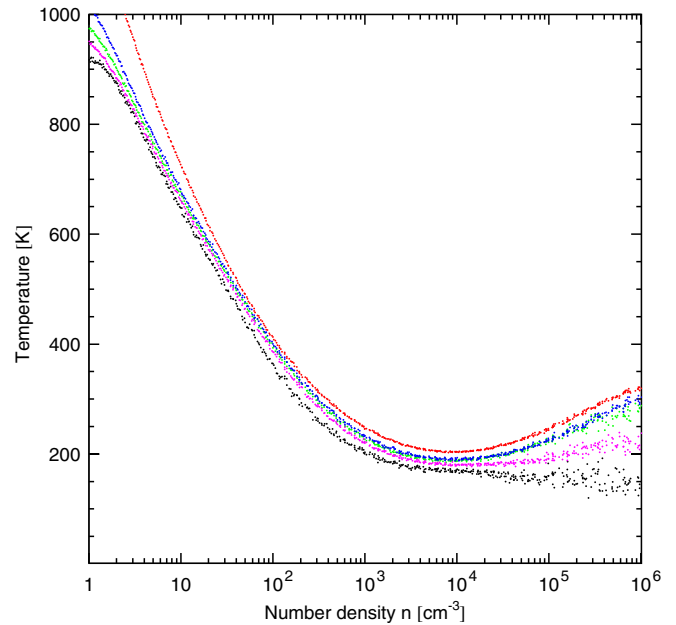

Figure 9. Evolution of a primordial cloud evolving in an initially ionized protogalactic halo using various associative detachment rate coefficients (Kreckel *et al* 2010). Each point corresponds to a spherical shell of material surrounding the center of the cloud. The black and red data use the previous upper and lower limits for the associative detachment reaction as discussed in Glover *et al* (2006). The green data use the experimentally benchmarked theoretical results of Kreckel *et al* (2010), while the magenta and blue data use a rate coefficient, respectively, 25% larger and smaller than this. During this epoch the Jeans mass is set by density at the minimum temperature reached, leading to a factor of 20 uncertainty with the old data and a factor of only 2 with the new.

hot medium. If the latter is the case, then the gas phases where clouds can exist are determined by the thermal cooling curve. This is the relationship between the gas temperature and the cooling rate (AGN3, chapter 3). If gas pressure equilibrium applies, then regions with very different kinetic temperatures and hydrogen densities can exist at the same gas pressure. This scenario dates back to early work done on the ISM (Field *et al* 1969) and was revived by Krolik *et al* (1981) for AGNs.

The form of the cooling curve results from massive amounts of atomic data. Collisional excitation and radiative decay rates are needed for thousands of lines while collisional and photoionization rates, together with radiative, dielectronic and charge transfer recombination rate coefficients, are needed for hundreds of ions. Dielectronic recombination is the most uncertain of these rates. Improvements in the dielectronic recombination data, mainly from storage ring measurements and expanded theory, have significantly affected our understanding of the stable phases (see the reviews of Schippers (2009) and Schippers *et al* (2010)). Atomic theory and experiment are now in far better agreement for the dielectronic recombination data with significantly larger low temperature rate coefficients than those of the previous generation.

Chakravorty *et al* (2008, 2009) revisited the thermal stability of AGNs using an updated version of the spectral simulation code Cloudy (Ferland *et al* 1998). This code uses, among many data sources, the compilation of recombination

rates from Badnell *et al* (2003) and Badnell (2006c). Chakravorty *et al* (2008, 2009) found that the updated dielectronic recombination rates produced significant changes in the predicted distribution of ions. The shape of the stability curve changed significantly as a result. These changes were large enough that the existence of certain gas phases were affected with implications for the final spectrum. However, the modern dielectronic recombination data do not extend to the low-charge, multi-electron systems that are needed to fully understand AGN clouds. This remains an outstanding need.

5.2. Molecular physics

5.2.1. Chemistry surrounding active galactic nuclei. Chemical models of x-ray dominated regions (XDRs) surrounding AGNs and YSOs (Maloney *et al* 1996) reveal significant abundances of doubly charged ions to be cospatial with H_2. The role of doubly charged ions as a diagnostic has been actively pursued since then. Dalgarno (1976) pointed out the potential importance of reactions involving these ions. Recently, Abel *et al* (2008) considered the effects on AGNs. Laboratory studies show that some $X^{2+} + H_2$ reactions occur rapidly at elevated temperatures. Chen *et al* (2003) measured a total rate coefficient for the reaction $S^{2+} + H_2$, while Gao and Kwong (2003) studied the reaction $C^{2+} + H_2$. Neither study, however, determined branching fractions among the various final chemical channels. Abel *et al* (2008) estimated what branching fractions would yield an observable effect on the SH^+ chemistry. They found that as long as the branch to $SH^+ + H$ was a few percent, doubly ionized chemistry would be the dominant pathway for SH^+ production. They also showed that S^{2+} was effectively destroyed once H_2 forms and that the S^{2+} abundance remains high in gas dominated by atomic hydrogen and not only in ionized gas as was previously thought. A key consequence of their calculations is that much of the mid-IR emission from [S III] at 18.7 and 33.5 μm may come from the XDR and not the ionized gas associated with an AGN. Recent detections of SH^+ in our Galaxy (Menten *et al* 2011) suggest the possibility for observing this molecular ion elsewhere and using the proposed diagnostics of Abel *et al* (2008).

6. Cosmology and fundamental physics

Cosmology and fundamental physics includes 'the early universe, the microwave background, the reionization and galaxy formation up to virialization of protogalaxies, large-scale structure, the intergalactic medium, the determination of cosmological parameters, dark matter, dark energy, tests of gravity, astronomically determined physical constants, and high energy physics using astronomical messengers' (Blandford *et al* 2010a).

6.1. Atomic physics

6.1.1. Primordial abundances. The abundances of the primordial elements H, D, ^{3}He, ^{4}He and ^{7}Li provide a key test of Big Bang cosmology. The data are taken from neutral gas in the Lyman-alpha forest for D, H II regions both within the Galaxy (^{3}He) and outside (^{4}He), and observations

of metal-poor stars for ^{7}Li (Steigman 2011). Corrections are made for the effects of post Big Bang nucleosynthesis (BBN) processing. For example, D and ^{7}Li are burned in stellar environments, and ^{7}Li is synthesized in cosmic ray interactions with nuclei in the ISM. For a recent discussion, see Charbonnel *et al* (2010).

The primordial ^{4}He abundance is usually measured in giant H II regions or dwarf irregular galaxies. In these extragalactic emission nebulae, H and He are photoionized. Corrections for stellar production of ^{4}He are determined from correlations with metallicity. A recent examination of 93 spectra for 86 low-metallicity extragalactic H II regions showed a linear dependence of ^{4}He on O/H, and yielded an extrapolated zero-metallicity ^{4}He mass fraction of 0.2565 ± 0.0010(stat) ± 0.0050(syst) (Izotov and Thuan 2010). Others have advocated more conservative errors (Aver *et al* 2010).

Accurate ^{4}He/H determinations from ratios of optical recombination lines require precise photo-production rates for electron recombination with H^+ (Storey and Hummer 1995) and ^{4}He$^+$. Recent atomic calculations for the two-electron system ^{4}He I (Benjamin *et al* 1999, Bauman *et al* 2005, Porter *et al* 2007) are in good agreement. Remaining issues include collisional processes involving the ground or metastable levels, photoionization cross-sections for non-hydrogenic moderate-n, small-l levels and transition probabilities for these levels (Porter *et al* 2009).

The abundance of D is important because of its sensitivity to the baryon-to-photon ratio η_B, varying as $\eta_B^{-1.6}$. From a limited set of high-red shift, low-metallicity QSO absorption line systems, $\log(D/H) = -4.55 \pm 0.04$ was found (Pettini *et al* 2008), in good agreement with the *Wilkinson Microwave Anisotropy Probe (WMAP)* determinations of η_B.

The observations of ^{7}Li in the atmospheres of old halo stars is constant to within measurement errors of 5% over a variety of masses and metallicities. While lithium is fragile in stellar environments, a well-formed 'plateau' is found at low metallicity, yielding an abundance ^{7}Li/H $= (1.23^{+0.34}_{-0.16}) \times 10^{-10}$ (Ryan *et al* 2000) that is about a factor of four below BBN predictions based on the *WMAP* η_B. Any astrophysical explanation of this anomaly would have to account for the stability of the plateau.

6.1.2. Protogalaxy and first star formation. In the early universe during the formation of protogalaxies and the first stars, commonly called Population III stars, H^- plays an important role in the formation of H_2, as is described in section 6.2.1. H_2 is an important coolant leading to the formation of structure during this epoch and reliable predictions of the H^- abundance are critical for reliable cosmological models. H^- can be destroyed by photodetachment

$$H^- + \gamma \rightarrow H + e^- \tag{1}$$

and by mutual neutralization

$$H^+ + H^- \rightarrow H + H. \tag{2}$$
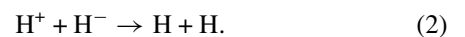
These processes decrease the H^- abundance, thereby limiting the amount of H_2 which forms and correspondingly reducing the cooling of the primordial gas.

Recent theoretical work has been carried out for each of these reactions. Miyake *et al* (2010) have calculated new photodetachment rates taking into account both the H^- resonance states lying near 11 eV and radiation fields characteristic of Population III stars, blackbody sources, power-law spectra and the hydrogen Lyman modulated sawtooth spectra of the high-redshift intergalactic medium. Stenrup *et al* (2009) have recently calculated new mutual neutralization data valid for temperatures relevant during protogalaxy and first star formation. Their results agree with previous theoretical calculations to within 30–40% (Bates and Lewis 1955, Fussen and Kubach 1986), but are about a factor of $2 - 3$ smaller than the experimental results of Moseley *et al* (1970), suggesting the need for further experimental work.

6.2. Molecular physics

6.2.1. Protogalaxy and first star formation. Ro-vibrational collisional excitation of H_2 followed by radiative relaxation is an important cooling mechanism in the early universe. H_2 is formed during this epoch by the associative detachment reaction

$$H + H^- \rightarrow H_2^- \rightarrow H_2 + e^-. \tag{3}$$
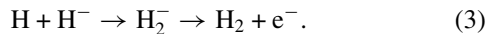
H_2 formation, in turn, can be limited by reactions (1) and (2), both of which compete with reaction (3) for H^- anions.

Until recently, there was nearly an order-of-magnitude uncertainty in the rate coefficient for reaction (3) (Glover *et al* 2006). This uncertainty severely limited our ability to model protogalaxies and metal-free stars forming from initially ionized gas, such as in ionized regions (i.e., H II regions) created by earlier Population III stars (Glover *et al* 2006, Glover and Abel 2008, Kreckel *et al* 2010). Recently, measurements for this reaction have been carried out using a merged-beam apparatus leading to an experimentally benchmarked theoretical rate coefficient with an uncertainty of $\pm 24\%$ (Bruhns *et al* 2010a, 2010b, Kreckel *et al* 2010). As a result, for example, the uncertainty in the model-predicted Population III Jeans mass due to errors in the atomic data has decreased from a factor of 20 to 2 (Kreckel *et al* 2010) (see also figure 9). As a result of all the experimental and theoretical work described here and in section 6.1.2, we are significantly closer to the point where remaining uncertainties in models for protogalaxy and first star formation tell us something about cosmology and not about the underlying chemistry.

6.3. Nuclear physics

6.3.1. Big Bang nucleosynthesis. The comparison between BBN calculations and primordial abundances is a cornerstone of modern cosmology, determining η_B (now confirmed by *WMAP*), and limiting the baryonic matter contribution to the universe to about 4% of the closure density (Olive 1999). Thus most of the dark matter is non-baryonic. BBN in combination with inventories of the matter in stars, inter-cluster diffuse gas, and the intergalactic medium indicate that a significant fraction ($\gtrsim 25\%$) of the baryonic matter is non-luminous (Silk 1999, Bregman 2007).

BBN calculations depend on the Maxwellian-averaged nuclear cross-sections for the various reactions of figure 10.
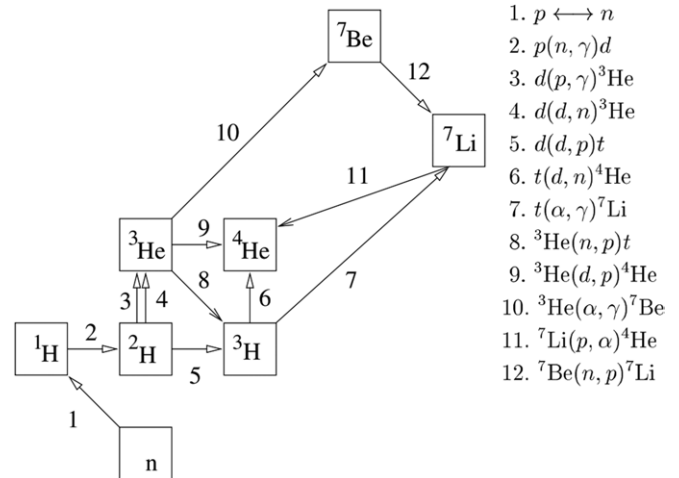

Figure 10. The reaction network for BBN, from Nollett and Burles (2000).

1. $p \longleftrightarrow n$
2. $p(n, \gamma)d$
3. $d(p, \gamma)^3He$
4. $d(d, n)^3He$
5. $d(d, p)t$
6. $t(d, n)^4He$
7. $t(\alpha, \gamma)^7Li$
8. $^3He(n, p)t$
9. $^3He(d, p)^4He$
10. $^3He(\alpha, \gamma)^7Be$
11. $^7Li(p, \alpha)^4He$
12. $^7Be(n, p)^7Li$

Comprehensive efforts have been made to assess the effects of cross-section uncertainties on BBN predictions (see, e.g., Nollett and Burles (2000) and Coc and Vangioni (2010)). Table 1 of Coc and Vangioni (2010) describes the impact of key nuclear physics uncertainties on the abundances of ^4He, D, ^3He and ^7Li, given the *WMAP* value of η_B. The ^4He yield is sensitive to weak rates now well constrained by neutron β decay (Lopez and Turner 1999). The reaction $n + p \rightarrow D + \gamma$ has a large impact on ^7Li by competing with $^7Be(n, p)^7Li(p, \alpha)^4He$ for neutrons: ^7Li is synthesized as ^7Be at the *WMAP* value for η_B. While there are meager low-energy data on this reaction, calculations based on effective field theory (EFT) treatments are believed to be accurate to 1% (Chen and Savage 1999, Ando *et al* 2006). New measurements (Tornow *et al* 2003) of the inverse reaction, made at energies of 2.39–4.05 MeV, are in excellent agreement with EFT predictions. ^7Li is also sensitive to the production channel rate for $^3He(\alpha, \gamma)^7Be$. Four new data sets, summarized in Adelberger *et al* (2011), have now determined this cross-section to $\pm 5.2\%$. Recent measurements (Leonard *et al* 2006) of a third reaction important to ^7Li, $^2H(d, p)^3H$, confirm earlier parameterizations of this cross-section.

Recent work has not uncovered a nuclear physics explanation for the discrepancy between BBN predictions and the ^7Li abundance determined from metal-poor stars. For a discussion, see Chakraborty *et al* (2010) and references therein.

6.3.2. Ultra-high-energy cosmic rays and neutrinos. Recent instrumentation advances in high-energy astrophysics include the Pierre Auger Observatory (Pierre Auger Collaboration 2010), for the study of ultra-high-energy (UHE) cosmic rays, the IceCube Observatory, a South Pole high-energy neutrino detector scheduled for completion in 2011 (Abbasi *et al* 2010), and prototype UHE neutrino detectors, such as the Antarctic Impulsive Transient Antenna (ANITA) experiment (Barwick *et al* 2006) and the Radio Ice Cherenkov Experiment (RICE) (Kravchencko *et al* 2006).

The Pierre Auger program includes measurements of the spectrum, anisotropies and composition of UHE cosmic rays, including at the GZK cutoff (Greisen 1966, Zatsepin

and Kuz'min 1966) of $\sim 5 \times 10^{19}$ eV. Interactions with the cosmic microwave background (CMB) limit the distances UHE protons/nuclei can travel. Interactions with the CMB and with IR, optical and UV background photons are well constrained by a large database of laboratory nuclear physics. The energy-loss mechanisms include single and multiple pion production off the proton, nuclear reactions such as photodisintegration, photo-pair processes and photoabsorption followed by re-emission. References to propagation models based on this input physics can be found in Kotera and Olinto (2011).

A key objective of the Pierre Auger science program, determining the primary energy and mass of UHE cosmic rays, requires a detailed model of the interactions of cosmic ray protons and nuclei with nuclei in the upper atmosphere. Cosmic rays above 10^{14} eV are measured indirectly, through the cascades of secondary particles that result from their atmospheric collisions. The energy and composition of the incident UHE cosmic ray are determined by comparing the observed extensive air showers with those predicted by models. Center-of-mass energies near the GZK cutoff are two orders of magnitude beyond the limits of our highest energy machines, the Large Hadron Collidor (LHC) and the Relativistic Heavy Ion Collidor (RHIC). Thus significant extrapolations are required. For a discussion of the uncertainties, see Alessandro *et al* (2011). Recent tests of existing codes against first LHC data are described in d'Enterria *et al* (2011).

Cosmic ray neutrinos are a tool for probing the universe at asymptotic energies and distances and for identifying point sources, as neutrinos are not deflected by magnetic fields. IceCube was designed to detect neutrinos with energies between 10^{10} and 10^{17} eV, through the Cerenkov light emitted by charged particles they produce. The extension to higher energies, required to detect the neutrinos from the nuclear reactions responsible for the GZK cutoff, requires ice volumes a factor ~ 100 beyond IceCube's km^3, as well as new detection techniques. Methods under development are based on coherent radio emission, the Askaryan effect (Askaryan 1962, Askaryan *et al* 1979). Recent laboratory tests of the Askaryan effect using targets of silica and rock salt confirmed that radio emission provides a means of detecting UHE neutrinos (Saltzberg *et al* 2001, Gorham *et al* 2005).

6.4. Particle physics

6.4.1. Baryon number asymmetry: experiment. The explanation for the excess of baryons over antibaryons in the early universe, and thus a non-zero η_B, is a key puzzle in cosmology. Baryogenesis requires charge-parity (CP) violation and baryon number violation. CP violation arises in the standard model through the Cabibbo–Kobayashi–Maskawa (CKM) phase and through the quantum chromodynamics (QCD) $\bar\theta$ parameter, and has been observed in the laboratory in kaon decays and at the B factories. However, the known CP violation is not sufficient to account for the baryon number asymmetry. Baryon number violation has not been seen in the laboratory, despite intense effort.

Static electric dipole moments (EDMs) require CP violation. As there is a significant gap between current experimental bounds on EDMs and standard-model predictions based on the CKM phase, detection of an EDM might indicate a new source of CP violation relevant to baryogenesis. Current limits come from atomic beam experiments on the electron EDM, $|d_e| < 1.6 \times 10^{-27}$ e cm (Commins *et al* 1994), and from trap experiments with ultracold neutrons, $|d_n| < 2.9 \times 10^{-26}$ e cm (Baker *et al* 2006). Alternatively, neutron and proton EDMs as well as CP-violating nucleon–nucleon (NN) interactions can be probed in neutral atoms. The ^{199}Hg vapor-cell experiment, $|d(^{199}\text{Hg})| < 3.1 \times 10^{-29}$ e cm, provides the most stringent limits on the proton and quark chromo EDMs, and on the strength of scalar, pseudoscalar and tensor CP-violating semileptonic interactions (Griffith *et al* 2009).

Baryogenesis could have arisen from the decays of heavy right-handed neutrinos, with the symmetry violation communicated to the baryons through mechanisms within the standard model (so-called 'sphalerons'; Fukugita and Yanagida (1986)). Recent laboratory discoveries—non-zero neutrino masses and two large mixing angles—have made this scenario quite plausible. The CP-violating observable is proportional to a product that involves the three mixing angles and the Dirac CP phase. A great deal of laboratory effort is now focused on both short- and long-baseline neutrino oscillation experiments to measure the third mixing angle and to detect leptonic CP violation at low energies by comparing neutrino oscillation channels, e.g. $\nu_\mu \rightarrow \nu_e$ and $\bar\nu_\mu \rightarrow \bar\nu_e$. Experiments in progress include the Daya Bay (Lin 2011) and Double Chooz (Palomares 2009) reactor experiments, and the Tokai-to-Kamioka (T2K) long-baseline neutrino oscillation experiment (Rubbia 2011). FermiLab 'intensity frontier' plans include a search for neutrino CP violation (see http://www.fnal.gov/pub/science/experiments/intensity/).

Laboratory limits on baryon number violation come from proton decay searches. The Super-Kamiokande Collaboration (Nishino *et al* 2009) has placed limits on the partial lifetimes for modes favored by minimal SU(5) Grand Unified Theories (GUTs), $p \rightarrow e^+\pi^0$ and $p \rightarrow \mu^+\pi^0$, of 8.2×10^{33} yr and 6.6×10^{33} yr, respectively, at a 90% confidence level. The collaboration has also established (Kobayashi *et al* 2005) stringent limits on modes favored by supersymmetric GUTs, $p \rightarrow \mu^+K^0$, $n \rightarrow \bar\nu K^0$, $p \rightarrow \mu^+K^0$, and $p \rightarrow e^+K^0$ of 2.23×10^{34} yr, 1.3×10^{32} yr, 1.3×10^{33} yr and 1.0×10^{33} yr, respectively.

6.4.2. Baryon number asymmetry: theory. In theory, no major paradigm shift has occurred in the last ten years. (For a review of baryogenesis models, see Dine and Kusenko (2003).) However, considerable progress has been made in refining the predictions of various scenarios and new possibilities have been proposed. In one class of models, the baryon asymmetry is produced at the electro-weak phase transition, as a result of new physics at the electro-weak scale, such as supersymmetry. While the basic scenario for electro-weak baryogenesis (EWB) was described long ago (Kuzmin *et al* 1985), recent developments include a re-evaluation (Lee *et al* 2005) of the relevant source terms which bias the production of a net baryon number via sphaleron transitions (Huet and

Nelson 1996) and of the associated resonant relaxation effects (Lee *et al* 2005). Also, it was realized that the supersymmetric parameter which is space compatible with the production of enough baryon asymmetry possesses a two-resonances structure (Cirigliano *et al* 2006, 2010). One of the two resonances corresponds to the scenario of 'bino-driven' EWB, where the origin of dark matter is deeply connected with that of the baryon asymmetry (Li *et al* 2009).

As possible experimental EWB tests, it was recently pointed out that the EDM size for the electron and for the neutron is bounded from below in EWB (Li *et al* 2010), as a result of unavoidable electro-weak two-loop contributions (Li *et al* 2008). The issue of producing a strong enough first-order phase transition in supersymmetry (Carena *et al* 2009) has also been investigated, together with the possibility of enhancing the first-order character altering the Higgs sector, for instance adding a singlet scalar field (Pietroni 1993, Apreda *et al* 2002, Profumo *et al* 2007). Questions related to the gauge dependence of criteria identifying strong enough first-order EW phase transitions have also been recently studied (Patel and Ramsey-Musolf 2011).

Numerous recent efforts targeted the 'coincidence problem' given by the ratio of the baryonic density Ω_b to non-baryonic dark matter density Ω_{DM} being of order unity ($\Omega_{DM}/\Omega_b \sim 5$). A variety of proposals have been recently put forward, including darkogenesis (Shelton and Zurek 2010), xogenesis (Buckley and Randall 2010) and hylogenesis (Davoudias *et al* 2010) that for reasons of space we cannot review here.

Remarkable progress has also been made on the front of leptogenesis models (for a comprehensive review see Giudice *et al* (2004)). Recent developments include the flavordynamics of leptogenesis (Pilaftsis 2005) and resonant leptogenesis near the electroweak phase transition (Pilaftsis and Underwood 2005). Some of these models might be testable with the LHC and with experiments sensitive to lepton-number and/or lepton-flavor violation (Pilaftsis 2009).

6.4.3. Direct dark matter detection. A wide spread experimental campaign is afoot to search for signatures of Galactic dark matter scattering off ordinary matter nucleons. These efforts are theoretically motivated by various compelling considerations (Goodman and Witten 1985) and typically target weakly interacting massive particles (WIMPs), although axion searches have also been very active in the last decade (Duffy and van Bibber 2009).

WIMPs can undergo elastic or inelastic scattering processes with nucleons (in the latter case exciting or ionizing the target atom, or producing the nuclear emission of a photon). The possibility of WIMPs transitioning themselves to an excited state has also been envisioned (Tucker-Smith and Weiner 2001). We briefly review here elastic dark matter scattering only, a process that can occur via spin-dependent or spin-independent interactions. The nuclear recoil induced by WIMP scattering can produce light (scintillation), charge (ionization) and/or phonon (heat) signals. In practice, current generation direct detection experiments are typically sensitive to two or more of these

signals, with the aim of achieving the best possible background rejection. Experiments that make use of scintillation and ionization include for instance XENON (Aprile *et al* 2010) and ZEPLIN (ZonEd Proportional scintillation in LIquid Noble gases; Akimov *et al* (2010)); among those that use scintillation and heat is CRESST (Cryogenic Rare Event Search with Superconducting Thermometers) (Angloher *et al* 2008), while CDMS (Cryogenic Dark Matter Search) (Akerib *et al* 2006) and EDELWEISS (Expérience pour DEtecter Les Wimps En Site Souterrain) (Gerbier 2010) make use of both ionization and heat. Other experimental setups that make use of one channel only include the scintillation experiment DAMA/LIBRA (DArk MAtter/Large sodium Iodide Bulk for RAre processes) (Bernabei *et al* 2010) or the ionization experiment CoGeNT (Contact Germanium Neutrino Telescope) (Aalseth *et al* 2008). Interestingly, the latter two experiments recently reported controversial signals that have been attributed to Galactic dark matter (Fitzpatrick *et al* 2010).

The first positive direct detection signal has been reported by the DAMA collaboration, with a rather impressive total exposure of 1.17 ton-yr (combining DAMA/NaI (DArk MAtter/Sodium–Iodine Target) and DAMA/LIBRA), which quotes an annual modulation in the recoil energy range of 2–6 keV electron equivalent at the 8.9σ confidence level (Bernabei *et al* 2010). The WIMP elastic-scattering interpretation of this signal is largely inconsistent with limits reported by XENON (Angle *et al* 2008) and CDMS (CDMS II Collaboration 2010). The CoGeNT experiment reported an exponential-like excess of events in the few keV energy range, compatible with a light-mass WIMP (Aalseth *et al* 2011). Anomalous events have also been reported by CRESST and CDMS, although with relatively low statistical significance. Figure 11 presents a sample of recent experimental and theoretical results on direct dark matter detection on the plane defined by the WIMP mass and the spin-independent WIMP-proton scattering cross-section. The regions shaded in light red are compatible with the DAMA/LIBRA modulation signal (Bernabei *et al* 2010), while the theoretical expectation for the scattering cross-section in the constrained minimal supersymmetric Standard Model (CMSSM) is shown with the blue and green shaded areas (see Trotta *et al* (2008) for more details). The figure also shows selected experimental limits, that rule out the corresponding upper-right corners of the plot. The limits shown are from the CDMS (dark blue), ZEPLIN (light blue) and CoGeNT (red dotted) experiments. We also indicate the projected reach of ton-size class experiments with a black dotted line. In summary, in the last ten years the field of direct dark matter searches reached a stage of full maturity. It is exploring interesting regions of theoretically favored parameter space and tantalizing signals are emerging from more than one experiment.

6.4.4. Indirect dark matter detection. Many theoretically motivated models for dark matter, including weakly interacting massive particles WIMPs, predict that dark matter pair-annihilates into ordinary Standard Model particles. Searches for the annihilation debris of dark matter are generically dubbed 'indirect dark matter detection'. In the last decade,
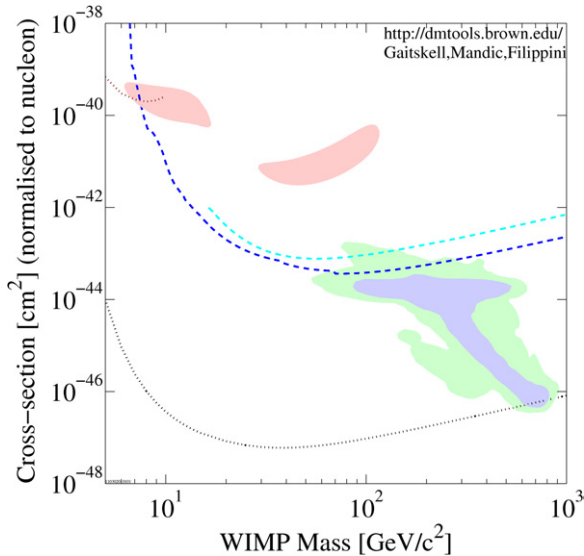
Figure 11. The plane of dark matter-proton spin-independent cross-section versus mass. The dark and light blue lines indicate constraints from CDMS and ZEPLIN, respectively, while the red dotted line is from CoGeNT: parameter space points above the lines are experimentally excluded. The light red areas represent regions compatible with the positive annual modulation signal from DAMA/LIBRA (Bernabei *et al* 2010). The light green and blue regions indicate theoretical predictions for the 95% and 68% confidence level regions of CMSSM parameter space as determined in Trotta *et al* (2008). Plot obtained through http://dmtools.brown.edu.

indirect detection has been one of the primary science goals of several new experiments and telescopes looking for high-energy gamma rays, neutrinos and antimatter.

Most notably, the *Fermi gamma-ray space telescope* (Atwood *et al* 2009) sets significant limits on the pair-annihilation rate of dark matter from the non-observation, in gamma rays, of nearby dwarf spheroidal galaxies (Abdo *et al* 2010a), of clusters of galaxies (Ackermann *et al* 2010a) and of monochromatic gamma-ray lines (Abdo *et al* 2010b). Atmospheric Cherenkov telescopes, such as the Very Energetic Radiation Imaging Telescope Array System (VERITAS), the High Energy Stereoscopic System (HESS) and the Major Atmospheric Imaging Cherenkov (MAGIC) telescope, have also produced interesting limits, for higher mass dark matter candidates (Aharonian *et al* 2006). Construction of the IceCube neutrino telescope at the South Pole was recently completed and the IceCube collaboration has delivered the first limits on dark matter annihilation in the Galactic Center (Abbasi *et al* 2010, 2011) and from particles captured from the center of the Sun (Heros 2010).

Anomalies in the high-energy flux of cosmic ray positrons, including the rising positron fraction measured by the *Payload for Antimatter Matter Exploration and Light-nuclei Astrophysics* (*PAMELA*) satellite (Adriani *et al* 2009) in the 10–100 GeV range and the hard positron-plus-electron flux reported by *Fermi* (Ackermann *et al* 2010b), triggered a great deal of excitement as possible signatures of dark matter annihilation (Arkani-Hamed *et al* 2009) or decay (Arvanitaki *et al* 2009). Astrophysical explanations, including nearby mature pulsars (Profumo 2008) as well as *in situ* secondary

particle acceleration (Blasi 2009), have also been put forward as plausible counterparts to the cosmic-ray electron–positron anomalies.

Other signatures that have been associated with Galactic dark matter annihilation include the *WMAP* haze (Hooper *et al* 2007), a diffuse radio emission that could be related to electrons and positrons produced by dark matter and possibly a gamma-ray haze (Dobler *et al* 2010). The evidence for the latter has been questioned (Linden and Profumo 2010). Recent re-analyses point toward two giant gamma-ray 'bubbles' whose morphology appears incompatible with a dark matter origin (Su *et al* 2010).

6.4.5. Dark matter theory. The last decade has seen giant leaps in theoretical studies concerning dark matter. On the one hand, simulation of structure formation in collisionless cold dark matter cosmologies has achieved unprecedented resolution and level of detail; on the other hand, model building inspired by possible experimental signals or by pure theoretical arguments has triggered interesting new particle physics scenarios.

In the field of *N*-body simulations, which only include gravitationally interacting dark matter, three milestones, among several other exciting simulations, have been the Millennium (Springel *et al* 2005), Via Lactea (Diemand *et al* 2007) and Bolshoi (Klypin *et al* 2011) simulations. While Millennium, in 2005, provided the basis for hundreds of studies on statistical properties of dark matter halos and on models for galaxy formation in a cosmological setting (including mock catalogues and merger trees), Bolshoi (completed in 2010) uses an updated set of cosmological parameters and will play a similar role in the immediate future. The Via Lactea suite of simulations specialized on Milky-Way-size dark matter structure, with important implications for indirect (Diemand *et al* 2007) and direct (Kuhlen *et al* 2010) dark matter searches. An important issue that will dominate future studies of the dark matter distribution is the effect of baryons on the dark matter density profiles (Duffy *et al* 2010).

On the model-building frontier, numerous studies explored in detail the phenomenology of supersymmetric models in collider, direct and indirect detection (Baer *et al* 2005). Several groups focused on statistical analyses of the supersymmetric (SUSY) parameter space, based upon, e.g., a Bayesian approach (Trotta *et al* 2008). Numerous theoretical model-building efforts concentrated on explaining observed anomalies in dark matter search experiments. These include leptophilic models (Fox and Poppitz 2009), models with a Sommerfeld enhancement at low dark matter relative velocities (Pospelov *et al* 2008), discussed to account for claimed indirect detection signals, and inelastic (Tucker-Smith and Weiner 2001) dark matter models, proposed to interpret direct dark matter signals.

7. Discussion and outlook for the future

Our astrophysical understanding of the cosmos continues to be propelled forward by advances in laboratory astrophysics. This review has touched on many, but far from all, of the

achievements of the past decade. The coming decade promises to be equally, if not more, fruitful. The Astro 2010 Survey Report and Panel Reports (Blandford *et al* 2010a, 2010b) have laid out a series of exciting scientific objectives, the achievement of which they point out is going to require numerous advances in laboratory astrophysics. We direct the reader to those reports for a detailed discussion.

Additional in depth discussions about the laboratory astrophysics needs and opportunities for the coming decade can be found in a number of white papers written over the past few years. These include those submitted by the Working Group on Laboratory Astrophysics (WGLA) to the Astro 2010 Survey (Brickhouse *et al* 2009a, 2009b, 2009c, 2009d, 2009e) as well as community input to Astro 2010 through the Science White Papers (http://sites.nationalacademies.org/BPA/BPA_050603) and the Laboratory Astrophysics White Papers (http://sites.nationalacademies.org/BPA/BPA_051118). Another white paper is that submitted by the WGLA to the US National Research Council Planetary Science Decadal Survey: 2013–2022 (Gudipati *et al* 2009). In plasma laboratory astrophysics, there have been a couple of reports recently released by the community (Prager *et al* 2010, Rosner and Hammer 2010). And most recently there is the white paper from the 2010 Laboratory Astrophysics Workshop sponsored by the Astrophysics Division of the Science Mission Directorate which covered atomic, molecular, condensed matter and plasma laboratory astrophysics (Savin *et al* 2011). These all point the way to the future and the richness of discovery which we can only just begin to guess.

Acknowledgments

Appendix. Acronyms

A complete list of the acronyms used throughout the text is given in table A1.

Table A1. List of acronyms used in the text.

Acronym	Phrase
AGB	asymptotic giant branch
AGN	active galactic nucleus
AGNs	active galactic nuclei
ANITA	ANtarctic Impulsive Transient Antenna
BBN	Big Bang nucleosynthesis
ccSNe	core collapse supernovae
CDMS	Cryogenic Dark Matter Search
CKM	Cabibbo–Kobayashi–Maskawa
CMB	cosmic microwave background
CN	carbon–nitrogen
CNO	carbon–nitrogen–oxygen
CoGeNT	Contact Germanium Neutrino Telescope
CP	charge-parity
CMSSM	constrained minimal supersymmetric Standard Model
CRESST	Cryogenic Rare Event Search with Superconducting Thermometers
CVs	cataclysmic variables
DAMA/LIBRA	DArk MAtter/Large sodium Iodide Bulk for RAre processes
DAMA/NaI	DArk MAtter/sodium–iodine target
DIB	diffuse interstellar absorption band
EDELWEISS	Expérience pour DEtecter Les Wimps En Site Souterrain
EDM	electric dipole moment
EOS	equations of state
EWB	electro-weak baryogenesis
FRIB	Facility for Rare Isotope Beams
FTIR	Fourier transform infrared
GRB	gamma ray burst
GUT	Grand Unified Theory
GZK	Greisen–Zatsepin–Kuz'min
HEDLA	High Energy Density Laboratory Astrophysics
HESS	High Energy Stereoscopic System
IAU	International Astronomical Union
IR	infrared
ISM	interstellar medium
KBO	Kuiper belt object
LHC	Large Hadron Collidor
LMC	Large Magellanic Cloud
LTE	local thermodynamic equilibrium
LUNA	Laboratory for Underground Nuclear Astrophysics
MAGIC	Major Atmospheric Imaging Cherenkov
MHD	magnetohydrodynamic
MRI	magnetorotational instability

Table A1. (Continued.)

MST	Madison Symmetric Torus
NN	nucleon–nucleon
PAH	polycyclic aromatic hydrocarbon
PAMELA	*Payload for Antimatter Matter Exploration and Light-nuclei Astrophysics*
PIC	particle-in-cell
QCD	quantum chromodynamics
QSO	quasi-stellar object
RHIC	Relativistic Heavy Ion Collidor
RICE	Radio Ice Cherenkov Experiment
SEM-EDX	scanning electron microscopy using energy-dispersive x-ray
SMC	Small Magellanic Cloud
SN	supernova
SNe	supernovae
SNO	Sudbury Neutrino Observatory
SNR	supernova remnant
SSM	standard solar model
SUSY	supersymmetric
TEM	transmission electron microscopy
TMC	Taurus molecular cloud
TNO	trans Neptunian object
TOF-SIMS	time of flight secondary ion mass spectrometry
TRACE	*Transition Region And Coronal Explorer*
T2K	Tokai-to-Kamioka
UHE	ultra-high-energy
UIR	unidentified infrared
UTA	unresolved transition array
UV	ultraviolet
VERITAS	Very Energetic Radiation Imaging Telescope Array System
YSO	young stellar object
WGLA	Working Group on Laboratory Astrophysics
WIMP	weakly interacting massive particles
WMAP	*Wilkinson Microwave Anisotropy Probe*
XDR	x-ray dominated region
XMM	*X-ray Multi-Mirror* mission
ZEPLIN	ZonEd Proportional scintillation in LIquid Noble gases
3D	three-dimensional

References

Aalseth C E *et al* 2008 *Phys. Rev. Lett.* **101** 251301

Aalseth C E *et al* 2011 *Phys. Rev. Lett.* **106** 131301

Abbasi R *et al* 2010 *Astrophys. J.* **732** 18

Abbasi R *et al* 2011 *Phys. Rev.* D **84** 022004

Abe K *et al* 2011 *Phys. Rev.* D **83** 052010

Abel N P, Federman S R and Stancil P C 2008 *Astrophys. J.* **675** L81–L84

Abdo A A *et al* 2010a *Astrophys. J.* **712** 147–58

Abdo A A *et al* 2010b *Phys. Rev. Lett.* **104** 091302

Ackermann M *et al* 2010a *J. Cosmol. Astropart. Phys.* **1005** 025

Ackermann M *et al* 2010b *Phys. Rev.* D **82** 092004

Adelberger E G *et al* 2011 *Rev. Mod. Phys.* **83** 195–245

Adriani O *et al* 2009 *Nature* **458** 607–9

Agúndez M, Cernicharo J and Guĺín M 2007 *Astrophys. J.* **662** L91–L94

Agúndez M, Cernicharo J and Goicoechea J R 2008a *Astron. Astrophys.* **483** 831–7

Agúndez M, Cernicharo J, Pardo J, Fonfría Expósito J P, Guélin M, Tenenbaum E D, Ziurys L M and Apponi A J 2008b *Astrophys. Space Sci.* **313** 229–33

Agúndez M *et al* 2010 *Astron. Astrophys.* **517** L2

Aharmim B *et al* 2010 *Phys. Rev.* C **81** 055504

Aharonian F *et al* 2006 *Phys. Rev. Lett.* **97** 221102

A'Hearn M F 2008 *Space Sci. Rev.* **138** 237–46

Akimov D Y *et al* 2010 *Phys. Lett.* B **692** 180–3

Akerib D S *et al* 2006 *Phys. Rev. Lett.* **96** 011302

Alessandro B *et al* 2011 arXiv:1101.1852

Allamandola L J, Tielens A G G M and Barker J R 1989 *Astrophys. J. Suppl. Ser.* **71** 733–75

Alonso-Medina A, Colón C and Rivero C 2005 *Phys. Scr.* **71** 154–8

Altun Z, Yumak A, Badnell N R, Loch S D and Pindzola M S 2006 *Astron. Astrophys.* **447** 1165–74

Altun Z, Yumak A, Yavuz I, Badnell N R, Loch S D and Pindzola M S 2007 *Astron. Astrophys.* **474** 1051–9

Amano T 2010 *Astrophys. J.* **716** L1–L3

Anderson H M, den Hartog E A and Lawler J E 1996 *J. Opt. Soc. Am.* B **13** 2382–91

Ando S, Cyburt R H, Hong S W and Hyun C H 2006 *Phys. Rev.* C **74** 025809

Angloher G *et al* 2008 The CRESST dark matter search *IDM2008: Identification of Dark Matter (Stockholm, Sweden, 18–22 Aug. 2008)* 014

Angle J *et al* 2008 *Phys. Rev. Lett.* **100** 021303

Apponi A J, Barclay W L Jr and Ziurys L M 1993 *Astrophys. J.* **414** L129–L132

Apreda R, Maggiore M, Nicolis A and Riotto A 2002 *Nucl. Phys.* B **631** 342–68

Aprile E and Profumo S 2009 *New J. Phys.* **11** 105002

Aprile E *et al* 2010 *Phys. Rev.* A **105** 131302

Araki M, Furuya T and Saito S 2001 *J. Mol. Spectrosc.* **210** 132–6

Arkani-Hamed N, Finkbeiner D P, Slatyer T R and Weiner N 2009 *Phys. Rev.* D **79** 015014

Arlandini C, Käppeler F, Wisshak K, Gallino R, Lugaro M, Busso M and Straniero O 1999 *Astrophys. J.* **525** 886–900

Arnett W D, Bahcall J N, Kirschner R P and Woosley S E 1989 *Annu. Rev. Astron. Astrophys.* **27** 629–700

Arnould M, Paulus G and Jorissen A 1992 *Astron. Astrophys.* **254** L9–L12

Arpesella C *et al* 2008 *Phys. Rev. Lett.* **101** 091302

Arvanitaki A, Dimopoulos S, Dubovsky S, Graham P W, Harnik R and Rajendran S 2009 *Phys. Rev.* D **80** 055011

Askaryan G A 1962 *Sov. Phys.—JETP* **14** 441–3

Askaryan G A, Dolgoshein B A, Kalinovsky A N and Mokhov N V 1979 *Nucl. Instrum. Methods* **164** 267–78

Asplund M, Grevesse N, Sauval A J, Allende Prieto C and Kiselman D 2004 *Astron. Astrophys.* **417** 751–68

Atwood W B *et al* 2009 *Astrophys. J.* **697** 1071–102

Aver E, Olive K A and Skillman E D 2010 *J. Cosmol. Astropart. Phys.* JCAP5(2010)003

Baby L T *et al* 2003a *Phys. Rev. Lett.* **90** 022501

Baby L T *et al* 2003b *Phys. Rev.* C **67** 065805

Bachiller R, Forveille T, Huggins P J and Cox P 1997 *Astron. Astrophys.* **324** 1123–34

Bacmann A, Lefloch B, Ceccarelli C, Castets A, Steinarker J and Loinard L 2002 *Astron. Astrophys.* **389** L6–L10

Bacmann A, Lefloch B, Ceccarelli C, Steinacker J, Castets A and Loinard L 2003 *Astrophys. J.* **585** L55–L58

Badenes C, Borkowski K, Hughes J P, Hwang U and Bravo E 2006 *Astrophys. J.* **645** 1373–91

Badenes C, Hughes J P, Cassam-Chenaï G and Bravo E 2008a *Astrophys. J.* **680** 1149–57

Badenes C, Bravo E and Hughes J P 2008b *Astrophys. J.* **680** L33–L36

Badenes C, Harris J, Zaritsky D and Prieto J L 2009 *Astrophys. J.* **700** 727–40

Badnell N R, O'Mullane M G, Summers H P, Altun Z, Bautista M A, Colgan J, Gorczyca T W, Mitnik D M, Pindzola M S and Zatsarinny O 2003 *Astron. Astrophys.* **406** 1151–65 http://amdpp.phys.strath.ac.uk/tamoc/DR/

Badnell N R 2006a *Astrophys. J.* **651** L73–L76
Badnell N R 2006b *J. Phys. B: At. Mol. Opt. Phys.* **39** 4825–52
Badnell N R 2006c *Astrophys. J. Suppl. Ser.* **167** 334–42
    http://amdpp.phys.strath.ac.uk/tamoc/RR/
Baer H, Mustafayev A, Profumo S, Belyaev A and Tata X 2005
    J. High Energy Phys. JHEP07(2005)065
Bahcall J N, Serenelli A M and Pinsonneault M 2004 *Astrophys. J.*
    614 464–71
Bahcall J N, Basu S, Pinsonneault M and Serenelli A M 2005a
    Astrophys. J. **618** 1049–56
Bahcall J N, Serenelli A M and Basu S 2005b *Astrophys. J.*
    621 L85–8
Bailey J E *et al* 2001 *J. Quant. Spectrosc. Radiat. Transfer*
    71 157–68
Bailey J E *et al* 2007 *Phys. Rev. Lett.* **99** 265002
Bailey J E, Gochau G A, Mancini R C, Igelsias C A, MacFarlane J J,
    Golovkin I E, Blancard C, Cosse Ph and Faussurier G 2009
    Phys. Plasmas **16** 058101
Balbus S A and Hawley J F 1991 *Astrophys. J.* **376** 214–22
Balbus S A and Hawley J F 1998 *Rev. Mod. Phys.* **70** 1–53
Baker C A *et al* 2006 *Phys. Rev. Lett.* **97** 131801
Bardayan D W *et al* 2000 *Phys. Rev.* C **62** 055804
Bardayan D W *et al* 2002 *Phys. Rev. Lett.* **89** 262501
Barwick S *et al* 2006 *Phys. Rev. Lett.* **96** 171101
Basu S and Antia M H 2008 *Phys. Rep.* **457** 217–83
Basu S 2010 *Astrophys. Space Sci.* **328** 43–50
Bates D R and Lewis J T 1955 *Proc. Phys. Soc. Lond.* A **68** 173–80
Bauman R P, Porter R L, Ferland G J and MacAdam K B 2005
    Astrophys. J. **628** 541–4
Bauschlicher C W, Ram R S, Bernath P F, Parsons C G and
    Galehouse D 2001 *J. Chem. Phys.* **115** 1312–18
Bauschlicher C W, Boersma C, Ricca A, Mattioda A L, Cami J,
    Peeters E, Sánchez de Armas F, Puerta Saborido G,
    Hudgins D M and Allamandola L J 2010 *Astrophys. J. Suppl.
    Ser.* **189** 341–5
Bean J, Kempton E M-R and Homeier D 2010 *Nature*
    468 669–72
Behar E, Sako M and Kahn S M 2001 *Astrophys. J.* **563** 497–504
Behar E, Rasmussen A P, Blustin A J, Sako M, Kahn S M, Kaastra J
    S, Branduardi-Raymont G and Steenbrugge K C 2003
    Astrophys. J. **598** 232–41
Beiersdorfer P 2003 *Ann. Rev. Astron. Astrophys.* **41** 343–90
Beiersdorfer P, Olson R E, Brown G V, Harris C L, Neill P A,
    Schweikhard L, Utter S B and Widmann K 2000 *Phys. Rev.
    Lett.* **85** 5090–3
Beiersdorfer P *et al* 2003 *Science* **300** 1558–60
Bekooy J P, Verhoeve P, Meerts W L and Dymanus A 1985 *J. Chem.
    Phys.* **82** 3868–9
Bellan P M 2005 *Phys. Plasmas* **12** 058301
Bellan P M, You S and Hsu S C 2005 *Astrophys. Space Sci.*
    298 203–9
Bemmerer D *et al* 2006a *Phys. Rev. Lett.* **97** 122502
Bemmerer D *et al* 2006b *Nucl. Phys.* A **779** 297–317
Bemmerer D *et al* 2009 *J. Phys. G: Nucl. Part Phys.* **36** 045202
Benjamin R A, Skillman E D and Smits D P 1999 *Astrophys. J.*
    514 307–24
Bergerson W F, Forest C B, Fiksel G, Hannum D A, Kendrick R,
    Sarff J S and Stambler S 2006 *Phys. Rev. Lett.* **96** 015004
Bernabei R *et al* 2010 *Eur. Phys. J.* C **67** 39–49
Bernstein M P, Dworkin J P, Sandford S A, Cooper G W and
    Allamandola L J 2002 *Nature* **416** 401–3
Bhardwaj A *et al* 2007 *Planet. Space Sci.* **55** 1135–89
Biémont E, Palmeri P, Quinet P, Zhang Z G and Svanberg S 2002
    Astrophys. J. **567** 1276–83
Blandford R *et al* 2010a *New Worlds, New Horizons in Astronomy
    and Astrophysics* (Washington, DC: National Academies Press)
Blandford R *et al* 2010b *Panel Reports—New Worlds, New Horizons
    in Astronomy and Astrophysics* (Washington, DC: National
    Academies Press)

Blasi P 2009 *Phys. Rev. Lett.* **103** 051104
Blondin J M, Fryxell B A and Konigl A 1990 *Astrophys. J.*
    360 370–86
Blustein A J, Branduardi-Raymont G, Behar E, Kaastra J S, Kahn S
    M, Page M J, Sako M and Steenbrugge K C 2002 *Astron.
    Astrophys.* **392** 453–67
Bockelée-Morvan D, Crovisier J, Mumma M J and Weaver H A
    2004 *COMETS II* ed M Festou *et al* (Tuscon, AZ: University of
    Arizona Press) pp 391–423
Bolton S 2006 *36th COSPAR Scientific Assembly, COSPAR, Plenary
    Meeting (Beijing)* vol 36, pp 3775
Bonetti R *et al* 1999 *Phys. Rev. Lett.* **82** 5205–8
Borucki W J *et al* 2010 *Science* **327** 977–80
Bouquet S *et al* 2004 *Phys. Rev. Lett.* **92** 225001
Bouwman J, Meeus G, de Koter A, Hony S, Dominik C, Waters L B
    F M 2001 *Astron. Astrophys.* **375** 950–62
Bouwman J, Cuppen H M, Bakker A, Allamandola L J and Linnartz
    H 2010 *Astron. Astrophys.* **511** A33
Bozier J C, Thiell G, Le-Breton J P, Azra S, Decroisette M and
    Schirmann D 1986 *Phys. Rev. Lett.* **57** 1304–7
Bradley J 2010 *Astromineralogy* (*Lecture Notes in Physics* vol 815)
    ed T Henning (Berlin: Springer) pp 259–76
Bregman J N 2007 *Annu. Rev. Astron. Astrophys.* **45** 221–59
Brickhouse N S and Schmelz J T 2006 *Astrophys. J.*
    636 L53–L56
Brickhouse N S *et al* 2009a arXiv:0902.4666
Brickhouse N S *et al* 2009b arXiv:0902.4681
Brickhouse N S *et al* 2009c arXiv:0902.4688
Brickhouse N S *et al* 2009d arXiv:0902.4747
Brickhouse N S *et al* 2009e arXiv:0902.4882
Brickhouse N S, Cranmer S R, Dupree A K, Luna G J M and
    Wolk S 2010 *Astrophys. J.* **710** 1835–47
Broggini C, Bemmerer D, Guglielmetti A and Menegazzo R 2010
    Annu. Rev. Nucl. Part. Sci. **60** 53
Bronson-Messer O E, Hix W R, Liebendörfer M and Mezzacappa A
    2003 *Nucl. Phys.* A **718** 449–51
Brown G V, Beiersdorfer P, Liedahl D A, Widmann K and
    Kahn S M 1998 *Astrophys. J.* **502** 1015–26
Brown G V, Beiersdorfer P, Liedahl D A, Widmann K and
    Kahn S M 2000 *Astrophys. J.* **532** 1245 (erratum)
Brown G V, Beiersdorfer P, Chen H, Chen M H and Reed K J 2001
    Astrophys. J. **557** L75–L78
Brown J M and Müller H S P 2009 *J. Mol. Spectrosc.*
    255 68–71
Brown M R, Cothran C D, Landreman M, Schlossberg D and
    Matthaeus W 2002 *Astrophys. J.* **577** L63–L66
Brown T A D, Bordeanu C, Snover K A, Storm D W, Melconian D,
    Sallaska A L, Sjue S K L and Triambak S 2007 *Phys. Rev.* C
    76 055801
Brownlee *et al* 2006 *Science* **314** 1711–16
Bruhns H *et al* 2010a *Rev. Sci. Instrum.* **81** 013112
Bruhns H, Kreckel H, Miller K A, Urbain X and Savin D W 2010b
    Phys. Rev. A **82** 042708
Brünken S, Gupta H, Gottlieb C A, McCarthy M C and Thaddeus P
    2007 *Astrophys. J.* **664** L43–L46
Buckley M R and Randall L 2010 arXiv:1009.0270
Burrows A, Ram R S, Bernath P, Sharp C M and Milsom J A 2002
    Astrophys. J. **577** 986–92
Burrows A, Dulick M, Bauschlicher C W, Bernath P F, Ram R S,
    Sharp C M and Milsom J A 2005 *Astrophys. J.* **624** 988–1002
Busquet M *et al* 2007 *High Energy Density Phys.* **3** 8–11
Busso M, Gallino R and Wasserburg G J 1999 *Annu. Rev. Astron.
    Astrophys.* **37** 239–309
Byun D-Y, Koo B-C, Tatematsu K and Sunada K 2006 *Astrophys. J.*
    637 283–95
Calder A *et al* 2002 *Astrophys. J.* **143** 201–29
Calvet N and Gullbring E 1998 *Astrophys. J.* **509** 802–18
Calzavara A J and Matzner C D 2004 *Mon. Not. R. Astron. Soc.*
    351 694–706

Cami J, Bernard-Salas J, Peeters E and Malek S E 2010 *Science* **329** 1180–2

Canto J, Tenorio-Tagle G and Rozyczka M 1988 *Astron. Astrophys.* **192** 287–94

Carena M, Nardini G, Quiros M and Wagner C E M 2009 *Nucl. Phys.* B **812** 243–63

Cartledge S I B, Meyer D M and Lauroesch J T 2003 *Astrophys. J.* **597** 408–13

Cartledge S I B, Lauroesch J T, Meyer D M and Sofia U J 2006 *Astrophys. J.* **641** 327–46

Castelli F, Gratton R G and Kurucz R L 1997 *Astron. Astrophys.* **318** 841–69

Castelli F and Kurucz R L 2004 *Astron. Astrophys.* **419** 725–33

CDMS II Collaboration 2010 *Science* **327** 1619–21

Cernicharo J, Guélin M, Agúndez M, Kawaguchi K, McCarthy M and Thaddeus P 2007 *Astron. Astrophys.* **467** L37–L40

Chafa A *et al* 2007 *Phys. Rev.* C **75** 035810

Chakraborty N, Fields B D and Olive K A 2010 *Phys. Rev.* D **83** 063006

Chakravorty S, Kembhavi A K, Elvis M, Ferland G and Badnell N R 2008 *Mon. Not. R. Astron. Soc.* **384** L24–L28

Chakravorty S, Kembhavi A K, Elvis M, Ferland G and Badnell N R 2009 *Mon. Not. R. Astron. Soc.* **393** 83–98

Charbonneau D *et al* 2005 *Astrophys. J.* **626** 523–9

Charbonneau D, Knutson H A, Barman T, Allen L E, Mayor M, Megeath S T, Queloz D and Udry S 2008 *Astrophys. J.* **686** 1341–8

Charbonnel C, Tosi M, Primas and Chiappini C 2010 *Light Elements in the Universe* (*Proc. IAU Symp.* vol 268) (Cambridge: Cambridge University Press)

Chastaing D, Le Picard S D, Sims I R and Smith I W M 2001 *Astron. Astrophys.* **365** 241–7

Chen D, Gao H and Kwong V H 2003 *Phys. Rev.* A **68** 052703

Chen G-X 2008 *Mon. Not. R. Astron. Soc.* **386** L62–L66

Chen J-W and Savage M J 1999 *Phys. Rev.* C **60** 065205

Chen G-X, Smith R K, Kirby K, Brickhouse N S and Wargelin B J 2006 *Phys. Rev.* A **74** 042709

Chevalier R A 1992 *Nature* **355** 691–6

Chevalier R A and Fransson C 2008 *Astrophys. J.* **683** L135–L138

Chevalier R A and Imamura J N 1982 *Astrophys. J.* **261** 543–9

Chiar J E and Tielens A G G M 2006 *Astrophys. J.* **637** 774–85

Chipps K A *et al* 2009 *Phys. Rev. Lett.* **102** 152502

Chowdhury P K, Merer A J, Rixon S J Bernath P F and Ram R S 2005 *Phys. Chem. Chem. Phys.* **8** 822–6

Christensen-Dalsgaard J, di Mauro M P, Houdek G and Pijpers F 2009 *Astron. Astrophys.* **494** 205–8

Chugai N N and Chevalier R A 2006 *Astrophys. J.* **641** 1051–9

Ciardi A, Lebedev S V, Frank A, Suzuki-Vidal, F, Hall G N, Bland S N, Harvey-Thompson A, Blackman E G and Camenzind M 2009 *Astrophys. J.* **691** L147–L150

Cirigliano V, Profumo S and Ramsey-Musolf M J 2006 *J. High Energy Phys.* JHEP07(2006)002

Cirigliano V, Li Y, Profumo S and Ramsey-Musolf M J 2010 *J. High Energy Phys.* JHEP01(2010)002

Clemett S J, Sandford S A, Nakamura-Messenger K, Horz F and McKay D S 2010 *Meteorit. Planet. Sci.* **45** 701–22

Coc A and Vangioni E 2010 *J. Phys.: Conf. Ser.* **202** 012001

Cody G D *et al* 2008 *Meteorit. Planet. Sci.* **43** 353–65

Cohen D, MacFarlane J, Bailey J and Liedahl D 2003 *Rev. Sci. Instrum.* **74** 1962–5

Cohen D H, Leutenegger M A, Wollman E E, Zsargó J, Hillier D J, Townsend R H D and Owocki S P 2010 *Mon. Not. R. Astron. Soc.* **405** 2391–405

Commins E D, Ross S B, DeMille D and Regan B C 1994 *Phys. Rev.* A **50** 2960–77

Confortola F *et al* 2007 *Phys. Rev.* C **75** 065803

Cordiner M and Millar T J 2009 *Astrophys. J.* **697** 68–78

Costantini H, Formicola A, Imbriani G, Junker M, Rolfs C and Strieder F 2009 *Rep. Prog. Phys.* **72** 086301

Cothran C D, Brown M R, Grat T, Schaffer M J and Marklin G 2009 *Phys. Rev. Lett.* **103** 215002

Cowan J J and Sneden C 2006 *Nature* **440** 1151–6

Cowan J J and Thielemann F-K 2004 *Phys. Today* **57** 47–53

Cranmer S R, Panasyuk A V and Kohl J L 2008 *Astrophys. J.* **678** 1480–97

Cravens T E 1997 *Geophys. Res. Lett.* **24** 105–8

Cravens T E, Robertson I P and Snowden S L 2001 *J. Geophys. Res.* **106** 24883–92

Crespo Lopez-Urrutia J R, Neger T and Jager H 1994 *J. Phys. D: Appl. Phys.* **27** 994–8

Crovisier J, Leech K, Bockelee-Morvan D, Brooke T Y, Hanner M S, Altieri B, Keller H U and Lellouch E 1997 *Science* **275** 1904–7

Crovisier J *et al* 2004 *Astron. Astrophys.* **418** 1141–57

Curry J J, den Hartog E A and Lawler J E 1997 *J. Opt. Soc. Am.* B **14** 2788–99

Dalgarno A 1976 *Atomic Processes and Applications* ed P G Burke (Amsterdam: North-Holland) p 109

Davoudias H, Morrissey D E, Sigurdson K and Tulin S 2010 *Phys. Rev. Lett.* **105** 211304

De Vries M S, Reihs K, Wendt H R, Golden W G, Hunziker H E, Fleming R, Peterson E and Chang S 1993 *Geochim. Cosmochim. Acta* **57** 933–8

Deamer D, Dworkin J P, Sandford S A, Bernstein M P and Allamandola L J 2002 *Astrobiology* **2** 371–81

Decrock P *et al* 1991 *Phys. Rev. Lett.* **67** 808–11

Delbar Th *et al* 1993 *Phys. Rev.* C **48** 3088–96

DeMeo F E, Barucci M A, Merlin F, Guilbert-Lepoutre A, Alvarez-Candal A, Delsanti A, Fornasier S and de Bergh C 2010 *Astron. Astrophys.* **521** A35

Deming D, Seager S, Richardson L J and Harrington J 2005 *Nature* **434** 740–3

Demorest P B, Pennucci T, Ransom S M, Roberts M S E and Hessels J W T 2010 *Nature* **467** 1081–3

den Hartog E A, Curry J J, Wickliffe M E and Lawler J E 1998 *Sol. Phys.* **178** 239–44

den Hartog E A, Wiese L M and Lawler J E 1999 *J. Opt. Soc. Am.* B **16** 2278–84

den Hartog E A, Fedchak J A and Lawler J E 2001 *J. Opt. Soc. Am.* B **18** 861–5

den Hartog E A, Wickliffe M E and Lawler J E 2002 *Astrophys. J. Suppl. Ser.* **141** 255–65

den Hartog E A, Lawler J E, Sneden C and Cowan J J 2003 *Astrophys. J. Suppl. Ser.* **148** 543–66

den Hartog E A, Herd M T, Lawler J E, Sneden C, Cowan J J and Beers T C 2005 *Astrophys. J.* **619** 639–55

den Hartog E A, Lawler J E, Sneden C and Cowan J J 2006 *Astrophys. J. Suppl. Ser.* **167** 292–314

den Hartog E A, Lawler J E, Sobeck J S, Sneden C and Cowan J J 2011 *Astrophys. J. Suppl. Ser.* **194** 35

Dennerl K 2010 *Space Sci. Rev.* **157** 57–91

d'Enterria D, Engel R, Pierog T, Ostapchenko S and Werner K 2011 *Astropart. Phys.* **35** 98–113

di Leva A *et al* 2009 *Phys. Rev. Lett.* **102** 232502

Diemand J, Kuhlen M and Madau P 2007 *Astrophys. J.* **657** 262–70

Dine M and Kusenko A 2003 *Rev. Mod. Phys.* **76** 1–30

Dobler G, Finkbeiner D P, Cholis I, Slatyer T and Weiner N 2010 *Astrophys. J.* **717** 825–842

Doron R and Behar E 2002 *Astrophys. J.* **574** 518–26

Dorschner J and Henning T 1995 *Astron. Astrophys. Rev.* **6** 271–333

Dos Santos S F, Kokoouline V and Greene C H 2007 *J. Chem. Phys.* **127** 124309

Doss F W 2011 *PhD Thesis* University of Michigan

Doss F W, Robey H F, Drake R P and Kuranz C C 2009 *Phys. Plasmas* **16** 112705

Doss F W, Drake R P and Kuranz C C 2010 *High Energy Density Phys.* **6** 157–61

Draine B T 2003 *Annu. Rev. Astron. Astrophys.* **41** 241–89

Drake R P 1999 *J. Geophys. Res.* **104** 14505–15

Drake J J, Ratzlaff P W, Laming J M and Raymond J 2009 *Astrophys. J.* **703** 1224–9

Duffy L D and van Bibber K 2009 *New J. Phys.* **11** 105008

Duffy A R, Schaye J, Kay S T, Dalla Vecchia C, Battye R A and Booth C M 2010 *Mon. Not. R. Astron. Soc.* **405** 2161–78

Dworkin L P, Deamer D W, Sandford S A and Allamandola L J 2001 *Proc. Natl Acad. Sci. USA* **98** 815–19

Edens A D, Ditmire T, Hansen J F, Edwards M J, Adams R G, Rambo P K, Ruggles L, Smith I C and Porter J L 2005 *Phys. Rev. Lett.* **95** 244503

Edwards M J, MacKinnon A J, Zweiback J, Shigemori K, Ryutov D D, Rubenchik A M, Keitlty K A, Liang E, Remington B A and Ditmire T 2001 *Phys. Rev. Lett.* **87** 085004

Eggert J, Brygoo S, Loubeyre P, McWilliams R S, Celliers P M, Hicks D G, Boehly T R, Jeanloz R and Collins G W 2008 *Phys. Rev. Lett.* **100** 124503

Elsila J E, Dworkin J P, Bernstein M P, Martin M P and Sandford S A 2007 *Astrophys. J.* **660** 911–18

Elsila J E, Glavin D P and Dworkin J P 2009 *Meteorit. Planet. Sci.* **44** 1323–30

Emery J P, Cruikshank D P and van Cleve J 2006 *Icarus* **182** 496–512

Epp S W *et al* 2007 *Phys. Rev. Lett.* **98** 183001

Fabian J 1996 *Phys. Rev.* B **53** 13864–70

Falgarone E *et al* 2010 *Astron. Astrophys.* **521** L15

Falize E, Bouquet S and Michaut C 2009a *Astrophys. Space Sci.* **322** 107–11

Falize E, Michaut C, Cavet C, Bouquet S, Koenig M, Loupias B, Ravasio A and Gregory C G 2009b *Astrophys. Space Sci.* **322** 71–5

Falize E *et al* 2011 *Astrophys. Space Sci.* **726** 41–9

Farley D R, Estabrook K G, Glendinning S G, Glenzer S H, Remington B A, Shigemori K, Stone J M, Wallace R J, Zimmerman G B and Harte J A 1999 *Phys. Rev. Lett.* **83** 1982–5

Fedchak J A, den Hartog E A, Lawler J E, Palmeri P, Quinet P and Biémont E 2000 *Astrophys. J.* **542** 1109–18

Federman S R, Knauth D C and Lambert D L 2004 *Astrophys. J.* **603** L105–L108

Ferland G F, Korista K T, Verner D A, Ferguson J W, Kingdon J B and Verner E M 1998 *Publ. Astron. Soc. Pac.* **110** 761–78

Fesen R A, Zastrow J A, Hammell M C, Shull J M and Silvia D W 2011 *Astrophys. J.* **736** 109

Field G B, Goldsmith D W and Habing H J 1969 *Astrophys. J.* **155** L149

Fiksel G, Almagri A F, Chapman B E, Mirnov V V, Ren Y, Sarff J S and Terry P W 2009 *Phys. Rev. Lett.* **103** 145002

Fink U 2009 *Icarus* **201** 311–34

Fitzpatrick A L, Hooper D and Zurek K M 2010 *Phys. Rev. D* **81** 115005

Flynn *et al* 2006 *Science* **314** 1731–5

Foord M E *et al* 2004 *Phys. Rev. Lett.* **93** 055002

Foord M E *et al* 2006 *J. Quant. Spectrosc. Radiat. Transfer* **99** 712–29

Formicola A *et al* 2004 *Phys. Lett.* B **591** 61–8

Fortney J J and Nettelmann N 2010 *Space Sci. Rev.* **152** 423–47

Fortney J J, Glenzer S H, Koenig M, Militzer B, Saumon D and Valencia D 2009 *Phys. Plasmas* **16** 041003

Foster J M *et al* 2005 *Astrophys. J.* **634** L77–L80

Fox C, Iliadis C, Champagne A E, Fitzgerald R P, Longland R, Newton J, Pollanen J and Runkle R 2005 *Phys. Rev.* C **71** 055801

Fox P J and Poppitz E 2009 *Phys. Rev. D* **79** 083528

Fragile P C, Murray S D, Anninos P and van Breugel W 2004 *Astrophys. J.* **604** 74–87

Frum C I, Engleman R Jr, Hedderich H G, Bernath P F, Lamb L D and Huffman D R 1991 *Chem. Phys. Lett.* **176** 504–8

Fujioka *et al* 2009 *Nature Phys.* **5** 821–5

Fukugita M and Yanagida T 1986 *Phys. Lett.* B **174** 45–7

Fullerton A W, Massa D L and Prinja R K 2006 *Astrophys. J.* **637** 1025–39

Fussen D and Kubach C 1986 *J. Phys. B: At. Mol. Opt. Phys.* **19** L31–L34

Gailitis A *et al* 2000 *Phys. Rev. Lett.* **84** 4365–8

Gallo L C, Boller Th, Brandt W N, Fabian A C and Vaughan S 2004 *Astron. Astrophys.* **417** 29–38

Gao H and Kwong V H 2003 *Phys. Rev.* A **68** 052704

García-Hernández D A, Manchado A, García-Lario P, Stanghellini L, Villaver E, Shaw R A, Szczerba R and Perea-Calderón J V 2010 *Astrophys. J.* **724** L39–L43

Garg U *et al* 2007 *Nucl. Phys.* A **788** 36–43

Garrod R T and Herbst E 2006 *Astron. Astrophys.* **457** 927–36

Geppert W D and Larsson M 2008 *Mol. Phys.* **106** 2199–226

Gerbier G 2010 arXiv:1012.2260

Gibb E L, Whittet D C B, Boogert A C A and Tielens A 2004 *Astrophys. J. Suppl. Ser.* **151** 35–73

Gillaspy J D, Lin T, Tedesco L, Tan J N, Pomeroy J M, Laming J M, Brickhouse N, Chen G-X and Silver E 2011 *Astrophys. J.* **728** 132–43

Gillett F C, Forrest W J and Merrill K M 1973 *Astrophys. J.* **183** 87–93

Giudice G F, Notari A, Raidal M and Strumia A 2004 *Nucl. Phys.* B **685** 89–149

Glosík J, Korolov I, Plašil R, Novotný O, Kotrík T, Hlavenka P, Varju J, Mikhailov I A, Kokoouline V and Greene C H 2008 *J. Phys. B: At. Mol. Opt. Phys.* **41** 191001

Glosík J, Plašil R, Korolov I, Kotrík T, Novotný O, Hlavenka P, Dohnal P, Varju J, Kokoouline V and Greene C H 2009 *Phys. Rev.* A **79** 052707

Glover S C, Savin D W and Jappsen A-K 2006 *Astrophys. J.* **640** 553–68

Glover S C O and Abel T 2008 *Mon. Not. R. Astron. Soc.* **388** 1627–51

Goodman M W and Witten E 1985 *Phys. Rev. D* **31** 3059–63

Gorham P W, Saltzberg D, Field R C, Guillian E, Milinčić R, Miočinovič P, Walz D and Williams D 2005 *Phys. Rev. D* **72** 023002

Greenwood J B, Williams I D, Smith S J and Chutjian A 2000 *Phys. Rev.* A **63** 062707

Greisen K 1966 *Phys. Rev. Lett.* **16** 748–50

Griffith W C, Swallows M D, Loftus T H, Romalis M V, Heckel B R, Fortson E N 2009 *Phys. Rev. Lett.* **102** 101601

Grillmair C J, Burrows A, Charbonneau D, Armus L, Stauffer J, Meadows V, van Cleve J, von Braun K and Levine D 2008 *Nature* **456** 767–9

Grosdidier Y, Moffat A F J, Joncas G and Acker A 1998 *Astrophys. J.* **506** L127–L131

Grosskopf M J, Drake R P, Kuranz C C, Miles A R, Hansen J F, Plewa T, Hearn N, Arnett D and Wheeler J C 2009 *Astrophys. Space Sci.* **322** 57–63

Grun J, Stamper J, Manka C, Resnick J, Burris R, Crawford J and Ripin B H 1991 *Phys. Rev. Lett.* **66** 2738–41

Grundy W M and Schmitt B 1998 *J. Geophys. Res.* **103** 25809–22

Grundy W M, Young L A, Spencer J R, Johnson R E, Young E F and Buie M W 2006 *Icarus* **184** 543–55

Grupen C 2005 *Astroparticle Physics* (Berlin: Springer)

Gu M F 2004 *Astrophys. J. Suppl. Ser.* **153** 389–93

Gu M F, Holczer T, Behar E and Kahn S M 2006 *Astrophys. J.* **641** 1227–32

Gudipati M S 2004 *J. Phys. Chem.* A **108** 4412–9

Gudipati M S and Allamandola L J 2004 *Astrophys. J.* **615** L177–L180

Gudipati M S and Allamandola L J 2006 *J. Phys. Chem.* A **110** 9020–4

Gudipati M S *et al* 2009 arXiv:0910.0442

Gunther H M, Lewandowska N, Hundertmark M P G, Steinle H, Schmitt J, Buckley D, Crawford S, O'Donoghue D and Vaisanen P 2010 *Astron. Astrophys.* **518** A54

Guo B and Li Z H 2007 *Chin. Phys. Lett.* **24** 65–8

Gupta H *et al* 2010 *Astron. Astrophys.* **521** L47

Guzman J and Plewa T 2009 *Nonlinearity* **22** 2775–97

Gyurky G *et al* 2007 *Phys. Rev.* C **75** 035805

Halfen D T and Ziurys L M 2004 *Astrophys. J.* **611** L65–L68

Halfen D T, Sun M, Clouthier D J and Ziurys L M 2009 *J. Chem. Phys.* **130** 014305

Hammache F *et al* 1998 *Phys. Rev. Lett.* **80** 928

Hammache F *et al* 2001 *Phys. Rev. Lett.* **86** 3985

Hanner M S and Zolensky M E 2010 *Astromineralogy* (*Lecture Notes in Physics* vol 815) ed T Henning (Berlin: Springer) pp 275–315

Hansen J F, Edwards M J, Froula D H, Edens A D, Gregori G and Ditmire T 2006 *Phys. Plasmas* **13** 112101

Harada N, Herbst E and Wakelam V 2010 *Astrophys. J.* **721** 1570–8

Harrison J J, Brown J M, Halfen D T and Ziurys L M 2006 *Astrophys. J.* **637** 1143–7

Hartigan P and Morse J 2007 *Astrophys. J.* **660** 426–40

Hartigan P, Foster J M, Wilde B H, Coker R F, Rosen P A, Hansen J F, Blue B E, Williams R J R, Carver R and Frank A 2009 *Astrophys. J.* **705** 1073–94

Hartigan P, Frank A, Foster J M, Wilde B H, Douglas M, Rosen P A, Coker R F, Blue B E and Hansen J F 2011 *Astrophys. J.* **736** 29

Hauschildt P, Warmbier R, Schneider R and Barman T 2009 *Astron. Astrophys.* **504** 225–9

Haxton W C and Serenelli A M 2008 *Astrophys. J.* **687** 678–91

Heger A, Langanke K, Martinez-Pinedo G and Woosley S E 2001 *Phys. Rev. Lett.* **86** 1678–81

Heger A, Kolbe E, Haxton W C, Langanke K, Martínez-Pinedo G and Woosley S E 2005 *Phys. Lett.* B **606** 258–64

Heil M, Käppeler F, Uberseder E, Gallino R, Bisterzo S and Pignatari M 2008 *Phys. Rev.* C **78** 025802

Henning T 2010 *Annu. Rev. Astron. Astrophys.* **48** 21–46

Henning T and Salama F 1998 *Science* **282** 2204–10

Henry R B C, Cowan J J and Sobeck J S 2010 *Astrophys. J.* **709** 715–24

Herbst E 1981 *Nature* **289** 656–7

Herbst E and Klemperer W 1973 *Astrophys. J.* **185** 505–34

Herbst E and van Dishoeck E F 2009 *Annu. Rev. Astron. Astrophys.* **47** 427–80

Hernanz M, José J, Coc A, Gómez-Gomar J and Isern J 1999 *Astrophys. J.* **526** L97–L100

Heros C d l 2010 arXiv:1012.0184

Hersant F, Wakelam V, Dutrey A, Guilloteau S and Herbst E 2009 *Astron. Astrophys.* **493** L49–L52

Hessels J W T, Ransom S M, Stairs I H, Freire P C C, Kaspi V M and Camilo F 2006 *Science* **311** 1901–4

Hicks D G, Boehly T R, Celliers P M, Eggert J H, Moon S J, Meyerhofer D D and Collins G W 2009 *Phys. Rev.* B **79** 014112

Hohenberger M *et al* 2010 *Phys. Rev. Lett.* **105** 205003

Hooper D, Finkbeiner D P and Dobler G 2007 *Phys. Rev.* D **76** 083012

Hora J L, Latter W B, Smith H A and Marengo M 2006 *Astrophys. J.* **652** 426–41

Horn A, Mollendal H, Sekiguchi O, Uggerud E, Roberts H, Herbst E, Viggiano A A and Fridgen T D 2004 *Astrophys. J.* **611** 605–14

Hörz *et al* 2006 *Science* **314** 1716–9

Hovde D C and Saykally R J 1987 *J. Chem. Phys.* **87** 4332–8

Huet P and Nelson A E 1996 *Phys. Rev.* D **53** 4578–97

Hwang U, Flanagan K A and Petre R 2005 *Astrophys. J.* **635** 355–64

IAU Commission 14 2011 http://iacs.cua.edu/IAUC14/

Iglesias-Groth S, Manchado A, García-Hernández D A, González-Hernández J I and Lambert D L 2008 *Astrophys. J.* **685** L55–L58

Iglesias-Groth S, Manchado A, Rebolo R, González-Hernández J I, García-Hernández D A and Lambert D L 2010 *Mon. Not. R. Astron. Soc.* **407** 2157–65

Iglesias-Groth S, Manchado A, Rebolo R, González-Hernández J I, García-Hernández D A and Lambert D L 2010 *Mon. Not. R. Astron. Soc.* **409** 880 (erratum)

Imbriani G *et al* 2005 *Eur. Phys. J.* A **25** 455–66

Indriolo N, Geballe T R, Oka T and McCall B J 2007 *Astrophys. J.* **671** 1736–47

Indriolo N, Fields B and McCall B J 2009 *Astrophys. J.* **694** 257–67

Innes D E, Giddings J R and Falle S A E G 1987 *Mon. Not. R. Astron. Soc.* **226** 67–93

Ivarsson S, Litzén U and Wahlgren G M 2001 *Phys. Scr.* **64** 455–461

Ivarsson S, Andersen J, Nordström B, Dai X, Johansson S, Lundberg H, Nilsson H, Hill V, Lundqvist M and Wyart J F 2003 *Astron. Astrophys.* **409** 1141–9

Izotov Y I and Thuan T X 2010 *Astrophys. J.* **710** L67–L71

Jager C, Huisken F, Mutschke H, Henning Th, Poppitz W and Voicu I 2007 *Carbon* **47** 2981–94

Jewitt D 1999 *Annu. Rev. Earth Planet. Sci.* **27** 287–312

Jewitt D C and Luu J 2004 *Nature* **432** 731–3

Ji H, Burin M, Schartman E and Goodman J 2006 *Nature* **444** 343–6

Juhasz A, Henning Th, Bouwman J, Dullemond C P, Pascucci I, Apai D 2009 *Astrophys. J.* **695** 1024–41

Julien K and Knobloch E 2010 *Phil. Trans. R. Soc.* A **368** 1607–33

Junghans A R, Mohrmann E C, Snover K A, Steiger T D, Adelberger E G, Casandjian J M, Swanson H E, Buchmann L, Park S H and Zyuzin A 2002 *Phys. Rev. Lett.* **88** 041101

Junghans A R *et al* 2003 *Phys. Rev.* C **68** 065803

Junghans A R, Snover K A, Mohrmann E C, Adelberger E G and Buchmann L 2010 *Phys. Rev.* C **81** 012801

Käppeler F, Beer H and Wisshak K 1989 *Rep. Prog. Phys.* **52** 945–1013

Käppeler F, Gallino R, Bisterzo S and Aoki W 2011 *Rev. Mod. Phys.* **83** 157–93

Kallman T R 2010 *Space Sci. Rev.* **157** 177–91

Kallman T R and Palmeri P 2007 *Rev. Mod. Phys.* **79** 79–133

Kaltenegger L and Sasselov D 2010 *Astrophys. J.* **708** 1162–7

Kalvans J and Shmeld I 2010 *Astron. Astrophys.* **521** A37

Kang Y G *et al* 2000 *Proc. SPIE* **3886** 489–95

Kaspi S *et al* 2002 *Astrophys. J.* **574** 643–62

Kaspi S, Netzer H, Chelouche D, George I M, Nandra K and Turner T J 2004 *Astrophys. J.* **611** 68–80

Kastner J H, Huenemoerder D P, Schulz N S, Canizares C R and Weintraub D A 2002 *Astrophys. J.* **567** 434–40

Kawaguchi K, Kasai Y, Ishikawa S and Kaifu N 1995 *Publ. Astron. Soc. Japan* **47** 853–76

Keller *et al* 2006 *Science* **314** 1728–31

Kelley M S and Wooden D H 2009 *Planet. Space Sci.* **57** 1133–45

Kharchenko V and Dalgarno A 2000 *J. Geophys. Res.* **105** 18351–60

Kifonidis K, Plewa T, Janka H-T and Muller E 2000 *Astrophys. J.* **531** L123–L126

Kifonidis K, Plewa T, Janka H-T and Muller E 2003 *Astron. Astrophys.* **408** 621–49

Kifonidis K, Plewa T, Sheck L, Janka H-T and Muller E 2006 *Astron. Astrophys.* **457** 963–86

Kim H, Wyrowski F, Menten K M, Decin L 2010 *Astron. Astrophys.* **516** A68

Kimoto P A and Chernoff D F 1997 *Astrophys. J.* **485** 274–84

Kirkpatrick J D 2005 *Annu. Rev. Astron. Astrophys.* **43** 195–245

Klein R I, McKee C F and Colella P 1994 *Astrophys. J.* **420** 213–36

Klein R I, Budil K S, Perry T S and Bach D R 2003 *Astrophys. J.* **583** 245–59

Klypin A, Trujillo-Gomez S and Primack J 2011 *Astrophys. J.* **740** 102

Knutson H A, Charbonneau D, Allen L E, Burrows A and Megeath S T 2008 *Astrophys. J.* **673** 526–31

Knutson H A, Charbonneau D, Allen L E, Fortney J J, Agol E, Cowan N B, Showman A P, Cooper C S and Megeath S T 2007 *Nature* **447** 183–6

Kobayashi K *et al* 2005 *Phys. Rev.* D **72** 052007

Koenig M *et al* 2006 *Phys. Plasmas* **13** 056504

Kohl J L, Noci G, Cranmer S R and Raymond J L 2006 *Astron. Astrophys. Rev.* **13** 31–157

Koldoba A V, Ustyugova G V, Romanova M M and Lovelace R V E 2008 *Mon. Not. R. Astron. Soc.* **388** 357–66

Konacki M, Torres G, Jha S and Sasselov D D 2003 *Nature* **421** 507–9

Konacki M, Torres G, Sasselov D D, Pietrzyński G, Udalski A, Jha S, Ruiz M T, Gieren W and Minniti D 2004 *Astrophys. J.* **609** L37–L40

Konigl A 1991 *Astrophys. J.* **370** L39–L43

Kotera K and Olinto A V 2011 *Annu. Rev. Astron. Astrophys.* **49** 119–53

Kotrík T, Dohnal P, Korolov I, Plašil R, Roučka Š, Glosík J, Greene C H and Kokoouline V 2010 *J. Chem. Phys.* **133** 034305

Koutroumpa D, Lallement R, Kharchenko V, Dalgarno A, Pepino R, Izmodenov V and Quemerais E 2006 *Astron. Astrophys.* **460** 289–300

Kraemer S B, Ferland G J and Gabel J R 2004 *Astrophys. J.* **604** 556–61

Krätschmer W, Lamb L D, Fostiropoulos K and Huffman D R 1990 *Nature* **347** 354–8

Krasnopolsky V A and Mumma M J 2001 *Astrophys. J.* **549** 634–4

Krasnopolsky V A, Mumma M J, Abbott M, Flynn B C, Meech K J, Yeomans D K, Feldman P D and Cosmovici C B 1997 *Science* **277** 1488–91

Kratz K-L, Pfeiffer B, Thielemann F-K and Walters W B 2000 *Hyperfine Interact.* **129** 185–221

Krause O, Tanaka M, Usuda T, Hattori T, Goto M, Birkmann S and Nomoto K 2008 *Nature* **456** 617–19

Kravchenko I *et al* 2006 *Phys. Rev.* D **73** 082002

Kreckel H *et al* 2005 *Phys. Rev. Lett.* **95** 263201

Kreckel H *et al* 2010 *Phys. Rev.* A **82** 042715

Kreckel H, Bruhns H, Čížek M, Glover S C O, Miller K A, Urbain X and Savin D W 2010 *Science* **329** 69–71

Krełowski J, Beletsky Y, Galazutdinov G A, Kołos R, Gronowski M and LoCurto G 2010 *Astrophys. J.* **714** L64–L67

Krolik J, McKee C M and Tarter C B 1981 *Astrophys. J.* **249** 422–42

Krongold Y, Nicastro F, Brickhouse N S, Elvis M, Liedahl D A and Mathur S 2003 *Astrophys. J.* **597** 832–50

Krongold Y, Nicastro F, Elvis M, Brickhouse N S, Mathur S and Zezas A 2005 *Astrophys. J.* **620** 165–82

Kroto H W, Heath J R, Obrien S C, Curl R F and Smalley, R E 1985 *Nature* **318** 162–3

Kuhlen M, Weiner N, Diemand J, Madau P, Moore B, Potter D, Stadel J and Zemp M 2010 *J. Cosmol. Astropart. Phys.* JCAP02(2010)030

Kuranz C C *et al* 2009 *Astrophys. J.* **696** 749–59

Kuranz C C, Drake R P, Grosskopf M J, Fryxell B, Budde A, Hansen J F, Miles A R, Plewa T, Hearn N C and Knauer J P 2010 *Phys. Plasmas* **17** 052709

Kurucz R L and Bell B 1995 *Kurucz CD-ROM 23: Atomic Line List* (Cambridge, MA: Smithsonian Astrophysical Observatory)

Kuzmin V A, Rubakov V A and Shaposhnikov M E 1985 *Phys. Lett.* B **155** 36–42

Laming J M 2004 *Phys. Rev.* E **70** 057402

Laming J M *et al* 2000 *Astrophys. J.* **545** L161–L164

Landi E and Cranmer S R 2009 *Astrophys. J.* **691** 794–805

Langanke K and Martinez-Pinedo G 2003 *Rev. Mod. Phys.* **75** 819–62

Lattanzi V, Walters A, Drouin B J, Pearson J C 2007 *Astrophys. J.* **662** 771–8

Lawler J E, Bonvallet G and Sneden C 2001a *Astrophys. J.* **556** 452–60

Lawler J E, Wickliffe M E, Cowley C R and Sneden C 2001b *Astrophys. J. Suppl. Ser.* **137** 341–9

Lawler J E, Wickliffe M E, den Hartog E A and Sneden C 2001c *Astrophys. J.* **563** 1075–88

Lawler J E, Sneden C and Cowan J J 2004 *Astrophys. J.* **604** 850–60

Lawler J E, den Hartog E A, Labby Z E, Sneden C, Cowan J J and Ivans I I 2007 *Astrophys. J. Suppl. Ser.* **169** 120–36

Lawler J E, den Hartog E A, Sneden C and Cowan J J 2008a *Can. J. Phys.* **86** 1033–8

Lawler J E, Sneden C, Cowan J J, Wyart J-F, Ivans I I, Sobeck J S, Stockett M H and den Hartog E A 2008b *Astrophys. J.* **178** 71–88

Lawler J E, Sneden C, Cowan J J, Ivans I I and den Hartog E A 2009 *Astrophys. J. Suppl. Ser.* **182** 51–79

Lebedev S V *et al* 2002 *Astrophys. J.* **564** 113–19

Lebedev S V, Ampleford D, Ciardi A, Bland S N, Chittenden J P, Haines M G, Frank A, Blackman E G and Cunningham A 2004 *Astrophys. J.* **616** 988–97

Lebedev S V *et al* 2005 *Mon. Not. R. Astron. Soc.* **361** 97–108

Lee C, Cirigliano V and Ramsey-Musolf M J 2005 *Phys. Rev.* D **71** 075010

Leith C E 1990 *Phys. Fluids* A **2** 297–9

Lemut A *et al* 2006 *Phys. Lett.* B **634** 483–7

Leonard D S, Karwowski H J, Brune C R, Fisher B M and Ludwig E J 2006 *Phys. Rev.* C **73** 045801

Lestinsky M *et al* 2009 *Astrophys. J.* **698** 648–59

Li Y, Profumo S and Ramsey-Musolf M 2008 *Phys. Rev.* D **78** 075009

Li Y, Profumo S and Ramsey-Musolf M 2009 *Phys. Lett.* B **673** 95–100

Li Y, Profumo S and Ramsey-Musolf M 2010 *J. High Energy Phys.* JHEP08(2010)062

Li Z H *et al* 2006 *Phys. Rev.* C **74** 035801

Lin C-H, Antia H M and Basu S 2007 *Astrophys. J.* **668** 603–10

Lin C-J 2011 arXiv:1101.0261

Linden T and Profumo S 2010 *Astrophys. J.* **714** L228–L232

Lis D C *et al* 2010 *Astron. Astrophys.* **521** L9

Lisse C M *et al* 1996 *Science* **274** 205–9

Lisse C M, Christian D J, Dennerl K, Meech K J, Petre R, Weaver H A and Wolk S J 2001 *Science* **292** 1343–8

Liszt H S, Lucas R and Pety J 2006 *Astron. Astrophys.* **448** 253–9

Loch S D, Pindzola M S, Ballance C P and Griffin D C 2006 *J. Phys. B: At. Mol. Opt. Phys.* **39** 85–104

Lodders K 2003 *Astrophys. J.* **591** 1220–47

Lodders K and Fegley B Jr 1999 *Asymptotic Giant Branch Stars* (*Proc. IAU Symp.* vol 191) ed T le Bertre *et al* (Cambridge: Cambridge University Press) pp 279–90

Lopez R E and Turner M S 1999 *Phys. Rev.* D **59** 103502

Lukić D *et al* 2007 *Astrophys. J.* **664** 1244–52

Lundberg H, Johansson S, Nilsson H and Zhang Z 2001 *Astron. Astrophys.* **372** L50–L52

Maercker M, Schoier F L, Olofsson H, Bergman P, Ramstedt S 2008 *Astron. Astrophys.* **479** 779–91

Maier J P, Walker G A H, Bohlender D A, Mazzotti F J, Raghunandan R, Fulura J, Garkusha I and Nagy A 2011 *Astrophys. J.* **726** 41

Malloci G, Joblin C and Mulas G 2007 *Chem. Phys.* **332** 353–9

Maloney P R, Hollenbach D J and Tielens A G G M 1996 *Astrophys. J.* **466** 561–84

Mancini R C, Bailey J E, Hawley J F, Kallman T, Witthoeft M, Rose S J and Takabe H 2009 *Phys. Plasmas* **16** 041001

Marta M *et al* 2008 *Phys. Rev.* C **78** 022802

Martin M C, Koller D and Mihaly L 1993 *Phys. Rev.* B **47** 14607–10

Mastrapa R M E and Brown R H 2006 *Icarus* **183** 207–14

Matsumoto C, Leighly K M and Marshall H L 2004 *Astrophys. J.* **603** 456–62

Matthews C N and Minard R D 2006 *Faraday Discuss.* **133** 393–401

Maxted P F L *et al* 2010 *Astron. J.* **140** 2007–12

McCall B J *et al* 2003 *Nature* **422** 500–2

McCarthy M C, Gottlieb C A Gupta H and Thaddeus P 2006 *Astrophys. J.* **652** L141–L144

McClendon J H 1999 *Earth-Sci. Rev.* **47** 71–93

McKeegan *et al* 2006 *Science* **314** 1724–8
McKernan B, Yaqoob T and Reynolds C S 2007 *Mon. Not. R. Astron. Soc.* **379** 1359–72
McWilliam A 1997 *Annu. Rev. Astron. Astrophys.* **35** 503–56
Medvedev M V and Loeb A 1999 *Astrophys. J.* **526** 697–706
Menten K M, Wyrowski F, Belloche A, Güsten R, Dedes L and Müller H S P 2011 *Astron. Astrophys.* **525** A77
Milam S N, Halfen D T, Tenenbaum E D, Apponi A J, Woolf N J and Ziurys L M 2008 *Astrophys. J.* **684** 618–25
Militzer B 2009 *Phys. Rev.* B **79** 155105
Miles A R, Braun D G, Edwards M J, Robey H F, Drake R P and Leibrandt D R 2004 *Phys. Plasmas* **11** 3631–45
Miller-Ricci E, Seager S and Sasselov D 2009 *Astrophys. J.* **690** 1056–67
Miyake S, Stancil P C, Sadeghpour H R, Dalgarno A, McLaughlin B M and Forrey R C 2010 *Astrophys. J.* **709** L168–71
Möller P, Pfeiffer B and Kratz K-L 2003 *Phys. Rev.* C **67** 055802
Molster F J and Waters L B F M 2003 *Astromineralogy* (*Lecture Notes in Physics* vol 609) ed T Henning (Berlin: Springer) pp 121–70
Moore A S, Gumbrell E T, Lazarus J, Hohenberger M, Robinson J S, Smith R A, Plant T J A, Symes D R and Dunne M 2008 *Phys. Rev. Lett.* **100** 055001
Monchaux R *et al* 2007 *Phys. Rev. Lett.* **98** 044502
Morton D C 2000 *Astrophys. J. Suppl. Ser.* **130** 403–36
Morton D C 2003 *Astrophys. J. Suppl. Ser.* **149** 205–38
Moseley J, Aberth W and Peterson J R 1970 *Phys. Rev. Lett.* **24** 435–9
Muller E, Fryxell B and Arnett D 1991 *Astron. Astrophys.* **251** 505–14
Müller H S P, Schlöder F, Stutzki J and Winnewisser G 2005 *J. Mol. Struct.* **742** 215–27
Muñoz Caro G M, Meierhenrich U J, Schutte W A, Barbier B, Arcones Segovia A, Rosenbauer H, Thiemann W H-P, Brack A and Greenberg J M 2002 *Nature* **416** 403–6
Murphy A St J *et al* 2009 *Phys. Rev.* C **79** 058801
Murphy G C, Dieckmann M E, Bret A and Drury L O C 2010 *Astron. Astrophys.* **524** A84
Mürtz P, Zink L R, Evenson K M and Brown J M 1998 *J. Chem. Phys.* **109** 9744–52
Nemes L, Ram R S, Bernath P F, Tinker F A, Zumwalt M C, Lamb L D and Huffman D R 1994 *Chem. Phys. Lett.* **218** 295–303
Netzer H 2004 *Astrophys. J.* **604** 551–5
Netzer H *et al* 2003 *Astrophys. J.* **599** 933–48
Neufeld D A *et al* 2010 *Astron. Astrophys.* **521** L10
Nilsson H, Ivarsson S, Johansson S and Lundberg H 2002a *Astron. Astrophys.* **381** 1090–3
Nilsson H, Ljung G, Lundberg H and Nielsen K E 2006 *Astron. Astrophys.* **445** 1165–8
Nilsson H, Zhang Z G, Lundberg H, Johansson S and Nordstrom B 2002b *Astron. Astrophys.* **382** 368–77
Nishikawa K I, Niemiec J, Hardee P E, Medvedev M, Sol H, Mizuno Y Zhang B, Pohl M, Oka M and Hartmann D H 2009 *Astrophys. J.* **698** L10–L13
Nishimura S *et al* 2011 *Phys. Rev. Lett.* **106** 052502
Nishino H *et al* 2009 *Phys. Rev. Lett.* **102** 141801
Nitz D, Kunau A E, Wilson K L and Lentz L R 1999 *Astrophys. J. Suppl. Ser.* **122** 557–61
Nollett K M and Burles S 2000 *Phys. Rev.* D **61** 123505
Nuevo M, Milam S N, Sandford S A, Elsila J E and Dworkin J P 2009 *Astrobiology* **9** 683–95
Öberg K I, van Dishoeck E F and Linnartz H 2009a *Astron. Astrophys.* **496** 281–93
Öberg K I, Garrod R T, van Dishoeck E F and Linnartz H 2009b *Astron. Astrophys.* **504** 891–913
Olive K A 1999 arXiv:astro-ph/9901231

Oliver P and Hibbert A 2010 *J. Phys. B: At. Mol. Opt. Phys.* **43** 074013
Osterbrock D E and Ferland G J 2006 *Astrophysics of Gaseous Nebulae and Active Galactic Nuclei* 2nd edn (Mill Valley, CA: University Science Press)
Otranto S and Olson R E 2011 *Phys. Rev.* A **83** 032710
Palmeri P, Quinet P, Wyart J-F and Biémont E 2000 *Phys. Scr.* **61** 323–34
Palomares C 2009 Double-Chooz neutrino experiment *EPS-HEP 2009: 2009 Europhysics Conf. on High Energy Physics (Krakow, Poland, 16–22 July 2009)* p 275
Pascoli G and Polleux A 2000 *Astron. Astrophys.* **359** 799–810
Patel H H and Ramsey-Musolf M J 2011 arXiv:1101.4665
Patel N A *et al* 2011 *Astrophys. J. Suppl. Ser.* **193** 17
Persson C M *et al* 2010 *Astron. Astrophys.* **521** L45
Pessah M E 2010 *Astrophys. J.* **716** 1012–27
Pessah M E and Goodman J 2009 *Astrophys. J.* **698** L72–L76
Petrignani A *et al* 2009 *J. Phys.: Conf. Ser.* **192** 012022
Pettini M, Zych B J, Murphy M T, Lewis A and Steidel C S 2008 *Mon. Not. R. Astron. Soc.* **391** 1499–510
Pfeiffer B, Kratz K-L, Thielemann F-K and Walters W B 2001 *Nucl. Phys.* A **693** 282–324
Piekarewicz J 2010 *J. Phys. G: Nucl. Part Phys.* **37** 064038
Pierre Auger Collaboration 2010 *Phys. Lett.* B **685** 239–46
Pietroni M 1993 *Nucl. Phys.* B **402** 27–45
Pilaftsis A 2005 *Phys. Rev. Lett.* **95** 081602
Pilaftsis A 2009 *J. Phys.: Conf. Ser.* **171** 012017
Pilaftsis A and Underwood T E J 2005 *Phys. Rev.* D **72** 113001
Piran T 1999 *Phys. Rep.* **314** 575–667
Polehampton E T, Menten K M, van der Tak F F S, White G J 2010 *Astron. Astrophys.* **510** A80
Poludnenko A Y, Dannenberg K K, Drake R P, Frank A, Knauer J, Meyerhofer D D, Furnish M, Asay J R and Mitran S 2004 *Astrophys. J.* **604** 213–21
Porter R L, Ferland G J and MacAdam K B 2007 *Astrophys. J.* **657** 327–37
Porter R L, Ferland G J, MacAdam K B and Storey P 2009 *Mon. Not. R. Astron. Soc.* **393** L36–L40
Porter S B, Desch S J and Cook J C 2010 *Icarus* **208** 492–8
Pospelov M, Ritz A and Voloshin M B 2008 *Phys. Lett.* B **662** 53–61
Pounds K A, Reeves J N, O'Brian P T, Page K A, Turner M J L and Nayakshin S 2001 *Astrophys. J.* **559** 181–6
Pounds K A, Reeves J N, King R A and Page K L 2004 *Mon. Not. R. Astron. Soc.* **350** 10–20
Prager S C, Rosner R, Ji H T and Cattaneo F 2010 *Research Opportunities in Plasma Astrophysics* (Princeton, NJ: Princeton Plasma Physics Laboratory) http://www.pppl.gov/conferences/2010/WOPA/index.html
Profumo S 2008 arXiv:0812.4457
Profumo S, Ramsey-Musolf M J and Shaughnessy G 2007 *J. High Energy Phys.* JHEP08(2007)010
Pudritz R E, Ouyed R, Fendt C and Brandenburg A 2007 *Protostars and Planets V* ed B Reipurth *et al* (Tucson, AZ: University of Arizona Press) pp 277–94
Pulliam R L, Savage C, Agúndez M, Cernicharo J, Guélin M and Ziurys L M 2010 *Astrophys. J.* **725** L181–L184
Puget J L and Léger A 1989 *Annu. Rev. Astron. Astrophys.* **27** 161–98
Qian Y-Z and Wasserburg G J 2007 *Phys. Rep.* **442** 237–68
Quinet P, Palmeri P, Biemont E, McCurdy M M, Rieger G, Pinnington E H Wickliffe M E and Lawler J E 1999 *Mon. Not. R. Astron. Soc.* **307** 934–40
Raiteri C M, Gallino R, Busso M, Neuberger D and Käppeler F 1993 *Astrophys. J.* **542** 400–3
Rapaport J and Sugarbaker E 1994 *Annu. Rev. Nucl. Part. Sci.* **44** 109–53
Raymond J C, Wallerstein G and Balick B 1991 *Astrophys. J.* **383** 226–32

Redman M P, Viti S, Cau P and Williams D A 2003 *Mon. Not. R. Astron. Soc.* **345** 1291–6

Reighard A B *et al* 2006 *Phys. Plasmas* **13** 082901

Reipurth B and Bally J 2001 *Annu. Rev. Astron. Astrophys.* **39** 403–55

Remijan A J, Hollis J M, Lovas F J Cordiner M A, Millar T J, Markwick-Kemper A J and Jewell P R 2007 *Astrophys. J.* **664** L47–L50

Remington B A, Drake R P and Ryutov D D 2006 *Rev. Mod. Phys.* **78** 755–807

Ren Y, Yamada M, Ji H, Dorfman S, Gerhardt S P and Kulsrud R M 2008 *Phys. Plasmas* **15** 082113

Ren Y, Almagri A F, Fiksel G, Prager S C, Sarff J F and Terry P W 2009 *Phys. Rev. Lett.* **103** 145002

Rest A *et al* 2008 *Astrophys. J.* **680** 1137–48

Reynolds S P, Borkowski K J, Hwang U, Hughes, J P, Badenes C, Laming J M and Blondin J M 2007 *Astrophys. J.* **668** L135–L138

Ricketts C, Contreras C, Walker R and Salama F 2011 *Int. J. Mass Spectrom.* **300** 26–30

Richardson J E, Melosh H J, Lisse C M and Carcich B 2007 *Icarus* **190** 357–90

Ritchey A M, Federman S R, Sheffer Y and Lambert D L 2011 *Astrophys. J.* **728** 70

Roberts H, Herbst E and Millar T J 2004 *Astron. Astrophys.* **424** 905–17

Robey H F, Perry T S, Klein R I, Kane J O, Greenough J A and Boehly T R 2002 *Phys. Rev. Lett.* **89** 085001

Rogers F J and Iglesias C A 1994 *Science* **263** 50–5

Rosen P A, Foster J M, Wilde B H, Hartigan P, Blue B E, Hansen J F, Sorce C, Williams R J R, Coker R and Frank A 2009 *Astrophys. Space Sci.* **322** 101–5

Rosner R and Hammer D A 2010 *Basic Research Needs for High Energy Density Laboratory Physics* (Washington, DC: US Department of Energy) http://www.science.energy.gov/fes/news-and -resources/workshop-reports/

Rothman L S *et al* 2005 *J. Quant. Spectrosc. Radiat. Transfer* **96** 139–204

Rubbia A 2011 March 16 talk *15th Int. Workshop on Neutrino Telescopes (Rome, 15–18 Mar. 2011)* http://agenda.infn.it/ conferenceOtherViews.py?view=standard&confId=3101

Runkle R C, Champagne A E, Angulo C, Fox C, Iliadis C, Longland R and Pollanen J 2005 *Phys. Rev. Lett.* **94** 082503

Ryan S G, Beers T C, Olive K A, Fields B D and Norris J E 2000 *Astrophys. J.* **530** L57–L60

Ryu D and Vishniac E T 1991 *Astrophys. J.* **368** 411–25

Ryutov D D, Drake R P, Kane J, Liang E, Remington B A and Wood-Vasey M 1999 *Astrophys. J.* **518** 821–32

Sakai N, Shiino T, Hirota T, Sakai T and Yamamoto S 2010 *Astrophys. J.* **718** L49–L52

Sako M *et al* 2003 *Astrophys. J.* **596** 114–28

Salama F 1998 *Solar System Ices* ed B Schmitt *et al* (Dordrecht: Kluwer) pp 259–80

Salama F 1999 *Solid Interstellar Matter: The ISO Revolution* ed L d Hendecourt *et al* (Berlin: Springer) pp 65–87

Salama F 2008 *IAU Symp. 251: Organic Matter in Space* ed S Kwok and S A Sanford (Cambridge: Cambridge University Press) pp 357–66

Salama F, Galazutdinov G, Krelowski J, Biennier L, Beletsky Y and Song I 2011 *Astrophys. J.* **728** 154–62

Saltzberg D, Gorham P, Walz D, Field C, Iverson R, Odian A, Resch G, Schoessow P and Williams D 2001 *Phys. Rev. Lett.* **86** 2802–5

Sandford *et al* 2006 *Science* **314** 1720–4

Sargent B A *et al* 2009 *Astrophys. J.* **690** 1193–207

Sarre P J 1980 *J. Chim. Phys. Phys.-Chim. Biol.* **77** 769–71

Sarre P J 2006 *J. Mol. Spectrosc.* **238** 1–10

Sasselov D D 2003 *Astrophys. J.* **596** 1327–31

Sako M *et al* 2003 *Astrophys. J.* **596** 114–28

Saumon D and Guillot T 2004 *Astrophys. J.* **609** 1170–80

Savage C, Apponi A J and Ziurys L M 2004 *Astrophys. J.* **608** L73–L76

Savin D W *et al* 2011 arXiv:1103.1341

Schartman E, Ji H, Burin M and Goodman J 2011 arXiv:1102.3725

Schectman R M, Cheng S, Curtis L J, Federman S R, Fritts M C and Irving R E 2000 *Astrophys. J.* **419** 207–23

Schilke P *et al* 2010 *Astron. Astrophys.* **521** L11

Schippers S 2009 *J. Phys.: Conf. Ser.* **163** 012001

Schippers S, Lestinsky M, Müller A, Savin D W, Schmidt E W and Wolf A 2010 *Int. Rev. At. Mol. Phys.* **1** 109–20

Schlemmer S, Asvany O, Hugo E and Gerlich D 2006 *Astrochemistry: Recent Successes and Current Challenges* ed D C Lis *et al* (Cambridge: Cambridge University Press) p 125

Schmidt E W *et al* 2006 *Astrophys. J.* **641** L157–L160

Schmidt E W *et al* 2008 *Astron. Astrophys.* **492** 265–75

Schoier F L, Maercker M, Justtanout K, Olofsson H, Black J H, Decin L, de Koter A, Waters R 2011 *Astron. Astrophys.* **530** A83

Seager S, Richardson L J, Hanse B M S, Menou K, Cho Y Y-K and Deming D 2005 *Astrophys. J.* **632** 1122–31

Sellgren K 1984 *Astrophys. J.* **277** 623–33

Sellgren K, Werner M W, Ingalls J G, Smith J D T, Carleton T M and Joblin C 2010 *Astrophys. J.* **722** L54–L57

Shelton J and Zurek K M 2010 *Phys. Rev. D* **82** 123512

Silk J 1999 The relationship between the bright and dark matter *The 3rd Stromlo Symposium: The Galactic Halo* (*ASP Conf. Ser.* vol 165) ed B K Gibson *et al* (San Francisco, CA: Astronomical Society of the Pacific) pp 27–33

Silva L O, Fonseca R A, Tonge J W, Dawson J M, Mori W B and Medvedev M V 2003 *Astrophys. J.* **596** L121–L124

Simon M C *et al* 2010 *Phys. Rev. Lett.* **105** 183001

Sims I R 2006 *Astrochemistry: Recent Successes and Current Challenges* ed D C Lis *et al* (Cambridge: Cambridge University Press) p 97

Singh B S, Hass M, Nir-El Y and Haquin G 2004 *Phys. Rev. Lett.* **93** 262503

Sisan D R, Mujica N, Tillotson W A, Huang Y M, Dorland W, Hassam A B, Antonsen T M and Lathrop D P 2004 *Phys. Rev. Lett.* **93** 114502

Smith N and Morse J A 2004 *Astrophys. J.* **605** 854–63

Smith R K, Chen G-X, Kirby K P and Brickhouse N S 2009 *Astrophys. J.* **700** 679–83

Smith R K, Chen G-X, Kirby K P and Brickhouse N S 2009 *Astrophys. J.* **701** 2034 (erratum)

Sneden C, Cowan J J and Gallino R 2008 *Annu. Rev. Astron. Astrophys.* **46** 241–88

Sneden C, Lawler J E, Cowan J J, Ivans I I and den Hartog E A 2009 *Astrophys. J. Suppl. Ser.* **182** 80–96

Snow T P and McCall B J 2006 *Annu. Rev. Astron. Astrophys.* **44** 367–414

Sobeck J S, Lawler J E and Sneden C 2007 *Astrophys. J.* **667** 1267–82

Soderberg A M *et al* 2008 *Nature* **453** 469–74

Sofia U J, Meyer D M and Cardelli J A 1999 *Astrophys. J.* **522** L137–L140

Sogoshi N, Kato Y, Wakabayashi T, Momose T, Tam S, DeRose M E and Fajardo M E 2000 *J. Phys. Chem. A* **104** 3733–42

Spence E J, Nornberg M D, Jacobson C M, Parada C A, Taylor N, Kendrick R D and Forest C B 2007 *Phys. Rev. Lett.* **98** 164503

Spitkovsky A 2008 *Astrophys. J.* **673** L39–L42

Springel V *et al* 2005 *Nature* **435** 629–36

Springer P T *et al* 1997 *J. Quant. Spectrosc. Radiat. Transfer* **58** 927–35

Steenbrugge K C, Kaastra J S, de Vries C P and Edelson R 2003 *Astron. Astrophys.* **402** 477–86

Steenbrugge K C, Kaastra J S, Sako M, Branduardi-Raymont G, Behar E, Paerels F B S, Blustin A J and Kahn S M 2005 *Astron. Astrophys.* **432** 453–62

Stefani F, Gundrum T, Gerbeth G, Rudiger G, Schultz M, Szklarski J and Hollerbach R 2006 *Phys. Rev. Lett.* **97** 184502

Steigman G 2011 Primordial nucleosynthesis: the predicted and observed abundances and their consequences *NIC XI: Proc. 11th Symp. on Nuclei in the Cosmos (Heidelberg, Germany, 11–23 July 2010)* 001

Stenrup M, Larson Å and Elander N 2009 *Phys. Rev.* A **79** 012713

Storey P J and Hummer D G 1995 *Mon. Not. R. Astron. Soc.* **272** 41–8

Strieder F *et al* 2001 *Nucl. Phys.* A **696** 219

Su M, Slatyer T R and Finkbeiner D P 2010 *Astrophys. J.* **724** 1044–82

Sun X, Intrator T P, Dorf L, Sears J, Fumo I and Lapenta G 2010 *Phys. Rev. Lett.* **105** 255001

Symes D R *et al* 2010 *High Energy Density Phys.* **6** 274–9

Tangri V, Terry P W and Fiksel G 2008 *Phys. Plasmas* **15** 112501

Tenenbaum E D and Ziurys L M 2008 *Astrophys. J.* **680** L121–L124

Tenenbaum E D and Ziurys L M 2010 *Astrophys. J.* **712** L93–L97

Tenenbaum E D, Woolf N J and Ziurys L M 2007 *Astrophys. J.* **666** L29–L32

Tenenbaum E D, Milam S N, Woolf N J and Ziurys L M 2009 *Astrophys. J.* **704** L108–L112

Tenenbaum E D, Dodd J L, Milam S N, Woolf N J and Ziurys L M 2010a *Astrophys. J.* **720** L102–L107

Tenenbaum E D, Dodd J L, Milam S N, Woolf N J and Ziurys L M 2010b *Astrophys. J. Suppl. Ser.* **190** 348–417

Terzieva R and Herbst E 2000 *Int. J. Mass Spectrom.* **201** 135–42

Thaddeus P, Gottlieb C A, Gupta H, Brünken S, McCarthy M C, Agúndez M, Guélin M and Cernicharo J 2008 *Astrophys. J.* **677** 1132–9

The L-S, El Eid M F and Meyer B S 2007 *Astrophys. J.* **655** 1058–78

Tielens A 2005 *The Physics and Chemistry of the Interstellar Medium* (Cambridge: Cambridge University Press)

Tikhonchuk V T *et al* 2008 *Plasma Phys. Control. Fusion* **50** 124017

Tinetti G *et al* 2007 *Nature* **448** 169–71

Tom B A *et al* 2009 *J. Chem. Phys.* **130** 031101

Tornow W, Czakon N G, Howell C R, Hutcheson A, Kelley J H, Litvinenko V N, Mikhailov S F, Pinayev I V, Weisel G J, and Witala H 2003 *Phys. Lett.* B **574** 8–13

Torres G *et al* 2011 *Astrophys. J.* **727** 24

Trotta R, Feroz F, Hobson M P, Roszkowski L and Ruiz de Austri R 2008 *J. High Energy Phys.* JHEP12(2008)024

Trujillo C A, Brown M E, Barkume K M, Schaller E L and Rabinowitz D L 2007 *Astrophys. J.* **655** 1172–8

Tucker-Smith D and Weiner N 2001 *Phys. Rev.* D **64** 043502

van Boekel R, Min M, Waters L B F M, de Koter A, Dominik C, van den Ancker M E, Bouwman J 2005 *Astron. Astrophys.* **437** 189–208

van der Holst B, Toth G, Sokolov I V, Powell K G, Holloway J P, Myra E S, Stout Q, Adams M L, Morel J E and Drake R P 2011 *Astrophys. J. Suppl. Ser.* **194** 23

van Veelen B, Langer N, Vink J, Garcia-Segura G and van Marle A J 2009 *Astron. Astrophys.* **503** 495–503

Vastel C, Caselli P, Ceccarelli C, Phillips T, Wiedner M C, Peng R, Houde M and Dominik C 2006 *Astrophys. J.* **645** 1198–211

Vernazza J E, Avrett E H and Loeser R 1976 *Astrophys. J. Suppl. Ser.* **30** 1–60

Vishniac E T 1983 *Astrophys. J.* **274** 152–67

Walker K M, Federman S R, Knauth D C and Lambert D L 2009 *Astrophys. J.* **706** 614–22

Walsh C, Harada N, Herbst E and Millar T J 2009 *Astrophys. J.* **700** 752–61

Wang F L, Fujioka S, Nishimura H, Kato D, Li Y T, Zhao G, Zhang J and Takabe H 2008 *Phys. Plasmas* **15** 073108

Wang L, Howell D A, Höflich P and Wheeler J C 2001 *Astrophys. J.* **550** 1030–5

Wang X K, Lin X W, Mesleh M, Jarrold M F, Dravid V P, Ketterson J B and Chang R P H 1995 *J. Mater. Res.* **10** 1977–38

Watson W D 1973 *Astrophys. J.* **183** L17–L20

Waxman E 2006 *Plasma Phys. Control. Fusion* **48** B137–B151

Westmoquette M S, Exter K M, Smith L J, and Gallagher J S 2007 *Mon. Not. R. Astron. Soc.* **381** 894–912

Whittet D C B 1997 *Orig. Life Evol. Biosph.* **27** 249–62

Whittet D C B 2003 *Dust in the Galactic Environment* 2nd edn (Bristol: Institute of Physics)

Wickliffe M E and Lawler J E 1997 *J. Opt. Soc. Am.* B **14** 737–53

Wickliffe M E, Lawler J E and Nave G 2000 *J. Quant. Spectrosc. Radiat. Transfer* **66** 363–404

Wiescher M, Gorres J, Uberseder E, Imbriani G and Pignatari M 2010 *Annu. Rev. Nucl. Part. Sci.* **60** 381–404

Wood K and Raymond J C 2000 *Astrophys. J.* **540** 563–71

Xu H L, Svanberg S, Quinet P, Garnir H P and Biémont E 2003 *J. Phys. B: At. Mol. Opt. Phys.* **36** 4773–87

Yamada M 2007 *Phys. Plasmas* **14** 058102

Yamada M, Kulsrud R and Ji H 2010 *Rev. Mod. Phys.* **82** 603–64

Yirak K, Frank A, Cunningham A and Mitran S 2008 *Astrophys. J.* **672** 996–1005

Yirak K, Frank A and Cunningham A 2012 *Astrophys. J.* at press (arXiv:1101.6020)

Young K, Cox P, Huggins P J, Forveille T and Bachiller R 1999 *Astrophys. J.* **522** 387–96

Zack L N, Ziegler N and Ziurys L M 2012 *Astrophys. J.* submitted

Zatsepin G T and Kuz'min V A 1966 *JETP Lett.* **4** 78–80

Zheng W J, Jewitt D and Kaiser R I 2009 *J. Phys. Chem.* A **113** 11174–81

Ziurys L M 2006 *Proc. Natl Acad. Sci. USA* **103** 12274–9

Zolensky *et al* 2006 *Science* **314** 1735–9

Zweibel E G and Yamada M 2009 *Annu. Rev. Astron. Astrophys.* **47** 292–332